NOTICE

AVIS

Canada

UNIVERSITY OF ALBERTA

COLLOIDAL STUDY OF A MONTMORILLONITE-FE-WATER
OIL SANDS SLUDGE MODEL

BY

JIANMING ZOU

A THESIS SUBMITTED TO

THE FACULTY OF GRADUATE STUDIES AND RESEARCH

IN PARTIAL FULFILLMENT OF THE REQUIREMENTS FOR THE DEGREE OF

MASTER OF SCIENCE

IN

MINING ENGINEERING

DEPARTMENT OF MINING, METALLURGICAL AND PETROLEUM
ENGINEERING

EDMONTON, ALBERTA

FALL, 1991

Canada

UNIVERSITY OF ALBERTA

RELEASE FORM

NAME OF AUTHOR: JIANMING ZOU

TITLE OF THESIS: COLLOIDAL STUDY OF A MONTMORILLONITE-FE-WATER OIL SANDS SLUDGE MODEL
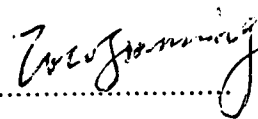
DEGREE: MASTER OF SCIENCE

YEAR THE DEGREE GRANTED: Fall, 1991

Permission is hereby granted to the University of Alberta Library to reproduce single copies of this thesis and to lend or sell such copies for private, scholarly or scientific research purposes only.

The author reserves other publication and other rights in association with the copyright in the thesis, and except as hereinbefore provided neither the thesis nor any substantial portion thereof may be printed or otherwise reproduced in any material form whatever without the author's prior written permission.

(SIGNED) ....

PERMANENT ADDRESS:
c/o Paul Pang
5204-22 Ave.
Edmonton, Alberta
Canada, T6L 2C5
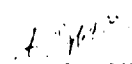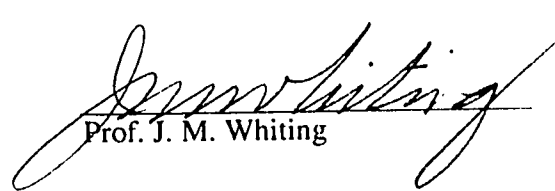
DATED: October 11, 1991

UNIVERSITY OF ALBERTA

FACULTY OF GRADUATE STUDIES AND RESEARCH

The undersigned certify that they have read, and recommend to the Faculty of Graduate Studies and Research for acceptance, a thesis entitled **COLLOIDAL STUDY OF A MONTMORILLONITE-FE-WATER OIL SANDS SLUDGE MODEL** submitted by **JIANMING ZOU** in partial fulfillment of the requirements for the degree of **MASTER OF SCIENCE** in **MINING ENGINEERING**.

_____
Prof. A. C. Pierre (Supervisor)

_____
Prof. J. M. Whiting

_____
Dr. R. Schutte

_____
Prof. S. E. Wanke

_____
Prof. S. A. Bradford

DATED: October 7, 1991

To my parents

for their unselfish support in my life and faith in me

and the sacrifice they made for me in the past.

And to my wife

for her boundless support and

the understanding of the tough life

as a student and a husband.

ABSTRACT

This study has been the design of a simple oil sands sludge model that fairly represents the real complex sludge system in terms of structure, settling and consolidation. A ternary model system, Montmorillonite-Fe(III)-Water, was selected.

The effects of electrolyte concentration, suspension pH, and the hydrolysis of Fe(III) on the settling and consolidation behavior of the model system have been examined. Experimental results show that settling and consolidation behavior depends largely on the fractal nature of flocs and the linkage strength between primary particles and flocs. Both electrolyte concentration and pH modify the double layer repulsion between clay particles, and consequently floc structure. With Fe (III) as the counterion, the interactions between plate-like clay particles become complex. Fe (III) has a triple role in the system: (1) as a counterion favoring edge-edge linkage; (2) as a former of Fe polymeric chemical complexes (when freshly prepared) which act as strong bonding agents; and (3) as an exchange cation anchoring the Fe complexes in the clay platelets. Drying experiments confirm the strong linkage between edges of platelets.

The structures of both model and real sludges after hypercritical drying under the scanning electron microscope is consistent with the diffusion-limited aggregation model. The observed structure differences can be attributed to the size differences.

A preliminary assessment of the effects of electrolyte concentration and suspension pH on drying behavior has been made on the model system. In addition, the swelling behavior of montmorillonite in aqueous media is assessed.

Comparison of the structure and settling behavior between the model system and real sludges shows the model is very useful for the understanding of the behavior of oil sands sludge, and provides valuable clues to preferred disposal methods.

ACKNOWLEDGEMENT

TABLE OF CONTENTS

LIST OF TABLES

LIST OF FIGURES

CHAPTER 1   INTRODUCTION

Alberta is rich in oil sands deposits. The Alberta oil sands deposits cover an area of 48,000 square kilometres, equivalent to the area of the province of New Brunswick. They comprise the Athabasca field, the world's largest single oil sands deposit, containing an estimated 862 billion barrels of heavy oil and bitumen of which 3.3 billion barrels are believed recoverable through surface mining (1). The commercial extraction of bitumen from oil sands has been possible since the development of the Hot Water Process in the 1920's by Dr. K.A. Clark of the Alberta Research Council. The Hot Water Process has been used by the only two existing oil sands plants operated on Athabasca oil sands deposit, Suncor and Syncrude Canada Ltd. It has been progressively improved in terms of bitumen recovery, energy consumption and production of oil sands tailings sludge. While it presents some drawbacks, and many alternatives have been proposed or tested over the past, the Hot Water Process is still the only one currently used for commercial extraction of bitumen from surface mined oil sands. It has been the process of choice for all of the major proposed oil sands projects, such as Alsands, Canstar, Syncrude Expansion and OSLO (2).

The major problem associated with the application of the Hot Water Process is the production of large quantities of **oil sands tailings sludge** and its net massive accumulation during the operation. Because of its toxic nature and environmental regulations, oil sands tailings sludge is impounded in tailings ponds where settling and consolidation occur slowly. Two major problems are incurred by the oil sands tailings sludge. First, the fine clay particles it contains settle very slowly, which makes the recycling of a large portion of water impossible. The recycling of water from tailings sludge is important since the Hot Water Process requires a tremendous amount of water. Water supply could become a problem for large oil sands operation. For example, the plant at Syncrude Canada Ltd is capable of processing over 300,000 tonnes of oil sands daily. It requires 250,000 cubic metres of water a day to remove 179,000 barrels of bitumen from the oil sands.

Secondly, and more important, the oil sands tailings sludge consolidates extremely slowly. After the solid content in tailings sludge reaches about 30-35%, the consolidation process virtually stops (3-7). At such a solid concentration, the tailings sludge remains a fluid, even after several years. It cannot be used for backfill or disposed of in an acceptable way.

From the environmental point of view, the oil sands tailings sludge has the following impacts. First, the large surface area of tailings ponds is not available for other uses for an extensive time period. Those oil sands deposits, if any, under the tailings ponds can't be recovered. Secondly, it may contaminate the groundwater. Tailings ponds also pose a threat to waterfowl and animals. Finally, liquefied tailings sludge constitutes a major hazard to the surrounding habitats and human beings, should a dyke failure occur, such as in case of earthquakes.

Therefore, the design of an efficient and economically acceptable method to transform the fluid-like tailings sludge into a form which can be easily disposed of, or the design of a new extraction process whereby the production of oil sands tailings sludge is minimized or eliminated, is generally considered as a major task to be achieved by the oil sands industry. Its accomplishment relies on a clear understanding of the behavior of tailings sludge and the determination of the effect of a number of factors, such as tailings sludge composition, the nature of flocculants and pH. The present study is intended as a contribution to the achievement of this task.

It is generally accepted that the presence of clays in the oil sands tailings sludge contributes to the long-term stability of oil sands tailings sludge with respect to consolidation. The problem caused by the clay component in tailings sludge was not fully anticipated despite the fact that the massive accumulation of tailings sludge was recognized as early as 1953. At that time, it was predicted that the oil sands tailings sludge would settle just as tailings from some other mining operation do, and would eventually form a compact sludge presenting no major problems for final disposal. However, because of the properties of clays, simple settling could not produce a sludge of which clay to water weight ratio is larger than 0.24 (8). The tailings sludge remains a fluid even after decades. A net bulking factor of 1.3-1.4 has been reported (3,9), which means the final volume of tailings sludge after water recycling is 30-40% larger than the volume mined. Consequently, large areas of tailings ponds were constructed to impound tailings sludge, and the contained tailings sludge volume is increasing quickly each year.

In the 1970's, the disposal of oil sands tailings sludge became of greater concern because of the growing public concern over the environment and the tougher environment legislation. Large amount of money and research efforts have been committed by governments, industries, universities and research institutions to try understanding the behavior of oil sands tailings sludge. A solution technically feasible and environmentally

safe is needed. Therefore, an important body of research results on tailings sludge is available.

It must be mentioned that tailings sludge is not only limited to the oil sands operation. It is very common to most mining industries. In general, **tailings sludge** can be defined as a heterogeneous dispersion of numerous substances, both organic and inorganic, with a wide particle size distribution ranging from colloidal to non-colloidal. Two of the major components of tailings sludges from various mining and extractive processes are water and clays. The water content of tailings sludge is high, typically higher than 60%, which is one of the main reasons that tailings sludges are difficult to be disposed of. However, different terminologies are used to describe the fluid-like tailings sludge in different mining industries. For example, tailings sludge from the extraction of alumina from bauxite is termed as red mud tailings. In phosphate mining operation in Florida, large amounts of tailings sludge called phosphatic clay are produced. Even different terms, such as clay slimes and sludge, are used to describe the same waste product: oil sands tailings sludge. For the sake of simplicity, the term tailings sludge designates in this work all tailings sludge from various mining and extractive processes that contain water and clays.

Most of the previous works have addressed the behavior and the treatment of the oil sands tailings sludge. The composition of the oil sands tailings sludge, however, is very complex. The studies made so far do not allow the prediction of its behavior when its composition, or more generally the procedure to extract bitumen from oil sands, is changed. It is felt that the oil sands industry need model systems where a number of important factors such as composition and the nature of flocculants can be varied easily and their effects can be assessed clearly. Ultimately, the best treatment methods of tailings sludge can be derived from such models.

Based on the literature review and the consultation with the "sludge fundamental consortium" administrated by the Alberta Oil Sands Technology and Research Authority (AOSTRA), a ternary tailings sludge model system, clay-Fe(III)-water, has been selected for the present study. Fe(III) is introduced as one of the ions present in the tailings sludge. There are other reasons for choosing Fe(III) as one component in the model system. First, ferric salts are widely used inorganic flocculants for the treatment of tailings sludge. Secondary, Fe(III) undergoes hydrolysis and the hydrolysis product is considered to have a major effect on clay-water systems. Because of the time and financial constraints, the clay being addressed in the present study is montmorillonite. However, similar studies can

be undertaken with other type of clays such as kaolinite. The approach adopted in this study can also be extended to the study of four component or five component model systems if it proves itself successful.

The present thesis includes a preliminary determination of the composition of the oil sands tailings sludge, then a study on the effects of the nature of electrolytes and pH on the settling and consolidation behavior of the model system. The "card-house" structure has long been suggested to explain the long-term stability of the oil sands tailings sludge with respect to consolidation, yet direct observation of the structure is rare, if at all. Therefore, the structure study of the oil sands tailings sludge and the model system will constitute a noteworthy part of this thesis. Natural dehydration (air drying) of the fluid-like tailing sludge to a certain water content below which the tailings sludge has enough shear stress to support the weight of vegetation or animals can also be considered a technique for the treatment of tailing sludge. A preliminary assessment of the effects on the drying behavior of the model system of the electrolyte concentration and suspension pH is also presented here. The results derived from the model system are compared with that of oil sands tailings sludge in most cases.

The thesis is organized as follow. The next chapter, chapter 2, is the literature review in which the most important information on the oil sands tailings sludge and the model system is gathered. It consists of five parts: (1) stability of colloidal dispersions; (2) oil sands and the Hot Water Process; (3) tailings sludge; (4) colloidal properties of clays, and (5) behavior of Fe(III) in aqueous medium. Next, chapter 3 briefly describes the experimental procedures and the various techniques used. The experimental results are reported in chapter 4. These results are discussed according to the well-established theories and other published experimental results in chapter 5. Conclusions pertaining to the behavior of the oil sands tailing sludge and the model system and comments on the usefulness of the model system, and suggestions for further work are given in the chapter 6 and chapter 7, respectively.

CHAPTER 2   LITERATURE REVIEW

The present review attempts to gather the most important information related to the behavior of oil sands tailing sludge and its components for the model being proposed: clays and Fe(III). It does not pretend to be an encyclopedia by itself, which would include all aspects of oil sands tailings sludge.

While some believe the presence of organics is critical, it is generally accepted that the stability of tailings sludge is due to the presence of clay particles with a colloidal size. The stability of colloidal dispersions has been extensively studied, and various theories are available to explain the interaction of dispersed particles, their aggregation or resistance to aggregation. These theories can usually be extended to explain the stability of tailings sludge, soils and suspensions to a certain extent. It is also known that various cations including Fe(III) are present in the oil sands tailings sludge and that most cations undergo hydrolysis. Hydrolysis reactions determine the identity, charge and stability of the hydrolysis products under a given set of conditions, which in turn control a number of important aspects of chemical behavior. For instance, they control the adsorption of the dissolved metal on the surfaces of mineral and soil particles, the tendency of the metal species to coagulate colloidal particles, and the solubility of the hydroxide or oxide of a metal (10). It is therefore necessary to address the hydrolysis of cations. Hydrolysis reactions of cations is very complex and varies from one cation to another.

The behavior of Fe(III) in aqueous medium is addressed specifically here, simply because Fe(III) is one of the three component in the present tailings sludge model. As mentioned in the introduction, Fe(III) is often considered to have a major effect on clay-water systems. In next sections, the literature reviews includes five parts: (1) stability of colloidal dispersions; (2) oil sands and the Hot Water Process; (3) tailings sludge; (4) colloidal properties of clays; and (5) behavior of Fe(III) in aqueous medium.

2.1 STABILITY OF COLLOIDAL DISPERSIONS

2.1.1. Terminologies

A Colloid can be defined as a dispersed solid matter which does not pass through dialysis membranes and yet does not settle readily under gravity. In practice, this corresponds to solid particles with a linear dimension between 10^{-7} cm (1 nm) and 10^{-4} cm (1 μm) (11).

However, this is an approximate size range, which depends largely on the nature of the solid. There are two types of colloidal systems: **lyophilic and lyophobic**. When the medium is water, these two systems are termed as **hydrophilic and hydrophobic**. Lyophilic systems are one-phase colloidal systems, for instance, liquid solutions with macromolecules dispersed uniformly in the medium. They are stable thermodynamically. Lyophobic systems are two-phase systems which are not stable thermodynamically but usually stable kinetically. For two-phase systems, the continuous phase (medium) or the dispersed phase (particles) can be a gas, a liquid or a solid. For the purpose of the present study, only the two-phase systems in which the dispersed phase is a solid and the continuous phase is an aqueous solution are addressed.

A **sol** can be defined as a stable dispersion of discrete colloidal solid particles in a liquid. A **gel** can be defined as an three-dimensional interconnected solid network expanded in a stable fashion through a liquid medium (12). One can transform a sol into a gel by passing through a gel point (discussed later). As mentioned previously, a colloidal system is only kinetically stable. Thermodynamically, the solid particles are bound to aggregate progressively, then settle under gravity when their mass becomes big enough. The laws explaining this kinetic stability are summarized in the next section.

Flocculation is usually defined as a process or technique whereby discrete particles with a colloidal size aggregate, which depends on the nature of liquids and the nature of electrolytes and their concentration. The terms **aggregation** and **coagulation** are also used to describe the so-called flocculation. The aggregates formed can be more or less open, and are called **flocs**. It must be pointed out that the flocculation may occur not only with colloidal particles, but also with bigger particle in the microscopic (micron) size up to visible particles in the millimetre size range (13) although particles larger than 1 micron will settle under gravity even if they do not build up flocs. **Sedimentation** refers to the settling of particles or flocs under the influence of gravity. It is well known that the settling kinetics of particles or flocs depends on the their size, shape and density. Since flocculation changes all these variables, very often the flocculation studies include sedimentation. **Colloid stability** is a widely used term that covers the interaction of dispersed colloidal particles, their aggregation and resistance to aggregation. Theories governing the stability of colloidal systems are used to explain the stability of tailings sludge to a certain extent.

2.1.2 DLVO theory

Most colloidal particles are charged, either positively or negatively. Particles usually obtain their charge in one of two ways: isomorphous substitution of cations with a different valence state as in case of clays and the preferential adsorption of certain specific ions (potential-determining ions) on the particle surface as in case of the adsorption of H^+ or OH^- by insoluble oxides or the adsorption of Ag^+ or I^- by the AgI lattice. To maintain the overall charge neutrality, an "atmospheric" distribution of counterions forms around the particle surface, which constitutes the so called **electric double layer**. The electric double layer consists of the particle charge and an equivalent amount of ionic charge which is accumulated in the solution near the particle surface (Fig.2.1). The electric double layer thickness is designated by κ^{-1}, where κ is related to the electrolyte conditions by:

$$\kappa = \left(\frac{4\pi e^2 N_A}{1000 \epsilon k_b T} \sum_i z_i^2 M_i \right)^{1/2}$$

(eq.2.1)

Where

z_i - the valence of ion i,

M_i - the molar concentration of ion i,

ϵ - the relative dielectric constant of the medium,

e - electron charge (1.60×10^{-19} C),

N_A - Avogadro's number,

k_b - Boltzmann's constant,

T - temperature.
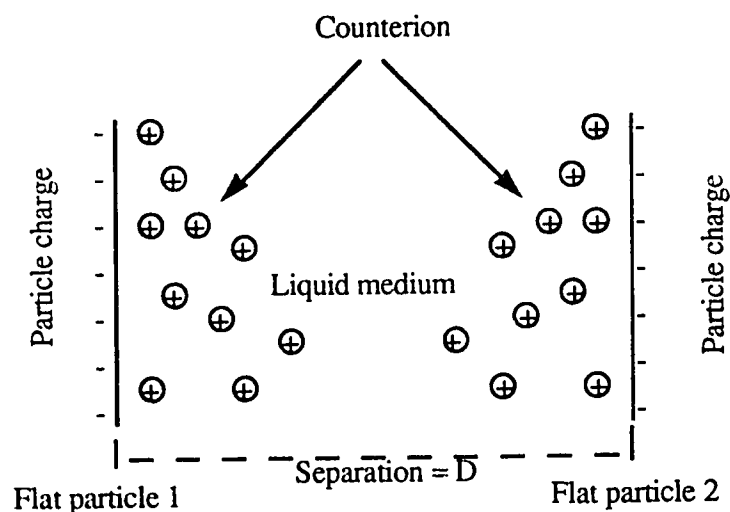
Fig.2.1 Electric double layer structure at a particle interface

A number of forces can operate between the dispersed particles. The most frequent interactions are (1) the dipole or **van der Waals interaction**, mostly attractive; (2) **electrostatic repulsion**; and (3) the **steric interaction** due to the adsorption of macromolecules on the surface of the particles. With magnetic colloidal particles, especially with Fe, **magnetic interactions** should also be considered (12,14-15).

It is clear that the stability of a colloidal dispersion depends on the combination of these interactions. When only the van der Waals attraction and the electrostatic repulsion are present, the systems are called "electrostatic". Such systems can be addressed with the DLVO theory (11). The DLVO theory (named after its inventors B. Derjaguin, L. D. Landau, E. J. W. Verwey, and J. Th. G. Overbeek) is the most successful stabilization theory. It can be best illustrated by a curve that shows the total potential interaction energy, Φ, of a pair of colloid particles as a function of their separation distance (Fig.2.2).
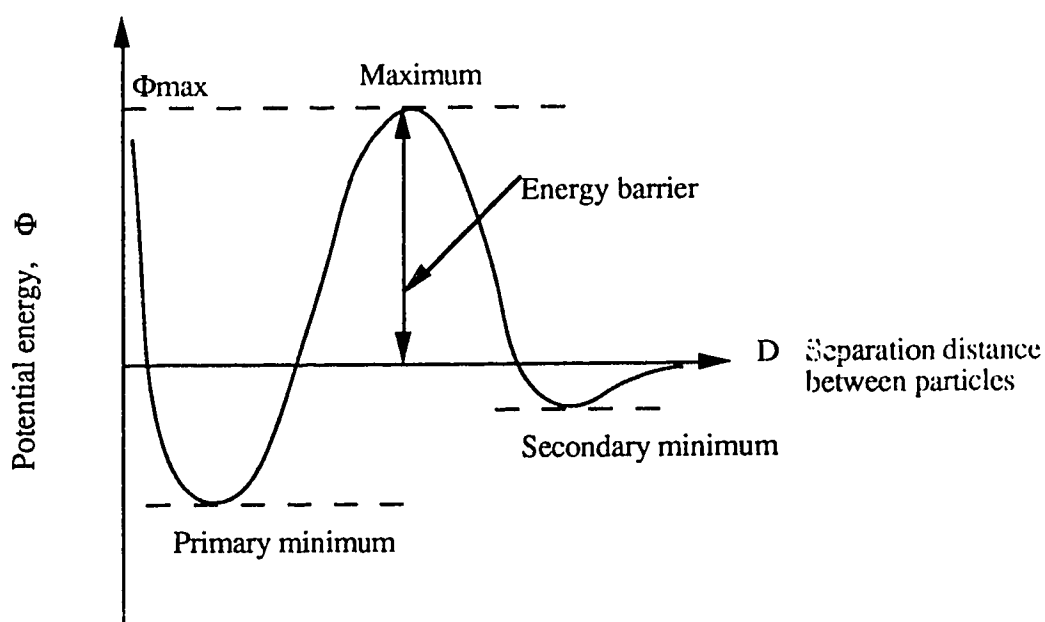
Fig.2.2 Qualitative sketch of the total potential interaction energy, Φ, as a function of separation distance, D, between two particles

The van der Waals attraction dominates at small and large separation. The electrostatic repulsion may or may not dominate at intermediate separation, depending on the electrolyte concentration and the valence of ions composing the electrolyte. For a stable colloid, this

curve usually shows a maximum and two minima. The height of the maximum above $\Phi=0$ is the so called "energy barrier". The shallower minimum is called the secondary minimum, it corresponds to hard contact between the particles. The deeper minimum is the primary minimum. When the thermal energy, k_bT (k_b - Boltzmann's constant and T-temperature), of particles undertaking the Brownian motion is larger than or comparable with the energy barrier, flocculation occurs statistically. And when a floc becomes sufficiently dense and big, sedimentation occurs. In practice, the magnitude of the energy barrier, Φmax, determines whether a colloid will be relatively stable or undergo flocculation.

Φ can be written: $\qquad \Phi = \Phi_R + \Phi_A \qquad\qquad\qquad\qquad$ (eq.2.2)

Φ_R is the repulsion potential energy due to the electrostatic interaction, and Φ_A is the attraction potential energy. For two blocks with a flat face, like clay particles, at separation D (see Fig.2.1):

$$\Phi_R = \frac{64n_0k_bT\gamma_0^2}{\kappa} \exp\left(\frac{-D}{\kappa^{-1}}\right) \qquad\qquad (eq.2.3)$$

or $\qquad\qquad \Phi_R = (const\ 1)n_0^{1/2}\exp[-(const2)n_0^{1/2}] \qquad$ (eq.2.4)

Where n_0 is the ion concentration (in the number of ions per cubic centimetre) far from the surface, κ^{-1} is the double layer thickness defined previously, and γ_0 is defined as follows:

$$\gamma_0 = \frac{Exp(ze\psi_0/2k_bT)-1}{Exp(ze\psi_0/2k_bT)+1} \qquad\qquad (eq.2.5)$$

Where ψ_0 is the potential at the interface, and z is the valence number of symmetrical z:z type electrolytes.

The relation between the number concentration and molar concentration is given by

$$n_i = \frac{M_iN_A}{1000} \qquad\qquad\qquad (eq.2.6)$$

Since the repulsion originates from the overlapping of the double layers, κ, and especially κ^{-1} are very important parameters. It can be seen that when the ion concentration or the valence of the ion increases, the double layer thickness decreases, and the repulsion between two particles or the height of the energy barrier decreases. It explains well that the addition of electrolytes which do not modify the electric potential of the particles (non-potential determining electrolytes) to colloidal dispersions often induces flocculation.

The attraction potential energy, Φ_A, is given by

$$\Phi_A = -\frac{A}{12\pi} D^{-2} \qquad (eq.2.7)$$

Where A is the effective Hamaker constant. It is determined by the dipolar nature of the dispersed and continuous phase.

Therefore, the total potential energy, Φ, will be

$$\Phi_{total} = \frac{64n_0 k_b T \gamma_0^2}{\kappa} \exp\left(\frac{-D}{\kappa^{-1}}\right) - \frac{A}{12\pi} D^{-2} \qquad (eq.2.8)$$

To induce flocculation, one can increase Φ_A, generally a secondary effect; or reduce Φ_R by modifying the concentration of electrolytes or the valence of ions. As mentioned earlier, one has the least control over the effective Hamaker constant. In practice, one can often obtain flocculation by changing the electrolyte concentration and the valence of ions. It must be pointed out that the treatment of colloidal stability is different for dilute and concentrated sols. For dilute sols, the electrostatic and van der Waals interactions can be considered as being bi-particle interactions. For concentrated dispersions, multi-particle interactions predominate, which is a more complex mathematical problem.

2.1.3 Critical flocculation concentration and Schulze-Hardy rule

The **critical flocculation concentration** or critical coagulation concentration (CFC, or C.C.C.) is defined as the electrolyte concentration below which fast flocculation does not occur. The flocculation state for a given colloidal system depends on the (1) standing time, (2) the uniformity or polydispersity of the dispersed phase, (3) the potential at the surface, (4) the value of A, and (5) the valence of the ions. In practice, the CFC is often determined by the flocculation series test in which items (1) to (4) remain constant so that the effect of the valence of added ions can be quantitatively measured. The effect of added electrolytes has been summarized in the Schulze-Hardy rule. The rule states that it is the valence of the ion of opposite charge (counterion) that has the principal effect on the stability of the colloid or CFC, and the effect of the valence or the type of the ions of the same charge is secondary. The Schulze-Hardy rule can be understood in term of the DLVO theory.

If we consider the approximation that rapid flocculation occurs when the height of the energy barrier is zero, then we have at the maximum

$$\Phi_{total} = 0 \qquad\qquad (eq.2.9)$$

and

$$\frac{d\Phi_{total}}{dD} = 0 \qquad\qquad (eq.2.10)$$

From eq.2.9 and eq.2.10, we can arrive at the following relationship between CFC and the valence of the ions

$$CFC \propto z^{-6} \qquad\qquad (eq.2.11)$$

According to eq.2.11, the CFC value is inversely proportional to the sixth power of the valence of all ions in solution, which is consistent with the Schulze-Hardy rule. Since the repulsion is mainly determined by the thickness of the double layer (eq.2.3), and the counterion plays the predominant role in the double layer (11), therefore, the valence of the counterion has a major effect on the interactions between particles. However, it must be pointed out the valence and the concentration of both ions of the same charge and counterions modify the double layer thickness (see eq.2.1). The ions of the same charge may also change the surface potential of particles, which in turn modifies the energy barrier.

2.1.4 Zeta potential

It is well known that when an electric field is applied to a colloidal dispersion, the particles move towards one of the electrodes. Such a phenomenon is called electrophoresis. When the particles move, part of the counterions will move with them. This leads to the definition of zeta potential (ζ). The zeta potential is defined as the electrical potential in the double layer at the shear plane between the liquid electrostatically attached to the particle and the free liquid. The location of this shear surface is difficult to determine. However, the zeta potential magnitude is usually considered as a measure of the repulsion between particles. The zeta potential sign is the same as the charge of the particle. The zeta potential can be calculated from the electrophoretic mobility, μ, of colloidal particles, itself an experimental quantity. When $\kappa R < 0.1$ (R, radius of the particle), the following Hückel equation can be used:

$$\mu = \frac{\varepsilon\zeta}{6\pi\eta} \qquad\qquad (eq.2.12)$$

When $\kappa R > 100$, one uses the Helmholtz-Smoluchowski equation:

$$\mu = \frac{\varepsilon \zeta}{4\pi\eta}$$

(eq.2.13)

Where η is the viscosity of the dispersion.

In general, with colloidal particles charged negatively, such as clay particles, zeta potential values above -14 millivolts (mV) indicate the beginning of flocculation. Values below -30 mv represent a sufficient mutual repulsion to result in stability. Values between -14 mV to -30 mV usually represent the transition. To assure a reasonable stability, the zeta potential should range between -45 mV to -70 mV (16). In details, the zeta potential changes with the electrolyte concentration and is also pH dependent.

2.1.5 Steric and electrosteric interactions

The steric interactions come from the adsorption of polymer molecules onto the particles. A theory has been initially developed by Flory and Huggins for the dissolution of a polymer (subscript 2) in a solvent (subscript 1). When one end of the polymer chain is adsorbed onto the particles, the partial molar free energy of dilution of the solvent is

$$\Delta G_1 = -R_g T \left(\frac{1}{2} - x_1\right)\Phi_2^2$$

(eq.2.14)

Where Rg is the gas constant, Φ_1 (=$1-\Phi_2$), and Φ_2 are the volume fraction of each component, and x_1 is a dimensionless parameter related to another dimensionless parameter ψ_1 by:

$$x_1 = \frac{1}{2} - \psi_1\left(1 - \frac{\theta}{T}\right)$$

(eq.2.15)

Where θ is a parameter with the dimension of a temperature, which characterizes the couple solvent-polymer solute. For $T=\theta$, there is no free energy of interaction between the polymer segments and the solvent. A high value of x_1, obtained for instance for $\theta > T$, corresponds to a high increase in the free energy, and the solvent is qualified as a "bad" solvent. On contrast, a low value of x_1, obtained for $T > \theta$ indicates a "good" solvent. In the last case, polymer interpenetration is avoided, which results in a repulsion effect between particles (17).

Polymers can comprise positively and/or negatively charged sites. These charged polymers are called polyelectrolytes. For polymers which are not charged, the interaction is usually steric. For polyelectrolytes, the interactions between particles include both electrostatic and steric. Such interactions are called electrosteric interaction. The steric and electrosteric interactions, a complicated topic, will not be addressed in this thesis.

2.1.6 Flocculation and Stokes' law

Types of flocculants

Inorganic salts and polyelectrolytes are the most widely used flocculants. Polyelectrolytes often have a high molecular weight in the range of 1 to 10 million. They are water-soluble or water-dispersible, and can be classified into three types according to their net charge: anionic, cationic and nonionic polyelectrolytes (18). Polymers which contain an excess of organic anions are anionic polyelectrolytes. Polymers in aqueous solution with an excess of organic cations are cationic. Polymers where the positive and negative sites balance each other are called nonionic polyelectrolytes. Polyelectrolytes are more efficient than electrolytes in term of stabilization or flocculating power. Very often, the terms flocculation and coagulation are used interchangeably. However, some prefer to use flocculation for aggregation due to polyelectrolytes and **coagulation** for aggregation due to electrolytes. In this thesis, the term flocculation only is used.

Mechanisms of flocculation

Flocculation of colloidal dispersions by inorganic salts can be well explained by the DLVO theory. That is, the addition of non-potential determining electrolytes depresses the thickness of the double layer around the charged particles, thereby reducing the energy barrier to be overcome by the particles undertaking the Brownian motion.

With non-charged polymers, flocculation occurs by a steric mechanism where the adsorbed polymers tend to phase-separate from the liquid solvent. With polyelectrolytes, flocculation occurs as a result of two mechanisms: by depression of the double layer, and by steric polymer/water separation. A number of more complex phenomena occur with polyelectrolytes (19):

(1) Bridging. When the length of a polymer chain extended from the particle surface into the solution is greater than the distance over which the interparticle repulsion operates, the

polymer can adsorb onto another particle, thereby bridging the two particles. This is the process by which nonionic and like-charged polymers flocculate the charged particles.

(2) <u>Charge neutralization</u>. the adsorption of the oppositely-charged polymers reduces the particle surface charge density, thereby decreasing the repulsion or the energy barrier.

(3) <u>Charge patch neutralization</u>. If the charge density of a polymer in its adsorbed state is higher than that of the surface, then patches of positive and negative charge will appear on the particle, thus allowing the possibility of flocculation due to the mutual attraction of oppositely-charged regions on different particles.

Flocculation kinetics

The flocculation of particles in dispersions depends on collisions between particles caused by their relative motion. This relative motion may arise from the Brownian motion that is natural thermal agitation, mechanical agitation (like ultrasonic mixing) and under external forces such as gravity. The rate of flocculation is determined by the collision frequency induced by the relative motion. If the interparticle repulsion or the energy barrier is small enough, then every collision leads rapidly to flocculation. If a significant repulsion or energy barrier exists, then the collision is slowed down as well as flocculation. Practically, it can even be stopped on a human life time scale. Therefore, the electrolyte concentration, the mode of agitation and the temperature have a major effect on the rate of flocculation. For a given system, agitation either natural or forced promotes the flocculation.

Stokes' Law and diffusion effect

The settling velocity, υ, of a spherical particle in a liquid can be addressed by Stokes' Law

$$\upsilon = \frac{2R^2(\rho_2 - \rho_1)g}{9\eta}$$ (eq.2.16)

Where

ρ_2 - density of the particle,

ρ_1 - density of the liquid,

R - radius of the particle,

g - acceleration due to gravity,

η - viscosity of the liquid.

For non-spherical particles and flocs, R can be replaced with an equivalent spherical radius. When particles flocculate, they build up flocs. The size of these flocs is larger than that of the individual particles. Consequently, the settling rate increases proportionally to the

square of floc radius although the density of flocs is lower because of the incorporation of water. This is consistent with the observed fast settling of flocculated particles.

It must be pointed out that when the particle or floc size is smaller than a certain value, the diffusion effect which opposes to sedimentation becomes significant. According to Fick's Law of steady-state diffusion, the flux (J_x) of the diffusing species in the x-direction due to the concentration gradient (dc/dx) is given by:

$$J_x = -D\frac{dc}{dx}$$
(eq.2.17)

Where D is the Brownian diffusion coefficient.

For a constant temperature and viscosity, the constant D is proportional to 1/R, where R is the radius of the particle diffusing. Comparing eq.2.16 for sedimentation with eq.2.17 for diffusion, it is clear that the settling rate, being a square law, decreases very rapidly while the latter increases rapidly as R decreases. Obviously, there exists a limiting size for R where diffusion is sufficiently rapid to prevent any significant degree of sedimentation. The limiting size for R is around 0.2 μm for a dense particle (20). Most of the clay particles are larger than 0.2 μm, the suspended clay particles usually settle quicker than those stable sols composed of particles less than 0.2 μm. This is one main reason that the term clay suspensions rather than clay dispersions is often used.

2.1.7 Gelation

Gelation is a process whereby a sol or a solution transforms into a gel. It consists in establishing links between the sol particles, or the solution molecules, so as to form a three-dimensional solid network (12).

Gelation can occur from polymers in solution, or from colloidal particles. In the first case, one speaks of polymeric gelation. It designates the transformation of a liquid into a solid by chemical reactions. Monomers with a functionality z>2 can yield an indefinitely large polymer structure which is limited by the size of the container through the condensation reaction. The first time a polymer of infinite size is formed is defined as the **gel point**. At the gel point, the viscous liquid transforms suddenly into a materials with elastic properties. In the liquid state, one can measure a viscosity which diverges towards an infinite value

when nearing the gel point. In the solid state, one can measure an elastic modulus starting from zero at the gel point (Fig.2.3).

For colloidal dispersions, gelation designates the successive addition of the colloidal particles to an open floc which slowly builds up an infinite network. Very often, gelation of colloidal sols can occur with the help of non-potential determining electrolytes. It is known that a critical gelation concentration (Cg) exists. When the non-potential determining electrolyte concentration C< C_g, the colloidal dispersion is stable. For C_g<C<CFC (rapid flocculation concentration defined before), the colloidal dispersion gels slowly. In this way, gelation can be considered as a special case of flocculation.
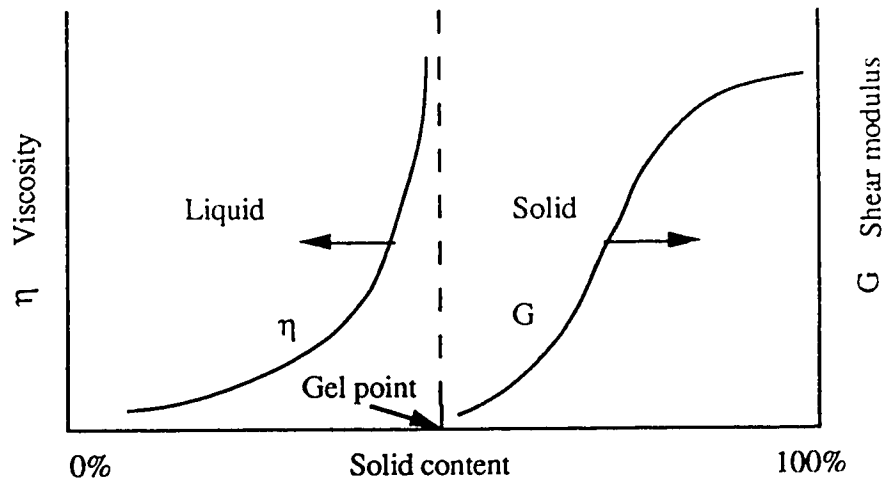
Fig.2.3　Schematic illustration of the sol-gel transition

In detail, the increasing concentration of non-potential determining electrolytes has the effect of decreasing the energy barrier to be overcome by particles undertaking the Brownian motion. If C< C_g, the energy barrier to be overcome is too high. Linking is unlikely statistically, the sol is kinetically stable. For C_g<C<CFC, linking between a pair of particles has a small but significant probability of occurring; therefore, flocculation occurs slowly . Since a third particle has a smaller energy barrier to overcome for a linear linking than for a lateral linking, a fibrous structure begins to form, eventually leading to the formation of a gel. If C>CFC, the energy barrier for a third particle to overcome so as to link with a pair of particles is low laterally as well as linearly, therefore flocculation occurs in dense aggregates (12). In terms of the DLVO theory, the conditions to obtain a gel are realized when the thickness of the double layer is comparable with the diameter of the colloidal spherical particles. In this case, the electrostatic repulsion is stronger for the lateral

approach than for the linear approach, by a coefficient , while the attractive van der Waals attraction remains the same (12).

Chander and Hogg (21) explained the gelation in terms of the rate of adhesion of particles (k_a) and the rate of sedimentation of flocs (k_s). When the rate of adhesion of particles is extremely rapid, a network of particles develops to form a gel structure. Then the gel structure may undergo a limited and slow self-consolidation. When the rate of adhesion of particles is similar to the rate of sedimentation of flocs, floc formation and floc sedimentation may occur simultaneously. Thus for gel formation, $k_a >> k_s$, and for sedimentation, $k_a \leq k_s$.

2.2 OIL SANDS AND THE HOT WATER PROCESS

Since the oil sands tailings sludge is a "by-product" of the Hot Water Process, it seems relevant to briefly describe the process and oil sands themselves.

Athabasca oil sands is a mixture of bitumen, mineral, and water. The bitumen content by weight ranges from 0 to 18%, averaging 12%. The water content is 3-6%. The mineral content, predominantly quartz, is 84-86%. The structure of an oil sand particle is often described as a sand grain surrounded by a thin layer of water envelope containing fine clay particles which, in turn, is surrounded by a bitumen film (Fig. 2.4). Whether this type of structure is true of oil sands is open to question. For a typical sand grain with a size of 100 μm diameter, the water film thickness is considered to be of the order of 2 μm, and the bitumen film thickness is 5-6 μm. The existence of any substantial amount of fine clay minerals suspended in the water layer surrounding sand grains is speculative (3). As a matter of fact, the clay minerals constitute less than 1% in oil sands (7). A substantial amount of clays present in the oil sands feed comes from the formation in the form of thin and discontinuous beds or bands varying from 1 inch to 6 feet (8). Both the amount and the nature of clays have an important influence on the performance of the Hot Water Process and the behavior of oil sands tailings sludge.

The commercial oil sands development consists of mining, extraction and upgrading. Generally speaking, surface mining includes the operation of overburden removal, and mining of oil sands with bucketwheel excavators. The extraction of bitumen from oil sands, currently, is realized with the help of the hot water in a primary step (the Hot Water

Process), and followed by centrifugation. Then, the bitumen is upgraded to synthetic crude oil before delivering to the market (Fig.2.5).
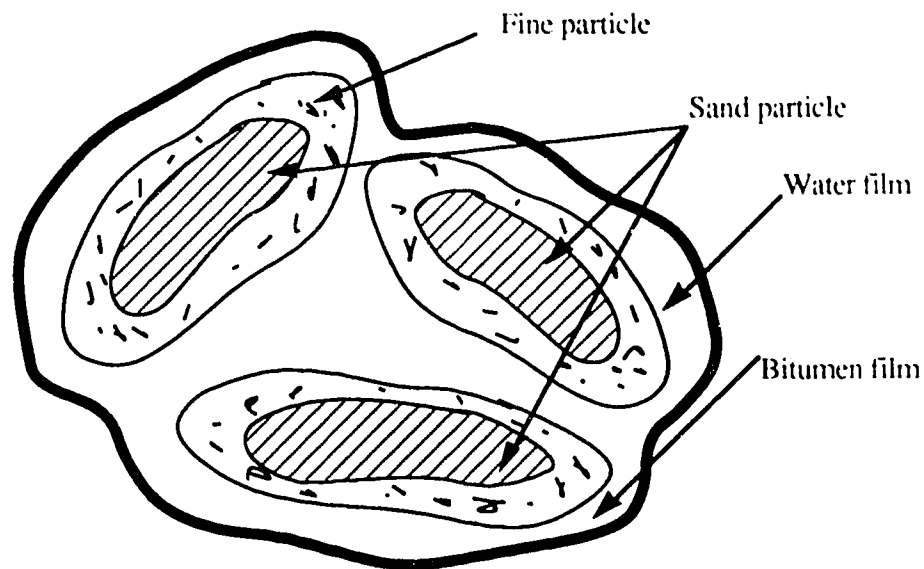
Fig. 2.4 Structure of oil sands particles
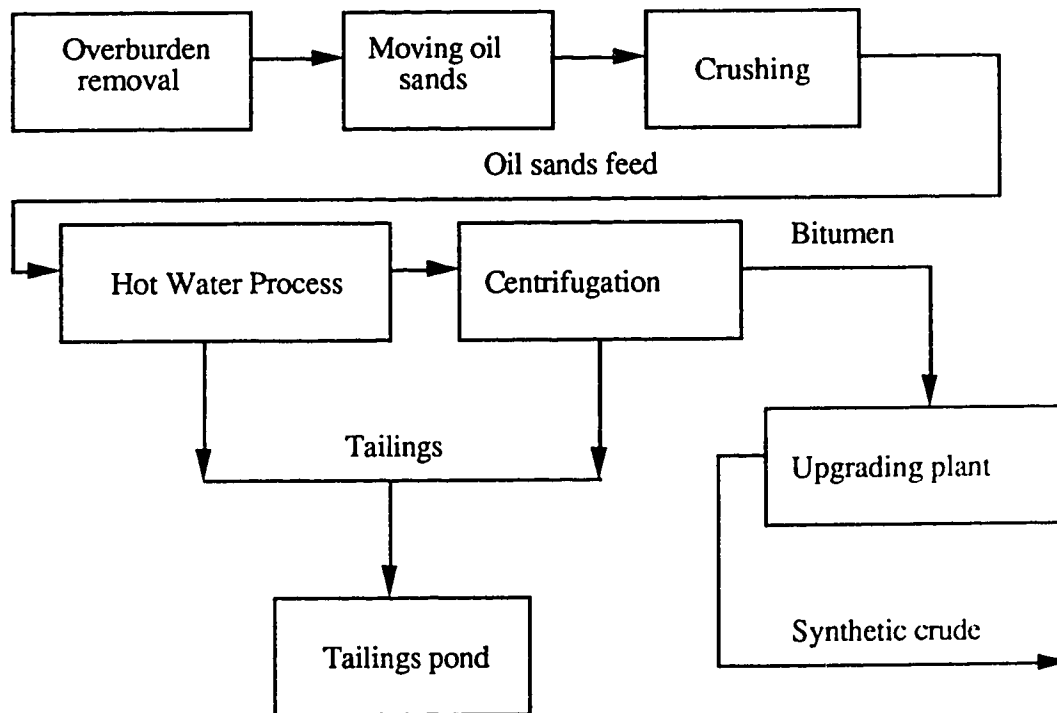
Fig.2.5 Flow-sheet of oil sands developing system

The Hot Water Process can be divided into three major steps: conditioning, separation and scavenging (Fig.2.6).

In the first step, conditioning, oil sands are mixed with water, and heated with open steam to form a slurry of 60 to 70% solids. Sodium hydroxide or other reagents are added as required to maintain the pH in the range 8.0-8.5. During this process, bitumen is stripped from the individual sand grains and aerated. At the same time, the clays in oil sands are well dispersed, which causes the tailings sludge settle to very slowly.

In the separation step, the conditioned oil sand slurry is screened to reject rocks and unconditioned lumps of oil sands and clays. The reject material, called "screen oversize," is discarded as a separate stream. The screened slurry is further diluted with water to promote a double settling process. Globules of aerated bitumen, essentially mineral-free, settle upward (float) to form the froth on the surface of the separation cell. Meanwhile, mineral particles, particularly sand, settle down and are removed from the bottom of the cell as tailings. The medium through which these two settling processes take place is called middlings. Middlings primarily consists of water, suspended fine minerals and bitumen particles.

The viscosity of middlings is a very important parameter. When the viscosity exceeds a certain value, the settling processes actually stop. As the amount of water increases, the middlings viscosity decreases. The ratio of the amount of clay to the amount of water in middlings also influences the middlings viscosity. As the feed clay content increases, a larger amount of water must be used in the process to control the middlings viscosity.

The third step of the hot water process is scavenging. This step is optional. Depending on the net process water input, it may or may not be necessary to withdraw a dragstream of middlings to maintain a separation cell material balance. If necessary, this stream of middlings can be scavenged to recover the bitumen within it.

The final extraction step is the froth cleanup. It is accomplished by centrifugation. Froth from the primary extraction is diluted with naphtha. Then, it goes through a two-stage centrifugation. This process yields an oil product of essentially pure, diluted bitumen. Water and minerals removed from the froth constitute an additional tailings stream which must be disposed of.
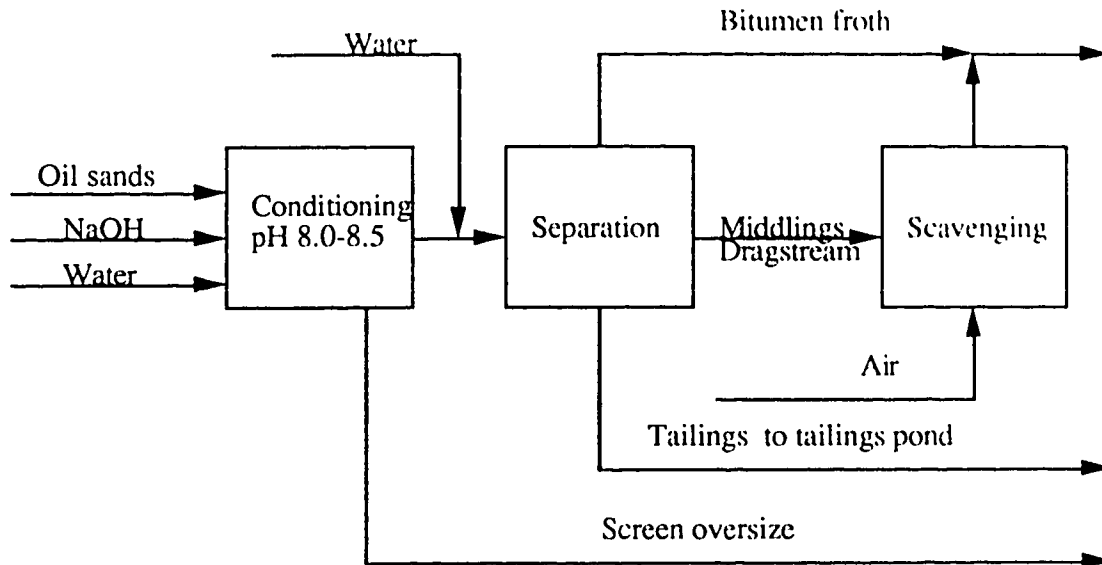
Fig.2.6   Hot Water Process

2.3 TAILINGS SLUDGE

A number of previous reviews (3-4, 8, 22-24) have dealt with the different aspects of the tailings sludge. A relatively comprehensive review of the properties of tailings sludge and its treatment was documented by Kasperski (25). In this part, the most important information on tailings sludge, particularly, the tailings sludge originated from Athabasca oil sands, is gathered. This allows me to introduce in a more appropriate fashion the objectives of the present study .

2.3.1 Origin and composition of oil sands tailings sludge

Origin

All tailings from the primary extraction and final extraction are sent to the tailings pond where the coarse sand and a portion of clay materials deposit on beaches and the remaining runs off towards the center. The sand fraction of the tailings is also used as the construction material for the dykes surrounding the tailings pond.

In the tailings pond, larger particles settle rapidly while those clay particles which are well dispersed in the Hot Water Process settle very slowly. Two layers can be identified according to the solid content by weight: the supernatant layer (top 5 to 10 feet of the tailings pond at Suncor), and the sludge layer. In general, the solid content in the supernatant layer is below 5% while it is higher than 5% in the sludge layer. It increases with the depth and settling time up to 35% (higher solid contents have been recorded, but they can be regarded as exceptional). A discontinuity exists in solid content in the sludge layer. A few feet below the supernatant layer, the solid content increases to 10-15% (3).

Tailings sludge usually refers to the sludge layer. Since the requirement of the solid content in the recycle water is less than 2%, only a portion of the water can be recycled. The sludge layer consolidates very slowly over several years to a solid content of 30-35% where it stabilizes (3-7) However, even at such solid content, the sludge layer is still fluid-like, which is a huge inconvenience for final disposal. Given the huge volume of oil sands processed every day, this means there is a tremendous accumulation of tailings sludge. For example, the volume of the tailings ponds at Syncrude Canada Ltd increases at a rate of about $3*10^6$ m^3 per month (4).

In summary, the origin of tailings sludge can be attributed to the following factors:
- Oil sands and its surrounding formation contain clays
- Large amount of water is required to control the viscosity of the middlings
- In the Hot Water Process, clays (in the form of lumps) end up being well dispersed
- Clay particles in aqueous solution settle very slowly
- Sludge layer consolidates very slowly

Composition

The composition of tailings sludge is complex. It changes with the time, the source of tailing sludge (fresh tailings or old pond tailings) and the location of sampling. In general, the major component of tailings sludge (before sending to the tailings pond) are water, sand (>44μm), silt (2-44μm), clay (2μm), residual bitumen and unrecovered naphtha. Tailings sludge also contains a small amount of dissolved organics, various cations and anions, and trace metals. **Table 2.1**, and **Table 2.2** show the solid (mineral) content increase with the depth of the tailings pond, and almost all the sand fraction is retained in dykes and beaches. **Table 2.1** also indicates the clay content remains rather stable in the sludge layer.

The amount and nature of clays in the tailings sludge varies over a wide range as reflected in many reports. Camp (3) indicated the major clay minerals are kaolinite (51.7-75.5%), illite (6.6-15%), and montmorillonite (8-9%), mixed with quartz (7-8%) while Kessick (22) reported kaolinite (22-76%), illite (7-10%) and montmorillonite (1-8%). Other minerals less than 2μm in size include chlorite, calcite, dolomite, siderite, feldspar and ankerite as well as zircon, ilmenite, leucoxene and rutile (3, 22).

Table 2.1 Composition of Tailings Sludge at Suncor (Data taken from(3))

	Sand tailings from dykes	Sludge layer at different depths 6 m	12 m	18 m
Composition, wt. %				
Bitumen	0.2	3.3	3.9	4.5
Water	22.8	74.7	70.1	65.5
Mineral (solid content)	77.0	22.0	26.0	30.0
Particle size, wt. % Mineral				
Sand	95.3	≈0	≈0	≈0
Silt	3.2	59	62	58.5
Clay	1.5	41	38	41.5
Clay/Water ratio	0.05	0.12	0.14	0.19

Table 2.2. Solid Content and pH of Tailings sludge at Syncrude Canada Ltd. (Data taken from (4))

Variable	Pond depth 0-5 m	6-9 m	10-15 m	>15 m
Total solids %	0.72±0.13	1.29±0.68	3.16±1.26	13.49±9.43
Suspended solids %	0.58±0.13	1.18±0.63	2.97±1.5	12.44±8.7
pH	8.1±0.2	8.2±0.2	8.2±0.2	8.3±0.3

Also various cations and anions are present in tailings sludge. The major cations are Na^+, K^+, Ca^{2+}, Mg^{2+} with respective concentration of 300, 20, 6 and 5 mg/L. Al^{3+}, Fe^{2+}, Fe^{3+} and NH^{4+} are also present (4, 26). The total iron concentration is less than 2 mg/L (27). The major anions are Cl^-, SO_4^{2-}, and HCO_3^- with respective concentration (mg/L) 80, 180, 500. One also finds CO_3^{2-}, $H_2PO_4^-$ and HPO_4^{2-} (4, 26).

The organic composition of tailings sludge is complex. Various dissolved and clay-associated organics, besides residual bitumen have been detected. The major organic

components are organic acids and polyphenolic aromatic compounds (4, 25). Hepler et al. (26) gave a list of organic compounds in bitumen and tailings sludge.

Untreated tailings sludge are acutely toxic, with LC_{50} (LC stands for lethal concentration) of less than 10% for fish (rainbow trout and fathead minnows) and about 20% for the crustacean Daphnia magna by standard 96-hour bioassay (4). The dilution value at which 50% of the fish tested survives is defined as the LC_{50}. That means less than 10% sludge water from the tailings pond mixed with fresh water will kill 50% of the fish tested under the experimental condition specified by the 96-hour bioassay.

The density of the oil sands tailings varies over a wide range depending on the sampling locations. The bulk density of materials in the dyke and beach is 1570-1930 kg/m^3. The bulk density of the tailings sludge in tailings ponds ranges from 960 kg/m^3 to 1300 kg/m^3 (7, 9). The particle size of the tailings sludge shows a wide distribution. About 12% of the particles are less than 1 micron (7, 9). Clay particles in the oil sands tailings sludge have a zeta potential of about -60 mV (7). The low density, the high zeta potential and the plate-like shape of fine clay particles explain the slow settling behavior of the oil sands tailings sludge.

The behavior of oil sands tailings sludge is complex, depending on many factors: composition, pH, types and amount of electrolytes or flocculants, temperature etc. In the next sections, focus will be on the behavior of tailings sludge with very different compositions, then on the particle aggregation modes in oil sands tailings sludge.

2.3.2 Behavior of tailings sludge at large

While tailings sludge is a common problem for most mining industries, the environment hazards these tailings sludge pose and the extent of difficulty of their disposal are different from one operation to another. Currently, besides oil sands, there are four major industries that require large quantities of water in their mining or extraction processes and produce large amounts of tailings sludge which contains clays. Theses industries are phosphate pebble rock mining (Florida), china clay mining (U.K.), and diamond mining (South Africa), and bauxite refining (worldwide). Although tailings sludge produced from these industries all contain clays, their behavior, especially consolidation, are different, depending on the nature of clays. A comparison of the compositions of these tailings

sludges and their behaviors certainly can give an indication of how the composition affects the behavior of tailings sludge. Much of this section is based on a review by Kessick (22).

Tailings sludge from phosphate mining

The solid fraction composition of tailings sludge produced from phosphate mining in Florida varies over a wide range. In general, it consists of: (1) clay minerals, principally montmorillonite, attapulgite, kaolinite and illite; (2) phosphate minerals, mostly fine-grained carbonate-fluorapatite, with lesser amounts of aluminum phosphates, such as wavellite; (3) quartz, present as sand or silt-sized particles; (4) other minerals, such as feldspar, heavy minerals, and hydrated iron oxides, in minor amounts.

Attapulgite and kaolinite count for 44-69% of the total solids while montmorillonite ranges from 9% to 36% (28). Unlike oil sands tailings sludge, the phosphate tailings sludge contains no significant amount of organic materials, and its pH is slightly lower. However, its consolidation behavior is very close to that of oil sands tailings sludge. This indicates that the presence of organic component may not be important as far as the long term stability of tailings sludge to consolidation is concerned. Phosphate mining in Wyoming, Montana and Idaho, and in Morocco does not produce tailings sludge because the phosphate rock is hard rock that does not contain clays (29). It shows again that the presence of clays is the origin of tailings sludge.

The phosphate tailings sludge, as produced, contains 3-5% solids. In less than one year, it settles to about 15%, and reaches close to 20% after 10 years. The amount of attapulgite present has a major effect on both the early settling rate and the consolidation rate. The early settling rate decreases with an increase in attapulgite concentration (30). Attapulgite is fibrous and swells. It is believed to contribute to a "haystack" structure in the same way as montmorillonite may contribute a "card-house" structure, and thereby hindering the consolidation process. Hoppe (30) reported that phosphatic tailings sludge with solid content above 40% would eliminate the need for dams and allow the lands for impounding tailings sludge to be reclaimed and used productively.

Tailings sludge from china clay mining

Large scale hydraulic mining of china clay in England produces a large amount of micaceous tailings sludge. The mineralogy of this tailings sludge is variable. However, it is mainly composed of 50% coarse kaolinite, with the remainder being muscovite and lithionite with small quantities of biotite mica, quartz, tourmaline, potash and sodium

feldspar. The solid content of the tailings sludge in the tailings ponds ranges from 44% to 65%, which is much higher than those of the oil sands sludge and phosphatic tailings sludge. Unfortunately, information regarding the consolidation behavior is not available. That is, the question of whether the micaceous tailings sludge remains fluid-like at such high solid content remains unanswered. The micaceous tailings sludge contains no montmorillonite or swelling type of clays.

Tailings sludge from diamond recovery

In South Africa, diamonds are recovered from a type of rock known as "kimberlite." The rock is crushed in water, and the diamonds are separated from the slurry, which is in turn thickened and pumped into a tailings disposal area. The tailings sludge eventually settles to a solid content of 20%, and then the dewatering process almost stops. The component that contributes to the long-term stability to consolidation has been identified as saponite, a type of swelling clay similar to montmorillonite. The major components were identified as 50-60% saponite, 10-20% talc, and minor amounts of chlorite, illite and quartz (31).

Tailings sludge from bauxite refining

Almost all the alumina produced commercially in the world is extracted from bauxite. In the process of extracting alumina from bauxite, a tailings sludge often called red mud is produced. Red mud can be characterized as a highly alkaline slurry of very fine particles of unreacted silica, iron oxides and titanium oxides along with some other minor components (32). For every ton of alumina produced, about one ton of red mud is produced. The solid content of red mud ranges from 15% to 30%. Vogt and Stein (33) found that red mud with solid content reaching 50% could support the men and equipment and shows little tendency to flow.

In addition to the above-mentioned tailings sludges, slow settling tailings sludge are produced by sand washing operations of various Australian mines. The tailings sludge, as produced, contains 1-5% solids, and eventually settles to 40% solids in tailings ponds (34). The major component of the solids in this tailings sludge is kaolinite. There are trace amounts of quartz, mica, gibbsite and pyrite. Organic matter is also detected at some sites.

Summary

Oil sands tailings sludge and the above-mentioned tailings sludge have one thing in common: they all contain clays. However, the nature of the clays and the amount of each

type of clay are different from one type of tailings sludge to another; so are their settling and consolidation behaviors.

In general, the presence of a significant amount of montmorillonite, or other swelling clays such as saponite or attapulgite contributes to lower settling rate and final solid content while the opposite holds true for kaolinite. At GCOS (now Suncor), better compaction of tailings sludge was reported when kaolinite content increased (3). This is mainly because the size, the shape, and swelling behavior for each type of clays are different. For example, the size of kaolinite, both in thickness and width, are larger than montmorillonite despite that their shapes are both plate-like. Larger particles contribute to more compact sediments and higher solid content.

The structures of sediments formed by different clays are different, depending on the packing pattern of individual particle and aggregates. By comparing tailings sludges containing organic matter with those containing no organic matter (except clay-associated organics), it can be shown that the presence of organic matter in tailings sludges does not have a major effect on the consolidation process.

2.3.3 Structure of oil sands tailings sludge

A number of studies on the structure of oil sands tailings sludge have been done by previous workers. However, much less has been done on the direct observation of the structure of oil sands tailings sludge because of difficulties in preparing proper samples for observation under the scanning electron microscope (SEM) without destroying or modifying the original structure. It has been suggested that the long term stability of oil sand tailings sludge is caused by the formation of a "card-house" structure in the fluid-like tailings sludge. The water trapped in the porous structure that can be forced out by settling and the weight of overlaid tailings sludge is limited, therefore leading to the observed high water content.

Although the "card-house" structure model considered for clays and addressed in **Section 2.4** could well explain the long-term stability of oil sands tailings sludge, some questions remain to be answered: (1) what is the morphology of the clay particles in oil sands tailings sludge at the end of the Hot Water Process; (2) what are the actual building blocks responsible for the aggregate structure of tailings sludge; and (3) what is the packing pattern of these building blocks.

Crickmore et al. (35) considered that the building blocks of oil sands tailings sludge are aggregates of fine particles. In the consolidation process, these aggregates rearrange themselves from a fluffy structure to a denser one. This process can be modelled by a fractal dimension, which increases with time. Unfortunately, as mentioned before, direct observation of the structure of oil sands tailings sludge is scarce. A recent study by Mikula et al. (36) has made good progress. They used the freeze fracture technique to prepare samples for direct observation under a scanning electron microscope (SEM). Their results indicated the existence of a "card-house" structure, and they attributed the stability of oil sands tailings sludge to the longer range ordering of the "card-house" building blocks. However a number of artifacts may explain the results: like the formation of ice crystals during the freezing process or the displacement of particles during icing. The real structure of oil sands tailings sludge remains unknown.

2.3.4 Treatment of tailings sludge with flocculants

The ideal disposal technique with respect to oil sands tailings sludge would be one that causes both the rapid settling and the quick consolidation of oil sands tailing sludge so that a maximum amount of water can be recycled and a compact sediment that is easy to be disposed of can form. The rapid settling of tailings sludge of low solid content can be achieved usually by flocculation. The focus of flocculation studies regarding oil sands tailings sludge disposal is to select a flocculant that will cause the rapid settling and consolidation of the oil sands tailings sludge at an acceptable cost. However, such an objective is very difficult to achieve. First, the addition of flocculants very often increases the sediment volume considerably in comparison with the sediment without flocculants. Secondly, flocculants are generally not effective for high solid content (above 20%) tailing sludge. Thirdly, the cost of flocculants, especially organic flocculants, is high.

However, it is well known that the addition of flocculants to the oil sands tailings sludge of low solid content leads to flocculation of the suspended particles and increases the rate of sedimentation. It can also increase the amount of water available in the tailings pond for recycling. Both inorganic flocculants (electrolytes) and organic flocculants have been tested and proposed to treat the oil sands tailings sludge. A number of techniques or methods using flocculants to treat oil sands tailings sludge have been patented (37-41). Several hundred commercial flocculants had been evaluated in attempts to select a flocculant that would cause both the rapid settling and quick dewatering of phosphatic tailings sludge. It was found that high-molecular-weight organic polyacrylamide polymers were the most

efficient. Anionic polymers proved superior to nonionic or cationic polymers, and combinations of polymers were often more successful than single ones (42). However, none of flocculants have been used on a commercial scale because of the above-mentioned reasons.

Since the particles in the oil sands tailings sludge are charged negatively, various inorganic salts containing Na^+, Ca^{2+}, Mg^{2+}, Fe^{3+} and Al^{3+} have been proposed as flocculants for treating tailings sludge. Previous studies have often focused on the effect of electrolyte concentration, ion valence and pH of the suspensions on the stability and settling rate. Schulz and Morrison (43) found 50 mg/L of Al^{3+} or Fe^{3+} is as effective as 150 mg/L of Ca^{2+} or Mg^{2+} in terms of flocculating power. Hocking and Lee (44) found that HCl acid is more effective than $CaCO_3$ or $Al_2(SO_4)_3$. Hall and Tollefson (45) found that Ca^{2+} was about seven times as effective as Al^{3+} in terms of inducing flocculation. Schutte (40) showed that when the pH of oil sands tailings sludge was below 5.5-6.5, flocculation occurred. Stastny (46) found that the injection of CO_2 into tailings sludge induced the flocculation by reducing the pH of the tailings sludge. Hepp and Camp (41) indicated that a pH below 7.5 or above 9 would flocculate the suspended clay particles. Much less work has been done on the effect on the sediment volume or solid content of the electrolyte concentration, the valence of ions and pH.

2.4 COLLOIDAL PROPERTIES OF CLAYS

Clays are one of the major components of oil sands tailings sludge. They are also one of the components of the present clay-Fe(III)-water model systems. It is generally accepted that the slow settling and long term stability with respect to consolidation of the oil sands tailings sludge is due to the presence of clays with a colloidal size. Therefore, an examination of the physical and chemical properties, mainly the colloidal behavior, of clays, especially the clay-water systems, will certainly help in understanding the behavior of the oil sands tailings sludge.

There are a number of definitions of clays. Some are based on an assembly of certain properties such as plasticity, particle size and hardening on firing. Some regard particle size as of primary importance, the size range being limited to less than 10 microns. In general, clay can be defined as a material which has properties such as adsorption, hydration, solvation, ion-exchange and hardening on drying and firing, and demonstrates remarkable plasticity when wet. For the purpose of the present study, particle size is of the primary

concern, as the colloidal behavior of clays is very important to the understanding of the oil sands tailings sludge. However, we will refer to the definition of clays by Kin$_{\text{t}}$ery et al. (47), that is, clays are fine particle hydrous aluminum silicates which develop plasticity when mixed with water. They vary over wide limits in chemical, mineralogical, and physical characteristics, but a common characteristic is their crystalline layer structure, consisting of electrically neutral aluminosilicate layers, which leads to a fine particle size and plate-like morphology and allows the particles to move readily over one another, giving rise to physical properties such as softness, soapy feel, and easy cleavage.

The most common clays are based on the kaolinite structure, $Al_2(Si_2O_5)(OH)_4$. The ideal chemical formulas of the common clays are shown in **Table 2.3**. Besides SiO_2 and Al_2O_3, clays usually include a number of other components: Fe_2O_3, FeO, MnO, MgO, CaO and K_2O, which may or may not be crystalline materials.

Table 2.3 Ideal chemical formulas of common clays (47)

Kaolinite	$Al_2(Si_2O_5)(OH)_4$
Halloysite	$Al_2(Si_2O_5)(OH)_4 \cdot 2H_2O$
Pyrophyllite	$Al_2(Si_2O_5)(OH)_2$
Montmorillonite	$\left(Al_{1.67} \begin{array}{c} Na_{0.33} \\ Mg_{0.33} \end{array} \right)(Si_2O_5)_2(OH)_2$
Mica	$Al_2K(Si_{1.5}Al_{0.5}O_5)_2(OH)_2$
Illite	$Al_{2-x}Mg_xK_{1-x-y}(Si_{1.5-y}Al_{0.5+y}O_5)_2(OH)_2$

In general, clays can be divided into two major groups: kaolinites and montmorillonites. In the following sections, we review: (1) the shape, size, structure, charge and ion exchangeability of clays; (2) the modes of particle association and "card-house" structure; (3) factors such as pH and electrolytes governing the stability of clay suspensions; (4) the sedimentation and consolidation of clay suspensions; (5) the swelling property of montmorillonites; and (6) the drying behavior and mechanisms.

2.4.1 Shape, size, structure, charge and ion exchangeability of clays

Clays are plate-like (or rod-like such as attapulgite in some cases) particles. The size of clay particles ranges from a few hundredths of a micron to several microns (48), which

means part of the clay particles is in the colloidal range. Dispersion or flocculation and other colloidal properties of clays are attributed to their colloidal size fraction.

The principal building elements of clay minerals are two-dimensional arrays of silicon-oxygen tetrahedra and two-dimensional arrays of aluminum- or magnesium-oxygen-hydroxyl octahedra. In the silicon-oxygen sheets, the silicon atoms are coordinated with four oxygen atoms. The silicon-oxygen sheet is termed a **tetrahedral layer or silica sheet**. In the aluminum- or magnesium-oxygen-hydroxyl sheets, the Al or Mg atoms are coordinated with six oxygen or OH groups which are located around the Al or Mg atoms with their centers on the six corners of a regular octahedron. Such sheet is termed an **octahedral layer or alumina or magnesia sheet** (also termed gibbsite layer or brucite layer respectively). Fig.2.7 shows the simplified layer structure of kaolinite and montmorillonite. It can be seen that kaolinite is a two-layer mineral in which oxygen atoms are shared between one silica and one alumina or magnesia sheet, and montmorillonite is a three-layer mineral in which one alumina or magnesia shares oxygen atoms with two silica sheets, one on each side. The combination of an octahedral sheet with one or two tetrahedral sheets is called a unit layer. Most clays consist of such unit layers, which are stacked parallel to each other. The difference lies in the way they stack together (49).

Electrokinetic studies of clay suspensions indicate that clay particles are charged negatively when the pH of clay suspensions is above 2 or 3 (50). The origin of the negative charge is principally due to **isomorphous substitution** in which the atoms of higher positive valence in the clay lattice are replaced by atoms of lower positive valence, for instance, tetravalent Si in the tetrahedral sheet is replaced by trivalent Al, resulting in a deficit of positive charge. The excessive negative charge is compensated by the adsorption on the layer surface of cations which are too large to be accommodated in the interior of the lattice like Na^+ (49). Other types of lattice imperfections, such as the absence of a constituent metal atom from its place in the lattice, dislocations, or localized bond breakages, may also contribute to the negative charge (50). In aqueous solution, the compensating cations are mobile and can be easily exchanged by other cations available in the solution, leading to the "**cation exchange capacity (C.E.C)**." C.E.C. is usually expressed in milliequivalents per 100 grams dry clay. It indicates the degree of isomorphous substitution.

Montmorillonites are three-layer clays. They have a relatively high C.E.C. (typically 70-100 meq per 100 grams). In the tetrahedral sheet, tetravalent Si is sometimes replaced by

trivalent Al. In the octahedral sheet, trivalent Al may be replaced by Mg, Fe, Cr, Zn or Li. When montmorillonite is contacted with water or water vapor, the water molecules penetrate between unit layers, resulting in so-called interlayer swelling. The swelling of montmorillonites will be discussed later. Montmorillonites also admit organic compounds of a polar or an ionic character between unit layers.

The material involved has been removed because of copyright restrictions, see reference (47).

Fig.2.7   Layer structure of kaolinite and montmorillonite, dimension in 0.1 nm.

Illites are also three-layer clays. However, they differ from montmorillonites primarily by the absence of interlayer swelling with water or organic compounds. In illites, isomorphous substitution occurs predominantly in the tetrahedral sheet. The compensating cations are usually potassium ions. The potassium ions between the unit layers are fixed - not available for exchange. The nonswelling behavior of illites can be attributed to the special linking effect of the unit layers by the potassium ions. Since only the external cations of illites are exchangeable, the C.E.C. of illites is lower than that of montmorillonites. The C.E.C. of illites is about 20-40 meq per 100 grams.

Kaolinites are two-layer clays. Their C.E.C. is relatively low, ranging from 1 to 10 meq per 100 grams. When contacted with water or water vapor, kaolinites do not swell (49).

2.4.2 Modes of clay particle association and "card-house" structure

The plate-like clay particles have two types of surfaces: faces and edges. There is much evidence indicating the edges of clay particles are charged positively (49-55). An electron micrograph of a mixture of kaolinite and a negatively charged gold sol showed that the small negatively charged gold particles were exclusively adsorbed at the edges of the kaolinite platelets (49). Based on the fact that the faces of plate-like clay particles are charged negatively and the edges might be charged positively, van Olphen (49) proposed three modes of particle association: face-to-face (FF), face-to-edge (EF) and edge-to-edge (EE). While the FF association leads to oriented flakes (Fig.2.8c), the EF (Fig.2.8a) and EE (Fig.2.8b) association lead to the formation of three-dimensional "card-house" and "chain-like" network structures, responsible for the gelation of clays and the high clay sediment volume. The aggregates built in these cases are called flocs.

Calculation by Flegmann et al. (53) shows that the modes of kaolinite particle association are pH dependent. Because of a high energy barrier to the FF association in the pH range 3 to 4, the possibility of the FF association is small. The energy barrier for the EE association is smaller; therefore the EE association occurs to some extent. In the case of the EF association, the attraction between the edges and faces is strong; the EF association dominates. Below pH 7, the edge surface is positively charged, so EF association is favorable. Around pH 7 (near the zero point of charge of the edges), the EE association is favored. Some EF association is also possible. The energy barrier to the FF association is still very high. At pH 10, the energy barrier is high enough for all modes of association, and the clay particles are very stable.
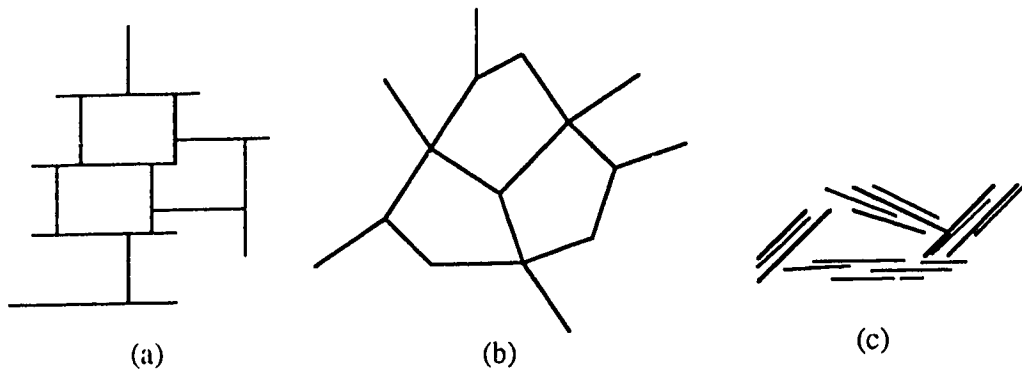
Fig.2.8. Structures built by plate-like clay particles: (a) EF association, card house; (b) EE association, chain-like network; (c) FF association, oriented flakes.
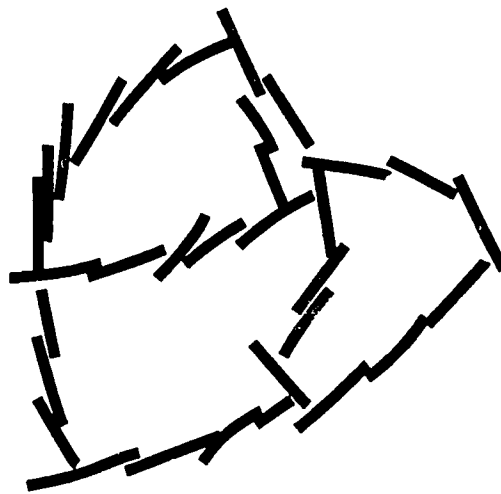
Fig.2.9 Card-house structure by FF and EF association, after O'Brien (56)

O'Brien (56) studied the structure of kaolinite in a flocculated state using two different techniques: freezing-drying and polyethylene glycol No. 6000 impregnation. He found that the modes of kaolinite particle association were mainly FF association. These flakes were arranged in a stair-step manner in each floc and the flocs were joined to each other in EF association (Fig.2.9). A similar structure was observed for illite in flocculated state. However, the artifact introduced by the formation of ice crystals can not be excluded.

Babchin et al. (57) believed that the hydration forces inherent to the interaction of quartz particles and the dipolar forces of clay particle interaction are responsible for the stability of tailings sludge. They proposed a different mechanism of "card-house" structure. In each plate-like particle, there are two dipole moments with opposite directions, and all plate-like particles, if the dipoles are symmetrical, can be represented as effective quadrupoles (Fig.2.10). Two such quadrupoles may attract or repel each other according to their mutual orientation, which leads to the formation of a "card-house" structure (Fig.2.8a). If the dipoles in clay particles are not symmetrical, the plate-like particles will be represented as effective dipoles rather than quadrupoles. A "chain-like" structure is formed like Fig.2.8b. It must be pointed out these authors ignored the diffusion effect of colloidal size particles (less than 0.2μm).

The material involved has been removed because of copyright restrictions, see reference (57).

Fig. 2.10 Repulsion and attraction forces between plate-like clay particles represented as quadrupoles, after Babchin, et al. (57).

Schutte, Czarnecki, and Liu (58) also recognized the existence of "card-house" and "chain-like" structures in oil sands tailings sludge. They believed that EF association is the

dominant association mode. Their explanation is that the probability of EF association is much higher than EE association as there is more surface on the face than the edge of plate-like clay particles. They also developed an energy model and derived analytical expressions describing the total interaction energy between clay particles as a function of the hinging angle between particles. They found that when clay particles are oriented perpendicular to each other, the total interaction energy (van der Waals attraction and electrostatic repulsion) is minimal. Therefore, EF association predominates.

2.4.3 Factors affecting the stability of clay suspensions

The stability of clay suspensions depends on many factors such as the particle size, the concentration and type of clays, the pH of the liquid, the concentration and nature of electrolytes and the hydrolysis of cations. In this section, the focus will be on two clays: kaolinite and montmorillonite.

Clay suspensions (clay-water systems in most cases) represent lyophobic colloidal systems. Their stability can be explained by the DLVO theory. However, the DLVO theory cannot be applied without several corrections to quantitatively explain the experimental data on clay suspensions. In the DLVO theory, the ion size, the hydration of clay particle surface, and the interaction between surface, counterion and the medium are not taken into consideration. In addition, clay particles have two types of faces. The charge on the face and edge could be different.

Electrolyte concentration

The flocculating power of a simple electrolyte can be measured by CFC. Because of the different methodologies in the CFC determination, for instance, the experiments were often conducted at different pH, considerable difference exists for the previously reported CFC of a given electrolyte. For example, the CFC of NaCl for Na-montmorillonite ranges from 7 to 20 mM/L (59); $CaCl_2$ for Ca-montmorillonite from 0.17 mM/L (49) to 0.5 mM/L (60); NaCl for Na-kaolinite from 0 to 5 mM/L (59). Swartzen-Allen and Matijevic (61) found the CFC decreased when the cation valence increased. However, for cations of the same charge, the flocculating power can differ significantly. The higher the atomic number, the lower the CFC. This is particularly true for polycations with the same valence. Due to the C.E.C. of clays and their varying affinity for different counterions, and the hydrolysis of cations of high valence, the Schulze-Hardy rule cannot be applied quantitatively to the clay suspensions without several corrections.

The effect of electrolyte concentration on the stability of clay suspensions can also be interpreted in term of its effect on the zeta potential or the electrophoretic mobility. The zeta potential or electrophoretic mobility of clay particles gives a measure of the interparticle repulsion. Studies by Swartzen-Allen and Matijevic (61 and 62) showed that for a given electrolyte at a given pH, a critical electrolyte concentration existed for Na-montmorillonite above which the electrophoretic mobility decreased dramatically, and this concentration was very close to its CFC at the same pH. As the cation valence increased from 2 to 3, the electrophoretic mobility was considerably reduced, which is in agreement with the Schulze-Hardy rule. However, there wasn't a significant difference between Al^{3+} and Th^{4+} except the latter reversed the charge of the montmorillonite at a concentration higher than 10^{-4} M.

pH effects

The stability of clay suspensions is very pH dependent. This is generally attributed to the pH effect on the particle charge and the modes of particle association. In the acidic condition, the edges of plate-like clay particles are positive and the net negative charge is lower; therefore the repulsion between particles is lower. Moreover, EF association results in partial flocculation before the addition of electrolytes. As a result, the clay suspensions are less stable than at higher pH where the positive edge charge is reduced or neutralized. In the latter case, the net negative charge or the interparticle repulsion is greater and the possibility of EF association is low. As mentioned before, at high pH, the energy barrier for all modes of particle association is high to prevent flocculation. In terms of CFC, the CFC increases as the pH of the clay suspension increases.

For Na-montmorillonite suspensions, Swartzen-Allen and Matijevic (61) found that the CFC of Na^+, Cs^+, Ca^{2+}, Co^{2+}, La^{3+} and Th^{4+} as a function of pH showed two plateaus. One plateau is between pH 4 and 6, and the other at pH>8 (Fig.2.11a). Between pH 6 and 8, the CFC increased rapidly. At pH<3.5 or pH>10.5, the amount of the acid or base added for pH adjustment reached the CFC and induced flocculation by itself.

For kaolinite suspensions, the CFC increases with pH (Fig.2.11b). Kaolinite suspensions are more stable than Na-montmorillonite suspensions mainly because montmorillonite has a higher C.E.C. and offers more exchangeable Al^{3+} than kaolinite. Less electrolyte is therefore needed to release a sufficient amount of Al^{3+} to induce Na-montmorillonite flocculation. Goldberg and Glaubig (63) found similar results.

The material involved has been removed because of copyright restrictions, see reference (61).

Fig. 2.11 CFC of various electrolytes as a function of pH: (a) for a Na-montmorillonite suspension (250 ppm); (b) for a Kaolinite suspension (25 ppm), from Swartzen-Allen and Matijevic (61).

The material involved has been removed because of copyright restrictions, see reference (62).

Fig.2.12 Electrophoretic mobilities of Na- and Cs-montmorillonite as a function of pH, with no added electrolytes, from Swartzen-Allen and Matijevic (62).

The material involved has been removed because of copyright restrictions, see reference (61).

Fig.2.13 CFC of $Al(NO_3)_3$ as a function of pH for a Na-montmorillonite suspension (250 ppm), from Swartzen-Allen and Matijevic (61).

The pH of clay suspensions also has a major effect on the zeta potential or electrophoretic mobility of clay suspensions. Swartzen-Allen and Matijevic (62) studied Na- and Cs-montmorillonite suspensions where the pH was adjusted only with HNO_3 or $NaOH$. They found the particles are negatively charged over the complete pH range from 3 to 12. At pH<8, the negative mobility is low and relatively constant. Between pH 8 and 10, the electrophoretic mobility increases very rapidly (Fig.2.12).

The sudden increase of the negative mobility of the montmorillonite particles at pH>8 is consistent with the coexistence of two kinds of charge on the clay particles. In a basic condition, the reaction of hydroxide anions with the positive particle edges neutralizes them or gives them a negative charge.

Hydrolysis effects

The hydrolysis of cations has a major effect on the stability of colloidal dispersions. In general, the hydrolysis of cations results in complexed species of lower charge, and decreases their flocculating power. However, in many cases, the replacement of water by hydroxyl groups in the coordination shell of a metal ion leads to much stronger adsorption on a wide variety of surfaces. Consequently, in spite of their reduced charge, hydrolyzed metal ions could be more effective in terms of flocculating power than the correspondingly unhydrolyzed ions, and even cause charge reversal and restabilization. For Fe(III) and Al(III) inorganic salts, highly charged products such as $Fe_2(OH)_2^{4+}$, $Fe_3(OH)_4^{5+}$, $Al_4(OH)_8^{4+}$ and $Al_8(OH)_{20}^{4+}$ formed. These species have a strong tendency to be adsorbed; therefore, they are very effective flocculants (64).

For highly charged cations such as Fe^{3+} and Al^{3+}, flocculation may occur according the following mechanisms:
(1) Flocculation by Fe^{3+} or Al^{3+} acting as simple counterions;
(2) Flocculation by the reduction of the particle charge due to the adsorption of hydrolysis products;
(3) The formation of Fe or Al hydroxide colloidal particles. These particles aggregate to form heterogeneous flocs or gelatinous precipitates with the clay particles.

Blackmore (65) studied the bonding of aggregates flocculated by the Fe(III) hydrolysis products. His results showed that stable aggregates formed when clays are mixed with freshly prepared $FeCl_3$ solutions. On the contrary, the gelatinous precipitates resulting from the full hydrolysis of $FeCl_3$ was not an effective aggregating agent, i.e, most of the

aggregates disintegrated after redispersion. The intermediate Fe hydrolysis products, which are positively charged, are strongly adsorbed on the clay particle surface and stable bonding between clay particles were achieved. Lutz (66) suggested a double role for iron in bonding: the soluble iron species acted as a counterion and the gelatinous precipitates acted as a cement. El Rayah and Rowell (67) also reported that freshly prepared iron and aluminum hydroxides acted as bonding agents. Upon ageing, the fresh iron hydroxide transformed into discrete hydrated iron oxide particles fixed on the clay particle surface while aluminum oxide acted as a bonding agent. However, these authors did not study the pH effect on the hydrolysis of cations.

Swartzen-Allen and Matijevic (61) studied the hydrolysis effect on the CFC of various electrolytes in the pH range 4 to 10. They found the CFC of Na^+, Cs^+, Ca^{2+}, Co^{2+}, La^{3+} and Th^{4+} salts for Na-montmorillonite all showed similar dependence on pH in spite of the difference in cation valence (see Fig.2.11a). Yet, Na^+, Cs^+, and Ca^{2+} do not undergo hydrolysis over the pH range 3.5 to 10 while Co^{2+} undergoes considerable hydrolysis at pH > ~7.5, La^{3+} at pH > ~8, and Th^{4+} at pH > ~4. They concluded therefore that the hydrolysis of cations might not have a a major effect on the CFC of electrolytes. However, the CFC of $Al(NO_3)_3$ as a function of pH shows a different trend (Fig.2.13). It increases first up to around pH 4; decreases between pH 4 and 6, due to the formation of highly charged hydrolysis products like $Al_8(OH)_{20}^{4+}$; then increases at pH > 6. This can be explained by a reduction of the cationic charge upon further hydrolysis at pH>6, leading eventually to the precipitation of aluminum hydroxide.

They also studied the effect of the hydrolysis of cations on the electrophoretic mobility of Na-montmorillonite. At the CFC of $Al(NO_3)_3$, the mobility of Na-montmorillonite increases monotonically with pH in the range 4 to 10 (Fig.2.14), which is different from the CFC of $Al(NO_3)_3$ vs. pH curve (Fig.2.13). This indicates a complex role of aluminum in the destabilization of montmorillonite suspensions. Over the pH range 4 to 10, aluminum ions are first hydrolyzed, then precipitated as hydroxide and finally, at the highest pH, ending up in anionic aluminate species (62). At the lowest pH, the hydrolyzed aluminum species reduce the particle charge considerably, indicating adsorption. With increasing pH, the particle charge at the CFC becomes more negative, yet the CFC is lowered as pH rises from 4 to 6. This could be explained as follows: as hydrolysis progresses, the effective charge per aluminum atom in the complex decreases, therefore lowering its charge-reducing ability; at the same time the total charge of the polymeric counterion complex itself increases, rendering it a more efficient flocculant. In the case of thorium (Th^{4+}) ions, the

effect of hydrolyzed thorium ions on the mobility of Na-montmorillonite is similar to unhydrolyzed thorium ions, that is, by charge reduction in addition to the release of aluminum counterion species. This indicates that the surfaces of clay particles do not show the same adsorptivity for hydrolyzed ions. In any case, the pH effect on hydrolysis differs from one cation to another, hence the effect on clay stability must be different.

The material involved has been removed because of copyright restrictions, see reference (61).

Fig.2.14 Mobilities of Na-montmorillonite at the CFC of $Al(NO_3)_3$ and with no added salt as a function of pH, from Swartzen-Allen and Matijevic (61).

2.4.4 Sedimentation and consolidation

Sedimentation can occur in both non-flocculated and flocculated colloidal systems each time the thermal energy k_bT is too low compared to the particle or floc weight, mg (m is the mass, g is the gravity). The settling rate increases with the particle or floc mass. Depending on the initial state of clay suspensions, the structure of sediments can be very different. It is well known that flocculated systems always result in a loose packed structure and high sediment volume whereas the well dispersed systems always result in a closely packed structure and low sediment volume.

For well dispersed clay suspensions, the kinetic units undertaking sedimentation are individual particles. The inter-particle space after settling is usually determined by the balance of two forces: weight of the consolidating mass itself, and the repulsive force, usually the double layer repulsion. Since the double layer repulsion, at best, is strong only at very small inter-particle distance, the sediment is relatively compact (Fig. 2.15a).

For flocculated clay suspensions, the kinetic units undertaking sedimentation are larger floc. The sediment volume is determined by the floc density, the packing pattern of primary particles inside the floc (or floc structure), the inter-particle linkage and the self-weight of the consolidating mass. In general, the self-weight of the consolidating mass is not large enough to break the linkage between particles, therefore, the sediment is loosely packed (Fig.2.15b).

While the addition of flocculants to suspensions can improve the settling rate significantly, it is often detrimental to the consolidation of the sediments. **Consolidation** can be defined as a process in which the constituent particles or flocs of sediments rearrange themselves progressively from a loose structure to a compact one under the external body forces.

Depending on the nature of flocs, two types of settling behavior can be observed for the flocculated systems: "free" settling and zone settling (68). In "free" settling, the individual flocs settle individually. There is a distribution of settling rates which depend on the size, density and permeability of the individual flocs. In zone settling, a single floc network forms so that all flocs have the same settling rate and a sharp flat interface forms between the settling mass and the supernatant liquid. In both cases, the density and permeability of the flocs are determined primarily by the floc size. The floc size is therefore the most important factor controlling the settling rate. In fact, Hogg et al. (69) found the settling rate

of flocculated kaolinite or quartz particle suspensions increased linearly with the floc size. They also found that for polymeric flocculants, agitation during the polymer addition is a very important factor in determining the settling behavior. Agitation is needed to provide adequate mixing of the flocculant with the suspension and to increase the collision frequency necessary for floc growth. At the same time, agitation leads to floc breakdown. Therefore, a limiting floc size exists. Both the rate of floc growth and the limiting floc size generally increase with the rate of polymer addition. Continued agitation without further polymer addition leads to essentially irreversible floc breakage.

Before settling   After settling

a

b
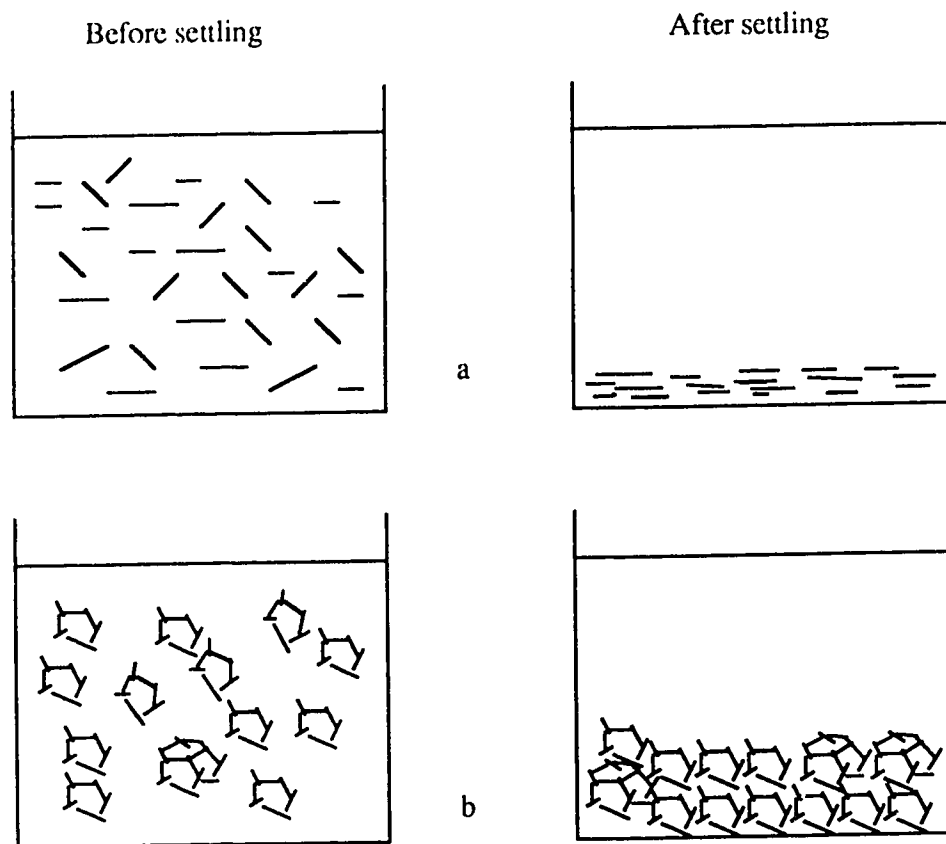
Fig. 2.15 Sedimentation in a well dispersed suspension (a); and in a flocculated suspension (b).

Smellie and La Mer (70) studied the settling of phosphatic tailings sludge by plotting the supernatant liquid/settling mass interface position as a function of time. They found two types of curves depending on the flocculant concentration (Fig. 2.16).

For type I, slow flocculation, some induction time, ab, is required for the formation of flocs with a certain size. For type II, rapid flocculation, settling occurs immediately due to the rapid formation of flocs with a certain size. After the constant settling rate (bc and ac in Fig.2.16) maintains for both types for some time in both cases. Then the consolidation begins, which is a very slow process.
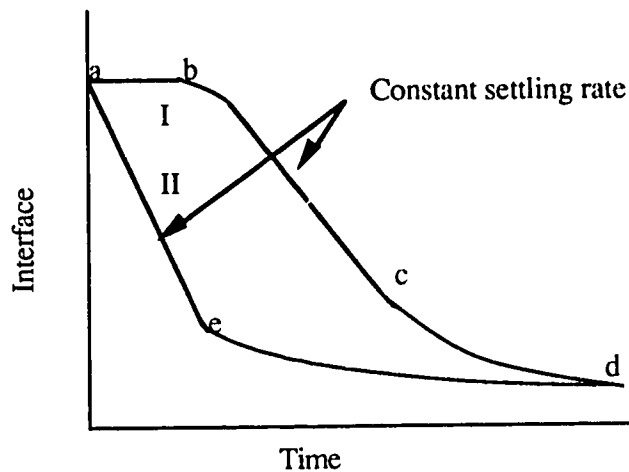
Fig. 2.16 Types of settling curves: I, slow flocculation; II, rapid flocculation.

Michaels and Bolger (71) found three types of settling curves for flocculated kaolinite suspensions depending on the solid concentration and the geometry of the container (Fig. 2.17).

The material involved has been removed because of copyright restrictions, see reference (71).

Fig.2.17 Three types of settling curves, after Michaels and Bolger (71)

For very dilute suspensions (volume fraction < 0.7%), curve a on Fig.2.17 is obtained. It comprises a straight-line segment. When the particle volume fraction increases above 0.7%, the flocs settle as a network, so that the settling curve has the shape of b. The initial settling rate is low, then increases with time, reaching its maximum value at t_1. When the container diameter is less than a certain value (yield diameter), settling proceeds slowly, at an ever-decreasing rate, similar to consolidation. The settling curve looks like Fig.2.17 c. According to their report, the inside diameter of the container must be larger than 0.24 cm for the wall effect to be negligible, in the case of suspensions with 3.2 % solid content (by volume).

The consolidation process involves the transport of liquid through the network of particles, breakage of existing inter-particle linkage and the formation of new inter-particle contacts. The study of consolidation behavior usually use methods based on the volume and compressibility of the sediment (21).

Hogg et al. (69) showed that the floc density was a factor controlling the consolidation process. The floc size has less importance although large flocs usually have a lower density. For example, very large flocs might contain as low as 4 to 5% solids by volume in comparison with more than 50% for very small flocs. The strength of linkage between flocs also has effect on the consolidation. High strength flocs (low compressibility) usually contribute to a low density and a high sediment volume. This also suggests that a higher compaction density could be achieved by controlling the floc size through agitation or by forming weakly bonded flocs with a low polymer concentration. Unfortunately, little has been done to study how the nature of flocculants and pH affect the size and structure of flocs.

Several techniques or methods based on the breakdown of flocs and the increase of density of flocs have shown encouraging results in the treatment of phosphatic tailings sludge. An efficient one consists in dewatering with moving screens (42). The slowly moving screens break up the gel-like structure to liberate a large percentage of the interstitial water. Laboratory tests have shown that tailings sludge having an initial solid content between 4.7 and 11.9% could be consolidated to 16.8% and 25.2%, respectively, in 3.5 days. The speed at which the screens move is a critical variable. To achieve significant improvement in consolidation, the screen speed must be slow, which is not practical considering the large amount of phosphatic tailings sludge produced.

Another efficient technique consists in mixing sands with the tailings sludge (30). Laboratory tests have shown that when fine grain sands were sprinkled over the tailings sludge with a 12% solid content, the sands penetrated and mixed with the tailings sludge, liberating water and producing a thick sand-tailings sludge mixture with about 45% solid content. Field tests on a 20-acre and 500-acre site duplicated the laboratory results. In fact, mixing sands with the tailings sludge accomplishes two things: the breakdown of flocs and the densification of flocs, both of them favoring the consolidation process.

2.4.5 Swelling of montmorillonites

The swelling of montmorillonite has been known for long time. When montmorillonites are placed in contact with water or water vapor, two stages of swelling are observed: interlayer swelling and physical or "osmotic" swelling (49, 72-73).

In the first stage, interlayer swelling, water molecules are adsorbed in successive monolayers between the clay atomic layers and push these unit layers apart. In this stage, the principal driving force is the hydration energy of the clay surface. Interlayer swelling leads to , at most, a doubling of the volume of the dry clay when four layers of water are adsorbed.

In the second stage, physical swelling, the swelling is due to the double layer repulsion by which the particles or the unit layers may be pushed further apart. The volume during this stage can increase by about 20 times (72). Such swelling leads to the formation of the montmorillonite gels. Upon stirring with more water, a montmorillonite sol or suspension forms.

It is well understood that the physical swelling is a result of long-range particle interaction, i.e., the double layer repulsion, compared with the short range particle interaction-swelling due to the surface hydration . As the double layer repulsion is controlled by many factors such as electrolytes, pH and dielectric constant of the dispersed medium, the effects of these factors on the swelling behavior of montmorillonite will be examined.

Norrish (72) and Emerson (74) showed that the swelling volume of montmorillonites decreased with the electrolyte concentration. The extent of swelling also decreased with the decrease of cation exchange capacity (C.E.C.) (72). At low Na^+ concentrations, swelling was very pH dependent. Between pH 4 and 8, the swelling volume remained constant.

However, when the pH increased above 8, the swelling volume increased dramatically (74). These results can be explained as follows: When the electrolyte concentration increases, the double layer repulsion decreases, and so does swelling. For montmorillonites, the double layer repulsion increases rapidly when the pH is above 8 (see Fig.2.12), so does the swelling. As for C.E.C., there is a relationship between surface charge density (σ) and C.E.C. (75) :

$$\sigma = C.E.C./100S \qquad\qquad (eq.2.18)$$

Where S is the specific surface area of the clay. The surface potential (ψ^0) of clay particles is:

$$\psi^0 = \frac{4\pi\sigma}{\varepsilon\kappa} \qquad\qquad (eq.2.19)$$

The surface potential decreases with decreasing surface charge density; therefore, when the C.E.C. decrease, the repulsion decreases.

The medium a;   ct ect on the swelling behavior of montmorillonite. According to eq.2.1, th· ·l·· .   .. ιnickness decreases with the dielectric constant ; therefore, the double layer re;··· .n decreases. ᴿor aqueous solution, the dielectric constant near a clay particle surface is mεch lower than the value of 78.3 for bulk water. It is generally believed the effective dielectric constant in the aqueous medium increases from a low value (<10) close to the particle to its bulk value over a distance of several molecular diameters (76). This is due to an ordering by rotation of the permanent water molecule dipoles, near the surface of the particle.

2.4.6 Drying of clays

This section outlines the generally accepted views on the mechanism of moisture movement during drying and those factors affecting rate of drying.

Mechanisms

The drying of all moist materials including clays under the conditions of constant air temperature, humidity and velocity can be divided into two or three distinct periods as shown in Fig.2.18: constant-rate period (AB), first falling-rate period (BC) , and second falling-rate period (CD) (77). If the drying rate is plotted against moisture content, a

different type of curve can be obtained (Fig.2.19). For some materials, only a single falling
rate period can be identified.
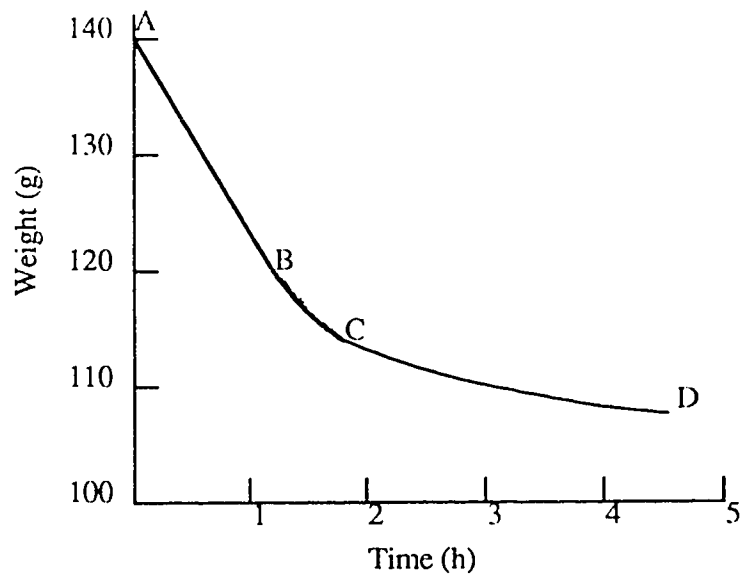
Fig.2.18 Typical drying curve
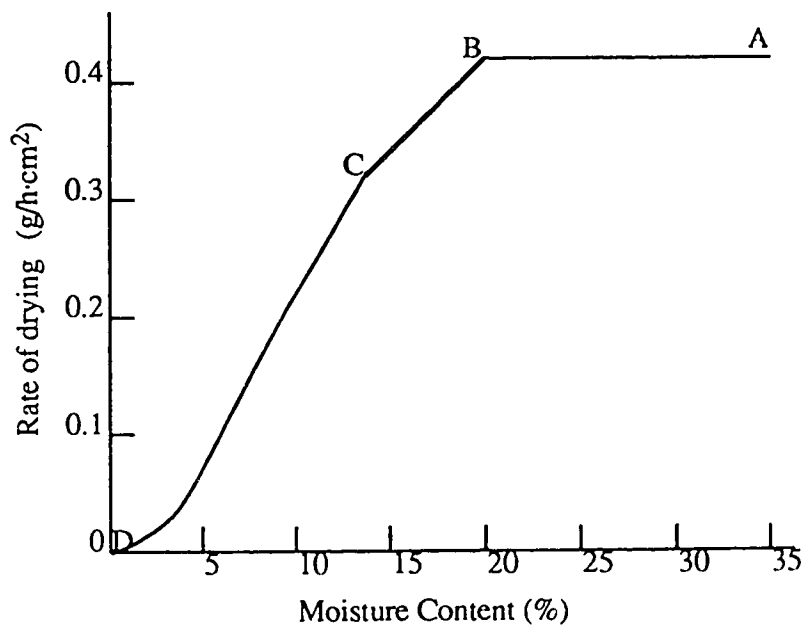
Fig.2.19 Rate of drying curve

The mechanism of moisture movement for each period is given below.

Constant-rate period (C.R.P.)

During the C.R.P., the rate of drying under constant conditions is independent of the nature of materials, and the surface of the material can be treated as a free water surface. The rate of evaporation is controlled by the rate at which vapor can diffuse through the comparatively stagnant layers adjacent to the surface. When the air velocity increases, the thickness of the stagnant layer decreases, thereby increasing evaporation rate. At a given condition, the rate of evaporation is proportional to (e_s-e_a), where e_s is the equilibrium vapor pressure over the surface, and e_a is the actual vapor pressure in the surrounding air.

In plastic clays, the particles are separated by a water film. As drying proceeds, shrinkage takes place as these films are reduced in thickness due to the evaporation of water. During this period, the decrease in volume is equal to the volume of water lost. It is generally accepted that, during this period, moisture is transferred in the liquid phase. Two mechanisms have been proposed to explain the moisture movement in the drying: capillary mechanism, and osmosis (12 and 77). However, there is a divergence of opinion as to whether the capillary force (i.e. surface tension) or osmotic force or both are the drying force for the moisture movement.
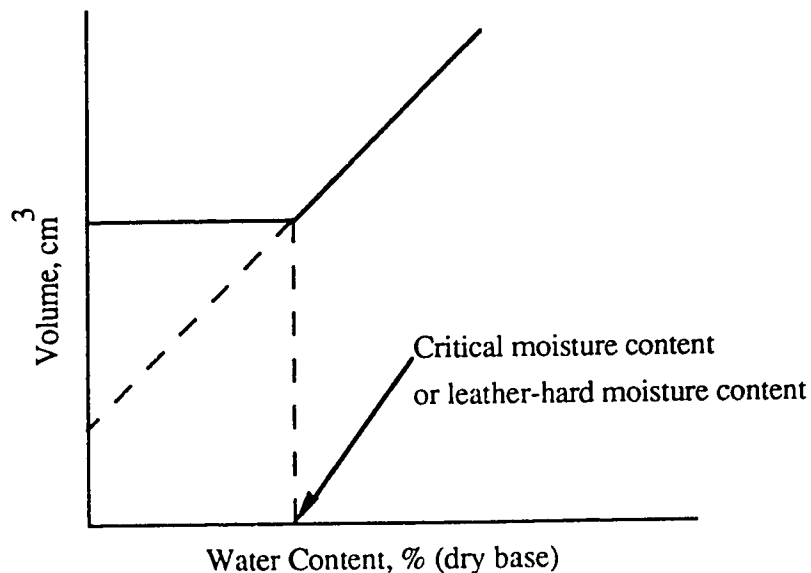
Fig.2.20 Drying curve for volume vs. water content

At the end of the C.R.P., the clay particles come into mutual contact, forming a loose packed assembly. Further contraction is not possible; therefore, no further shrinkage occurs. The remaining water is trapped in the voids between particles, and the water content at this point (called the critical point of shrinkage) is known as the critical moisture content (C.M.C). C.M.C. is also referred to as the leather-hard moisture content. If the volume of the plastic clay is plotted against the water content (dry basis), then the following type of curve can be obtained (Fig.2.20).

First falling-rate period (1st F.R.P.)

During this period, water cannot arrive at the surface fast enough to maintain the saturation of the surface air film. The rate of evaporation is controlled by the rate at which water can flow to the surface and the rate at which vapor can diffuse through the surface air film. It must be pointed out that this period is not always observable. Whether moisture travels as liquid or vapor during this period is still open to question.

Second falling-rate period (2nd F.R.P.)

During this period, the surface is dry or nearly so. Evaporation occurs within the solid, vapor reaching the surface by molecular diffusion through pores. The rate of vapor diffusion in the pores is the factor controlling the drying rate, and the external factors such as air humidity and velocity have little effect. In this final stage of drying, it is generally accepted that the evaporation occurs in the interior and moisture travels as vapor.

Factors affecting drying behavior

Temperature, humidity, air velocity, particle size, exchangeable cations, surface tension, flocculant concentration, and water content all have important effects on the drying behavior of clays. For example, a smaller particle size will increase the drying shrinkage since the number of water films increases as particle size decreases.

There are two major forces between particles; one is the repulsion due to the particle charge, and the other is the compressing force exerted by the capillary pressure that depends on the surface tension and the radius of curvature at the surface. In addition, there is the van der Waals attraction which is considerably smaller than the capillary pressure in the plastic range.

Kingery and Francl (78) concluded, in their study on the effect of the surface tension of liquid on the drying behavior of clay-water systems, that (1) drying shrinkage increases

linearly with the surface tension ; (2) consequently, the dry bulk density increases also linearly with the surface tension; (3) the C.M.C. is lowered as the surface tension increases; (4) The rate of drying during the C.R.P. decreases as surface tension increases.

The addition of flocculants changes the pore size and the thickness of water film, i.e. the packing pattern of clay particle., and the repulsion between particles, thereby affecting the drying behavior. In general, the flocculated systems have a higher C.M.C. than the stable systems because clay particles in the former are loosely packed (20).

2.5 BEHAVIOR OF FE (III) IN AQUEOUS MEDIUM

Iron is a transition metal which can possibly have two valence states: +2 or +3. Its behavior in an aqueous medium is very complex. A number of soluble iron species can be formed leading to the precipitation of various gelatinous products. However, Fe (II) is thermodynamically unstable in the presence of oxygen, and oxidizes to Fe (III). As for Fe(III), the interaction of clays with organic complexes containing this cation is not important to the present research topics. Consequently, only the aqueous chemistry of Fe(III) inorganic precursors is presented here. The precursor refers to the initial salts, for example, $FeCl_3$. A large number of papers including the recent review by Livage et al. (79) have addressed this subject . The aqueous chemistry of Fe^{3+} inorganic precursors involves a succession of bimolecular reactions, divided into hydrolysis and condensation reactions. In both cases, the cation, the anion and water participate in the trans ormation.

2.5.1 Hydrolysis

In general, hydrolysis can be defined as a chemical reaction in which a substance is split or decomposed by water. In inorganic chemistry, hydrolysis often refers to solutions of salts and the reactions by which they are converted to new ionic species or precipitates − oxides, hydroxides, or basic salts (10). The hydrolysis reactions follow a similar pattern for most cations, mainly because most metal atoms form strong bonds to oxygen and the OH⁻ ligand is always present in water. With Fe (III), they can be described as follows.

When dissolved in pure water, Fe^{3+} surrounds itself with a shell of 6 water molecules, each being captured according to the following chemical equation:

$$Fe^{3+} + :O\overset{H}{\underset{H}{\diagdown}} \longrightarrow \left[Fe-O\overset{H}{\underset{H}{\diagdown}} \right]^{3+} \qquad (eq.\ 2.20)$$
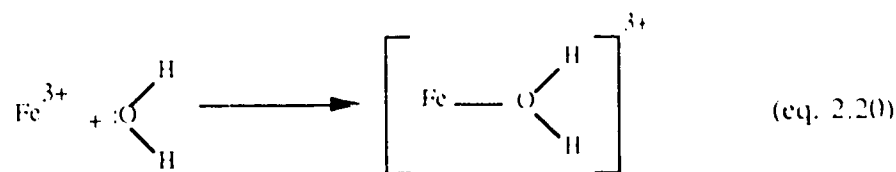
This transformation, called solvation, leads to the formation of a partially covalent bond.

A partial charge transfer occurs from the filled $3a_1$ bonding orbital of the water molecule to the empty d orbitals of Fe^{3+} ion. The positive partial charge on the hydrogen atoms increases, and the water molecule, as a whole, becomes more acidic. Depending on the magnitude of the transfer, each solvated water molecule may lose 1 or 2 protons according the following reactions :

$$[Fe(OH_2)_6]^{3+} + H_2O \Leftrightarrow [Fe(OH)(OH_2)_5]^{2+} + H_3O^+ \qquad K1 = 3*10^7 s^{-1} \qquad (eq.2.21)$$

$$[Fe(OH)(OH_2)_5]^{2+} + H_2O \Leftrightarrow [Fe(OH)_2(OH_2)_4]^+ + H_3O^+ \qquad K2 = 6.1*10^4 s^{-1} \qquad (eq.2.22)$$

$$[Fe(OH)(OH_2)_5]^{2+} + H_2O \Leftrightarrow [FeO(OH_2)_5]^+ + H_3O^+ \qquad (eq.2.23)$$
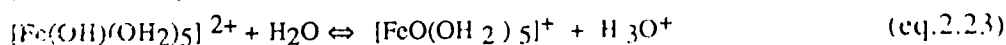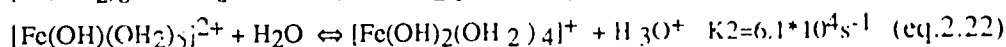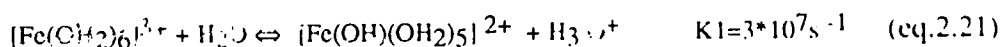
Considering only hydrogen and oxygen, three kinds of chemical groups called ligands can be linked to Fe^{3+}: aquo ligands (OH_2), hydroxo ligands (-OH) and oxo ligands (=O). If N is the number of water molecules covalently bound to Fe^{3+} (coordination number), the rough formula for any Fe^{3+} inorganic chemical complexes can be written as $[FeO_NH_{2N-h}]^{(3-h)+}$, where h is defined as the molar ratio of hydrolysis. When h=0, the complex is an "aquo-ion" $[Fe(OH_2)_N]^{3+}$ while for h=2N, it is an "oxo-ion" $[FeO_N]^{(2N-3)-}$. If 0<h<2N, the complex can be either an oxo-hydroxo complex $[FeO_x(OH)_{N-x}]^{(N+x-3)-}$ (if h>N), an hydroxo-aquo complex $[Fe(OH)_h(OH_2)_{N-h}]^{(3-h)+}$ (if h<N) or an hydroxo complex: $[Fe(OH)_N]^{(N-3)-}$ (if h=N).

A charge-pH diagram established by Jorgensen (80) can be used to explain the nature of ligands bound to the cation before condensation occurs (Fig.2.21). Three domains can be defined: domain I, oxo complexes $[MO_N]^{(2N-z)-}$; domain II, hydroxo complexes $[MO_NH_{2N-h}]^{(z-h)+}$; and domain III, aquo complexes $[M(OH_2)_N]^{z+}$. This diagram gives the nature of the complexes as a function of the formal charge z of the cation M^{z+} and the pH of the aqueous solution.

Let us consider a hydroxo complex in domain II. When the pH is increased, this cation complex behaves like an acid and liberates protons. A cleavage of the O-H bond occurs due to the Fe atom's large polarization:

$$\overset{\delta'}{} \quad \overset{\delta}{} \quad \overset{\delta'}{}$$
$$(Fe - O - H)aq. + H_2O \Leftrightarrow (Fe - O^-)aq. + H_3O^+ \qquad (eq.2.24)$$
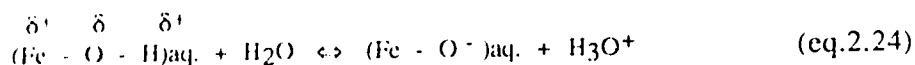
In the above equation, δ is the partial charge of each atom, and aq.designates the other H_2O ligands.

The main Fe complexes known to behave as acids are:

$$[Fe(OH)(OH_2)_5]^{2+} \quad and \quad [Fe(OH_2)_6]^{3+}$$

On the contrary, when the pH is lowered, the limiting reaction is the cleavage of the Fe-O bond arising from the low polarization of the Fe atom. The Fe complexes tend to behave like bases according to the reaction:

$$(Fe-OH)aq \rightarrow Fe^+_{aq} + OH^-_{aq} \qquad (eq\ 2.25)$$

The main Fe complexes known to behave like a base are:

$$[FeO(OH)_3]^{2-} \quad and \quad [Fe(OH)_4]^-$$
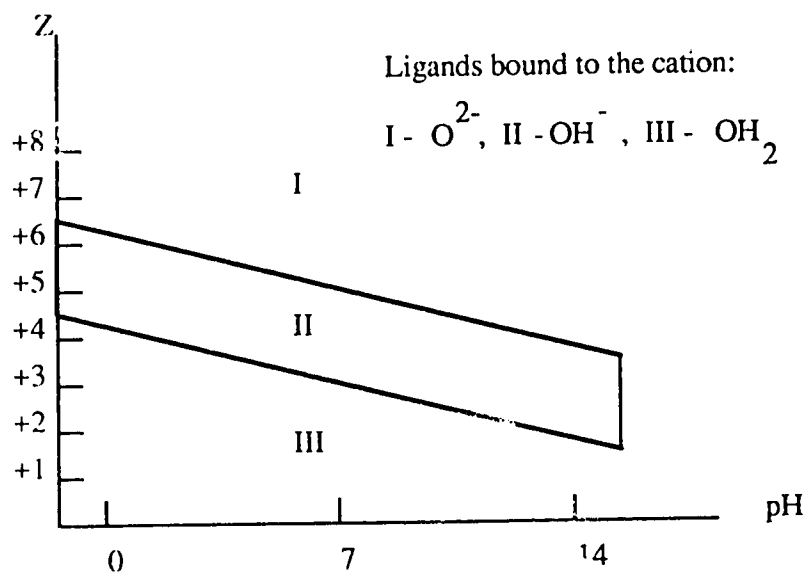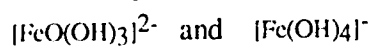
Fig.2.21 Charge-pH diagram, according to Jorgensen (80)

These results are in agreement with the "charge-pH" diagram on Fig. 2.21, where low-valent cations (Z<+4) give rise to aquo hydroxo and/ or hydroxo complexes over the whole pH range.

2.5.2 Condensation

General

Condensation can be defined as the bimolecular addition of cation complexes. Condensation in aqueous solutions can occur through two simple mechanisms that can be related to the coordination unsaturation:

i) If the preferred coordination is already fulfilled in the initial molecular complexes, condensation occurs via a substitution reaction:

$$Fe - OX + Fe - OY \rightarrow Fe - \overset{X}{O} - Fe + OY \qquad (eq.2.26)$$
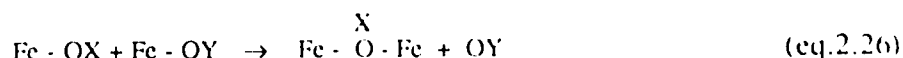
In this case, an entering group OX and a leaving group OY must be present around Fe in order to keep the coordination number unchanged.

ii) If the preferred coordination is not fulfilled in the initial molecular complexes, addition reactions become possible:

$$Fe - OX + Fe - OY \rightarrow Fe - \overset{X}{O} - Fe - OY \qquad (eq 2.27)$$
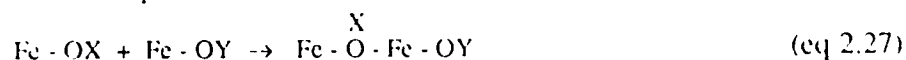
An increase in the coordination number occurs so that no OY group needs to be eliminated.

The mechanism of actual condensation depends on the availability of entering groups and leaving groups. With oxo complexes, oxo ligands are good nucleophiles (entering group) and very poor leaving groups. Condensation can only occur via addition of complexes. With aquo complexes, as no entering group is available, condensation cannot occur. For hydroxo complexes, where both entering groups and leaving groups are available, condensation through substitution reactions can thus be n as soon as one hydroxo ligand appears in the coordination. According to the "charge-pH" diagram, the system must be brought from the aquo (low-valent cations) or oxo (high-valent cations) domain into the hydroxo one (middle domain) in order to obtain a sol, a gel or a precipitate. With iron complexes, there are two ways to achieve condensation reactions. One is to increase the pH (eq. 2.28); the other is to oxidize Fe^{2+} to Fe^{3+} (eq.2.29):

$$[Fe(OH_2)_6]^{3+} + 3OH^- \rightarrow [Fe(OH)_3 (OH_2)_3]^\circ + 3H_2O \qquad (eq.2.28)$$

$$2Fe^{2+} + 5H_2O + 1/2O_2 \Leftrightarrow Fe(OH)_3(S) + 4H^+ \qquad (eq.2.29)$$
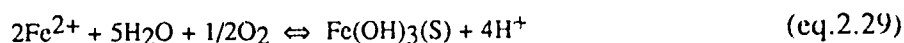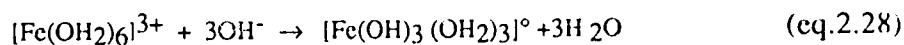
There is also a possibility of forming the deprotonation reaction (eq.2.21) by heating, a process called thermohydrolysis.

Condensation by olation

Very often, the group OX in eq.2.26 and eq.2.27 is replaced by OH⁻. In this case, condensation occurs by olation, which is the formation of a hydroxo or "ol" bridge Fe-OH-Fe. Such a condensation process occurs with hydroxo-aquo complexes $[Fe(OH)_x(OH_2)_{N-x}]^{(z-x)+}$ where x<N. Several kinds of bridges can form according to reactions called respectively, $_2(OH)_1$ (eq.2.30), $_3(OH)_1$ (eq.2.31), $_2(OH)_2$ (eq.2. 32), and $_2(OH)_3$ (eq.2.33).

$$Fe - OH + Fe - OH_2 \longrightarrow Fe - \overset{H}{\underset{}{O}} - Fe + H_2O \quad (eq.2.30)$$

$$\underset{Fe}{\overset{Fe}{>}}OH + Fe - OH_2 \longrightarrow \underset{Fe}{\overset{Fe}{>}}OH - Fe + H_2O \quad (eq.2.31)$$

$$H_2O - Fe - OH + Fe - OH_2 \longrightarrow Fe \underset{O,H}{\overset{H,O}{<>}} Fe + 2H_2O \quad (eq.2.32)$$

$$(K_h = 6*10^{-4})$$

$$Fe - OH - Fe \longrightarrow Fe < \overset{H,O}{\underset{O,H}{}} > Fe + H_2O \quad (eq.2.33)$$
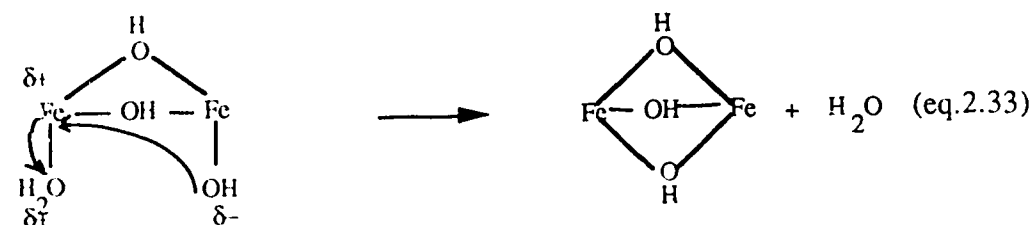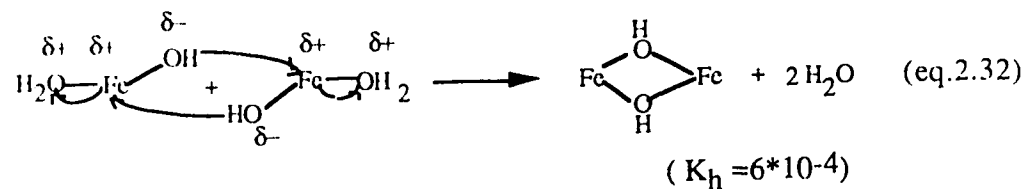
In a bridge symbolized by $_x(OH)_y$, x is the number of metal Fe atoms linked by one "ol" bridge and y is the number of bridges between these x Fe atoms. Since oxygen cannot have more than four covalent bonds, the limiting value for x is 3. In all cases, an aquo ligand must be removed from the coordination sphere. The kinetics of olation , therefore, depends strongly on the lability of the $(Fe - OH_2)$ bond. This lability depends mainly on the charge, size, electronegativity and electronic configuration of Fe atom.

Charged complexes (z-h≥1) cannot condense indefinitely to form indefinitely big polycations. This is mainly because the nucleophilic strength of the hydroxo group δ(OH) varies during the condensation process. The partial charge of hydroxo groups changes during the condensation process, owing to the departure of donor water molecules. In general, condensation is limited to dimers. These polycations must be considered as end points in hydrolysis and condensation reactions of monomeric precursors in a given range of pH.

On the contrary, zero charged precursors (h=z) are able to nucleate a solid phase through infinite condensation of "ol" groups. The final term of this process must be a hydroxide $M(OH)_z$ provided oxolation does not occur.

Condensation by oxolation

Oxolation refers the formation of an oxo bridge M-O-M between two metal cations. Such a condensation process is observed when no aquo (OH_2) ligand is available in the coordination sphere of the metal. In general, it occur, with oxo-hydroxo complexes $[MO_x(OH)_{N-x}]^{(N+x-z)-}$ where x<N. As for Fe(III), condensation by oxolation is limited since Fe(III) gives rise only to aquo hydroxo and/ or hydroxo complexes over the whole pH range. When $\delta(H_2O)<0$, the "ol" bridge remains stable and oxolation does not occur. When the partial charge of $\delta(H_2O)>0$, the "ol" bridge is not stable and oxolation can compete with olation.

2.5.3 Effects of anions

In most cases, an anion is present when an inorganic salt is dissolved in water. In some cases, organic or inorganic anionic species are added to the solution so as to control the precipitation process. In any case, anions have marked effect on hydrolysis and condensation reactions. Later in the process, therefore they modify therefore the colloid stability and the structure of solids being formed.

A large variety of anions X^- can enter into the Fe^{3+} aqueous complexes, such as ClO_4^-, NO_3^-, HSO_4^-, $H_2PO_4^-$ or CH_3COO^-. These anions can replace two water molecules and produce $[Fe(X)(OH_2)_4]^{2+}$ species, which can themselves dissociate partly (eq.2.34) or undertake hydrolysis (eq.2.35)

$$[Fe(X)(OH_2)_4]^{2+}_{aq.} \Leftrightarrow [Fe(OH_2)_6]^{3+}_{aq.} + X^-_{aq.} \qquad \text{(eq.2.34)}$$

$$[Fe(OH)(HX)(OH_2)_4]^{2+}_{aq} \leftrightarrow [Fe(OH)(OH_2)_5]^{2+}_{aq} + HX_{aq} \qquad (eq.2.35)$$
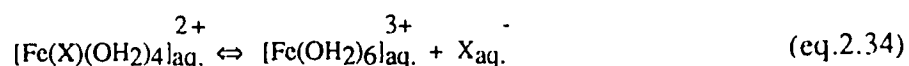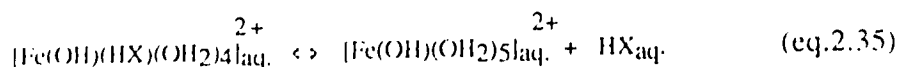
Depending on the strength of the acid HX in aqueous solution, the hydrolyzed species can be reprotonated leading to the non-hydrolyzed $[Fe(OH_2)_6]^{3+}$ precursor. The ability to form complexes for a given anion X^- depends on the electronegativity of X^- and the hydrolysis ratio h of the precursor i.e. the pH of the solution. Studies show that highly electronegative anions such as perchlorates are not able to coordinate Fe·· because of ionic dissociation. They behave as counter ions. However, the hydrolysis ratio h can be decreased by lowering the pH, and complexation occurs under highly acidic conditions. On the other hand, less electronegative anions such as HCO_3^- are able to coordinate Fe^{3+} when the hydrolysis ratio is high, i.e. at high pH. As a consequence, they behave mostly as counter ions except under basic conditions. Some anions such as the sulfates with a mean electronegativity close to that of H_2O are able to form stable complexes over the whole pH range. These anions have a strong effect on both hydrolysis and condensation processes. Special mention must be made of a type of complexation called chelation. It consists in bridging a ligand to a cation by intermediate of several bonds. For example, the Fe^{3+} aqueous species is modified by a strong chelating ligand such as $[(OOCCH_2)_2N - CH_2 - CH_2 - N(CH_2COO)_2]4-$ (or EDTA). In this case, the hydrolysis equation (eq.2.21) and condensation (eq.2.32) must be replaced respectively by (eq.2.36) and (eq.2.37).

$$[Fe(OH_2)_2EDTA]^- + H_2O \leftrightarrow [Fe(OH)(OH_2)EDTA]^{2-} + H_3O^+ \quad Kh = 10^{-2.5} \quad (eq.2.36)$$
$$2[Fe(OH)(OH_2)EDTA]^{2-} \leftrightarrow [Fe_2(OH)_2(EDTA)_2]^{4-} + 2H_2O \quad Kh = 10^{2.95} \quad (eq.2.37)$$
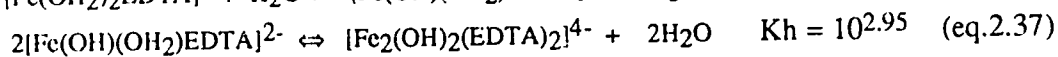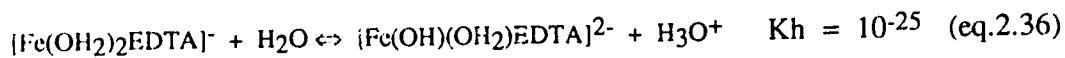
Practically, hydrolysis is prevented by EDTA while condensation is favored. That is to say the formation of a more linear polymer is enhanced.

2.5.4 Sols, gels and precipitates

Calculated values of the water molecule's partial charge $\delta(H_2O)$ in equilibrium with pure aquo-hydroxo complexes and pure hydroxide are given in **Table. 2.4**. These are compared with the solid phases actually known to form. It can be seen that when $\delta(H_2O)<0$, a hydroxide $Fe(OH)_3$ precipitates. On the contrary, when $\delta(H_2O)>0$, the hydroxide is not stable, oxolation occurs and an oxy-hydroxide, FeOOH is obtained.

The effect of the nature of anions on the nature and structure of the metal hydroxide particles generated in different salt solutions has been reported by Matijevic (81). For

example, by aging three different solutions of ferric salts: $Fe(NO_3)_3$, $FeCl_3$ and $Fe(ClO_4)_3$ under identical conditions, the shapes of the obtained particles are different. He also showed that sulfate ions played a crucial role in the formation of ferric hydrous oxide sols.

Table.2.4 Relation between partial charge and the Fe species formed

Aquo-hydroxo complexes	$\delta(H_2O)$ (theoretical)	Pure solid hydroxide formed by olation	$\delta(H_2O)$ (theoretical)	Crystalline phases being actually formed	$\delta(H_2O)$
$[Fe(OH)_2(OH_2)_4]^0$	-0.01	$Fe(OH)_3$	-0.02	$Fe(OH)_2,FeO$	<0
$[Fe(OH)_3(OH_2)_3]^0$	+0.03	$Fe(OH)_3$	+0.07	$FeOOH,Fe_2O_3$	>0

The formation of gels rather than precipitates from aquo-hydroxo inorganic complexes is a rather complicated process which depends on the chemical parameters discussed in the previous sections, that is:

(1) - The chemical composition of the aqueous solution

(2) - The concentration of all reactants

(3) - The temperature

(4) - The order of mixing of the reactants

(5) - The addition mode and the speed of agitation of the solution

Concerning the last point, for instance, when a drop of reactant like NaOH is added to a solution, a pH gradient exists around the drop. Hence, a distribution of different hydrolysis products is formed. All these parameters must be taken into account in order to develop a reproducible chemical recipe.

Monolithic gels are preferentially formed when the rate of condensation is slow. With Fe (III), because the rate of condensation is usually too fast, gelatinous precipitates form generally. Such precipitates can be obtained by addition of a base like NH_3 or NaOH to a number of precursors such as chlorides, sulfates, nitrates, perchlorates, acetates or oxalates. They are amorphous and may have a composition intermediate between α-FeOOH (goethite) and α-Fe_2O_3 (haematite). Upon aging, α-FeOOH is formed at pH>10 and α-Fe_2O_3 is formed at pH<4.

To summarize the process since the beginning, the iron complex $[Fe(OH)_2(OH_2)_4]^+$ (h=2) usually forms a polycation whose mean composition is $[Fe_4O_3(OH)_4]_n^{2n+}$. This polycation gives rise to spheres about 2-4 nm in diameter, which are responsible for the brown-red color of the colloidal solutions. Upon aging, or addition of a base, aggregation occurs

leading to α-FeOOH needles with the same diameter as the original polycation. These needles then undergo an ordered aggregation process producing rod-like particles. The latter form themselves fibrous units called tactoids responsible for the gelatinous aspect of the precipitate. The anions can modify substantially the overall process. In the presence of chloride ions, β-FeOOH precipitates are formed rather than α-FeOOH while in the presence of sulfate ions a base salt precipitates. At high temperature, the h=2 precursor does not form a polycation. It nucleates directly into α-Fe$_2$O$_3$ that may have various morphologies.

CHAPTER 3   EXPERIMENTAL PROCEDURES

3.1 OBJECTIVES OF THE EXPERIMENTAL WORK

As mentioned in **Introduction**, the ternary system, Montmorillonite-Fe(III)-Water, has been chosen as a simplified model of the real oil sands tailings sludge. How well this model represents the behavior and property of the real sludge is open to question. This is the reason why most of the experiments in this present study have been repeated on a reference real oil sands sludge provided by Syncrude Canada Limited.

First, all samples, model montmorillonite samples and sludge references, have been analyzed for their composition and structure by a number of techniques: X-ray diffraction, SEM, EDX and BET porosimetry.

Next, since the real sludge problem is a settling/consolidation problem, the model kinetics of settling and sedimentation have been studied extensively. The parameters include: the nature of electrolyte (water containing Fe), the electrolyte concentration and the pH of the suspensions. A few similar tests have been done also on the reference sludge for comparison purposes.

The structure of a sludge – gel or other – while in its liquid aqueous medium, is largely enigmatic. We could apply here a technique, called hypercritical drying, allowing access to the structure of the sludge with minimal modification. This technique has been applied both to the model and the sludge reference at various electrolyte conditions.

It is necessary to know if the state of a sludge in its aqueous liquid environment is an equilibrium (or quasi-equilibrium) situation . To solve this problem, it is necessary to perform an experiment opposite to settling, that is a swelling experiment. Settling and swelling allow one to "bracket" an eventual equilibrium state of the model and reference sludge.

Before swelling, it is necessary to dry the sample. This provides the opportunity to study the drying behavior. The results of drying at different electrolyte and pH conditions can provide information on a sediment, such as how the strength of its network opposes shrinkage.

The details of the techniques and equipment used are summarized in the next section.

3.2 EXPERIMENT SERIES AND TECHNIQUE

3.2.1 Materials and analysis equipment

Reference sludges and model montmorillonites

Three different types of samples were analyzed in this experiment series: oil sands tailings sludge, SWy-1 montmorillonite, and montmorillonite K10.

In the analysis of the oil sands tailings sludge, two types of samples were used: the first one was kindly provided by Syncrude Canada Limited, and the second one was kindly provided by CANMET. For the sake of simplicity, they will be called respectively reference 1 sludge and reference 2 sludge, unless otherwise specified. These wet samples were dried in an oven and reduced to powder by grinding for a short time (around 20 minutes) with a pestle and a mortar (for X-ray diffraction and SEM observation). It is necessary to point out that prolonged grinding produces marked structural disorder that often leads to complete destruction of the diffraction pattern (82 and 83).

Our model system montmorillonite comprises the reference clay, SWy-1 from the Clay Minerals Society's Source Clay Minerals Repository at the University of Missouri. The cation exchange capacity of this clay is 76 meq/100g and the principal exchange cations are Na and Ca. The surface area as measured by N_2 adsorption is 32 m^2/g (84). Many data have been published on clays from this source, which allows one to discuss their behavior on a consistent basis with respect to previous publications. The C.E.C. and surface area of some reference clays are given in **Table 3.1**.

Table 3.1 C.E.C and specific surface area of some reference clays (84)

	KGa - 1 Kaolinite	SWy - 1 Mont.	STx - 1 Mont.	SAz - 1 Mont.
C.E.C.	2.0 meq/100g	76.4 meq/100g	84.4 meq/100g	120 meq/100g
S.A.	10 m^2/g	32 m^2/g	84 m^2/g	97 m^2/g

Mont. - Montmorillonite; S.A. - Specific surface area with N_2 adsorption.

A second montmorillonite used in our model has been montmorillonite K10 from the Aldrich Chemical Company, Inc. Montmorillonite K10 is used as a catalyst and is

prepared by the chemical processing of montmorillonites. Unfortunately, the information on the chemical processing is not available. Its specific surface area is 220-270 m^2/g, and the bulk density is 300-370 g/L.

X-ray diffraction

A Philips PW-1380 X-ray diffractometer with a scintillation counter probe and a graphite single crystal monochromator was used to obtain the "powder diffraction pattern" of the samples. The radiation of CuKα at 30 kV and 15 mA. These "powder diffraction patterns" were compared with JCPDS (Joint Committee on Powder Diffraction Standards) powder diffraction files for the chemical identification of the samples.

SEM

An ISI (International Scientific Instruments)-60 SEM was used to determine the size and surface morphology of the constituent particles of the samples. SEM provides a magnified and three-dimensional view of clay particle morphology with great depth of focus (85). The powder samples were coated with carbon before observation under the SEM. Due to the resolution limit, the maximum useful magnification of this SEM is 10,000X. Another SEM, Cambridge Stereoscan 250, has been used in the observation of the structure of samples after the hypercritical drying.

EDX

A PGT (Princeton Gamma-Tech) System 4 EDX was used to determine the elemental composition of the samples. This system is qualitative in nature; it only shows what elements are present in the powder samples with no numerical value as to amount. Besides, it cannot detect elements with an atomic number lower than 11 (Na). The elemental composition of the sample surface as a whole and at four particular points were determined for each sample.

BET

The specific surface area of the samples was measured with an AUTOSORB®-1 from the Quantachrome Corporation. The AUTOSORB®-1 operates by measuring the quantity of a specific gas adsorbed onto or desorbed from a solid surface at some equilibrium vapor pressure by the static volumetric method. The volume-pressure data can be reduced by the AUTOSORB®-1 into BET (Brunauer-Emmett-Teller) surface area, Langmuir surface area, adsorption and/or desorption isotherms, pore size and surface area distributions, micropore

volume and surface area using t-plots, total pore volume and average pore radius. For the present study, the data of interest are the specific surface area and the pore size. Before analysis, all samples were outgassed for an hour at T=100°C. The same equipment is used later to determine the effect of flocculation on the specific surface area and pore size.

Hypercritical point drying

A jumbo critical point dryer from Polaron was used for the hypercritical drying.

Humidity Cabinet

A humidity cabinet, Model LHU-112M-U from ESPEC Corp., was used to control the temperature and humidity in the drying experiments.

Particle size analyzer

A LAB-TEC™100 size analyzer from Laser Sensor Technology Inc. was used for the analysis of particle size distribution.

3.2.2 Flocculation and sedimentation experiments

Montmorillonite-Fe(III)-Water model system

The solid content (by mass) of SWy-1 montmorillonite suspensions was chosen as 0.5%, after preliminary experiments showing that when the solid content increases to about 2%, a montmorillonite gel is formed instead of a suspension. 0.5% montmorillonite suspensions were prepared by adding the clay (as received) to distilled water and stirring the mixture for 30 minutes with a magnetic stirrer. The suspensions were prepared at room temperature (23°±1° C) just prior to their use, and their pH was measured and adjusted with an Accumet pH meter (Model 950). The pH of fresh 0.5% SWy-1 montmorillonite suspensions, without any adjustment, varied between 9.4 and 9.5. The pH adjustment was performed by adding HNO_3 or $NaOH$.

Seven initial pH values of the suspensions were investigated: 2.1, 4.1, 6.0, 8.0, 9.4 (no pH adjustment), 10.0 and 11.8. At each pH, six different $FeCl_3$ concentration were examined: 0 (pure clay), 0.5, 1, 2, 5 and 10-- in millimoles (mM) per litre. This was designed to evaluate the effects of the initial pH of the suspension and $FeCl_3$ concentration on the stability and settling of the montmorillonite suspensions. Note $FeCl_3$ solutions are acidic, and decrease the pH value of the suspensions. Fresh $FeCl_3$ solution was always prepared just prior to use.

Experiments were conducted by introducing suspensions with a given pH value into six 100 mL graduated cylinders with an inside diameter of 28 mm and adding an appropriate amount of the electrolyte, itself dissolved in water. The initial suspension volume for all samples was 100 mL. Just after preparation, the cylinders were covered with a parafilm to prevent water evaporation. Then, these cylinders were hand-shaken forcefully to distribute the components uniformly inside the suspensions. The cylinder diameter was sufficiently large to neglect the wall effect according to a previous study by Michaels and Bolger (71).

To investigate the effect of the nature of ions, supplementary experiments were carried out with the electrolytes $Fe_2(SO_4)_3$, $FeSO_4$ and $NaCl$, at pH=9.4 where no pH adjustment of the 0.5% montmorillonite suspensions was necessary.

Each time a sediment separated from the supernatant liquid, the type of interface (diffusive or sharp) was noted. Whenever a sharp separation occurred, the position of the separation plane was read every 10 minutes during the first hour, then every hour for the following three hours, and finally every 24 hours until 240 hours. The sedimentation data were obtained in a $23°\pm1$ °C constant temperature lab.

Montmorillonite K10 suspensions

The experimental procedure for 0.5% montmorillonite K10 suspensions was similar to 0.5% SWy-1 montmorillonite suspensions except for the following difference:
The pH of 0.5 % montmorillonite K10 suspensions varied between 3.7 and 3.9. In addition to $FeCl_3$, other electrolytes NH_4OH, H_2SO_4, HCl, and $Fe_2(SO_4)_3$ have also been used. Both the effect of electrolytes and the pH of the suspensions were investigated.

Reference sludge

In order to compare the results of the model system with those of reference sludges, flocculation and sedimentation experiments were also performed on the 0.5% reference 1 sludge suspensions with no pH adjustment.

The effect of pH on the stability of the oil sands tailings sludge has also been examined. The pH of the 0.5% reference 1 suspensions was adjusted with acids (HNO_3, H_2SO_4 and HCl) or bases ($NaOH$ and NH_4OH), added from a 50 mL titration burette. This was conducted in a 500 mL beaker with a 300 mL suspension volume. The concentration of acids or bases was decreased progressively from concentrated to very dilute so that a

critical pH value could be determined below which or above which flocculation occurred in a given standing time. The standing time was chosen as five minutes.

The effect of the solid content on the stability of tailings sludge was examined on 1%, 5%, 10%, and 15% reference 1 sludge suspensions. For this experiment, the standing time was chosen as 24 hours. $Fe_2(SO_4)_3$, $FeCl_3$ and H_2SO_4 were used as flocculants.

All chemicals used in this study were reagent grade.

3.2.3 SEM observation of the structure of sediments

This experiment series has focussed on the direct observation of the structure of the settled sediments and how flocculation affects the structure. Both model sediments and reference sludge sediments have been examined.

Hypercritical point drying technique

In this experiment, the hypercritical point drying technique (HPD) has been used to prepare samples for observation under the SEM. T . HPD technique makes use of the existence of a critical point beyond which no distinction between a liquid and its vapor can be made. This critical point is characterized by a critical temperature Tc and a critic pressure Pc. For pressures P<Pc, a phase transformation between the liquid and the ga , exists. It is described by a vaporization temperature Tvop, wh depends on the pressure P, and a latent heat. A sharp interface exists between the liquid and the gas.

The HPD technique consists in filling up completely a cell containing the sample to be dried with a liquid like liquid CO_2 (point I in Fig.3.1). The sample cell is filled with liquid and the liquid pressure is brought beyond Pc, and the cell is closed (point A in Fig.3.1). Then the temperature is raised above Tc (point B). We are now beyond the critical point, the pressure can be decreased below 1 atm, by pumping down to Point C. The fluid has transformed uniformly into a gas without forming a liquid-gas interface, even inside the sediment pores. It can be pumped out completely without creating a meniscus responsible for the sediment shrinkage. Finally, when empty (filled with air), the temperature can be decreased to room temperature. The drying route has turned around the critical point, and is called hypercritical. This technique has the advantage of preserving the morphology of samples containing liquid while limiting the shrinkage of samples to a minimal extent.

P

A ───────────────────► B

Pc ─ ─ ─ ─ ─ ─ ─ ─

Solid   1   Liquid

1 atm ─ ─ ─ ─ ─ ─ ─

Initial state

Critical point

Final state   Gas   C

20°C   Tm   Tc   T
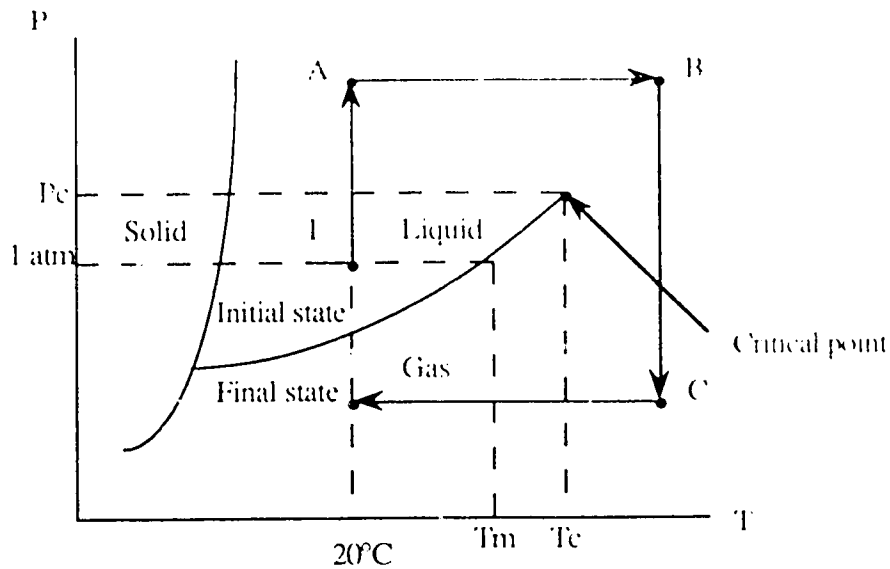
Fig.3.1 Illustration of the hypercritical drying route.

The hypercritical drying can be done with any fluid, particularly water. However, the critical point of water is very high, Tc= 374.15°C and Pc=22 11 MPa.. Hence, this is a dangerous one. It is much easier with carbon dioxide of which Tc=31.5°C and Pc=7.586 MPa. It requires therefore replacing the water in the sediment by liquid CO_2, which can be done progressively by diffusion.

Sample preparation

Actually, water is not easy to replace directly by liquid CO_2. It is more convenient to replace water first by acetone, then to substitute liquid CO_2 for acetone. Each of the samples has been prepared in the following ways: first, the wet sample was taken from the bottom sediments in the cylinders with a pipet and placed into a vial. Then, 99.5% (minimum) acetone was added to the vial to exchange with the water contained in the sample. Slowly, acetone diffuses into water. 15 minutes later, the supernatant liquid, an acetone-water solution, was again replaced by pure acetone. This procedure was repeated five times so that all or almost all water in the sample was replaced by acetone. Then, the sample was placed in a capsule permeable to liquid, but not to the sediment particles. The capsule was placed in the critical point drier. Liquid CO_2 was flushed several times to replace acetone. And finally, the hypercritical drying route was applied. The operating temperature was 35-40°C, and the operating pressure was 8.276-9.655 MPa.

The samples we have dried by this technique comprised SWy-1 montmorillonite models and reference sludges, all with 0.5% initial solid content. The reference sludge samples were made without any pH adjustment before FeCl₃ addition.

At the end of the flocculation and sedimentation experiments, two sa les from the sediments of the 0.5% SWy-1 montmorillonite suspensions at pH 9.4 were prepared using the hypercritical drying technique: one from the cylinder without any addition of FeCl₃, which has the lowest sediment volume, the other from the cylinder with 5 mM FeCl₃, which has the highest sediment volume. For reference 1 sludge, three samples from the sediments of 0.5% reference 1 sludge suspensions were prepared: the first without FeCl₃, the second with 1 mM FeCl₃, and the third with 5 mM FeCl₃.

For reference 2 sludge , the sample preparation was somewhat different. Three samples were prepared One was from the sediment of reference 2 sludge as supplied without any treatment (the solid content of the sediment was 25%). The second one was from the sediment of a 0.5% sludge refere 2 suspension flocculated by 5 mM FeCl₃. The 0.5% sludge reference 2 was prepared in the same way as the montmorillonite suspensions and reference 1 sludge suspensions in a 100 mL cylinder. The third sample was prepared from the sediment of a 0.5% reference 2 sludge suspension in which the initial liquid had been replaced by a 60% acetone and 40% distilled water solution. As will be explained in the next chapter, this solution had a special effect on the flocculation of sludge reference 2.

3.2.4 Drying behavior of the model system

Experiment 1   Aspects of dried materials

In this experiment, two groups of d   tests were conducted. For the first group, six 50 mm (outside diameter) x 70 mm (height) beakers were used. Each beaker contained 100g of 5% Wy-1 montmorillonite gel, and the non-potential determining electrolyte was Fe₂(SO₄)₃ with respective molarities: 0, 0.1, 0.5, 1, 2 and 5 mM. Clay content of 5% was chosen so that the volume of dried samples was high enough for observation. These samples were dried in the humidity cabinet set at R.H.=95% and T=25°C. The aspects of the dried material were examined. After drying, the dried samples were broken manually along the edges and observed under a SEM (the same model as used in sample analysis) so that their packing pattern could be examined. Later, it was found that the air velocity in the humidity cabinet was location dependent, and the drying rate of the samples was affected

significantly by their location in the cabinet. As a result, the drying data of this group was not valid for the assessment of the effect of electrolyte concentration.

To examine the effect of electrolyte concentration on the drying kinetics, a second group of samples was dried in constant lab conditions. This group consisted of eight 125 mm (outside diameter) x 65 mm (height) Pyrex crystallizing dishes, with one dish containing only distilled water for normalization purposes. The other dishes each contained 100 g of a 5% SWy-1 montmorillonite suspension with FeCl₃ as the electrolyte, at respective concentrations: 0, 0.5, 1, 2, 5, 10 and 20 mM. The evolution of the sample mass with time was recorded and corrected for the fluctuations in the drying environment, by calibrating against the drying of distilled water. After the drying was completed, distilled water was added to each dried sample to examine the effect of electrolyte concentration on the swelling of SWy-1 montmorillonite.

Experiment 2   Microstructure of 5% montmorillonite gel near leatherhard point

Two groups of identical samples were prepared. Each group consisted of six 70 mm (outside diameter) x 50 mm (height) crystallizing dishes. Each dish contain 100 g of 5% SWy-1 montmorillonite suspensions with the FeCl₃ concentration for dish #1 to #6 bein. 0, 0.5, 1, 2, 5 and 10 mM, respectively. The first group was for the determination of drying kinetics (mass vs. time). The second was for the SEM observation of the drying materials at the end of the constant drying period. In the scientific literature (see literature review Section 2.4), the end point of the constant drying period has been called the leatherhard point or drying critical point. To avoid confusion between the liquid critical point (concerning the hypercritical drying) and the drying critical point (concerning drying kinetics), the constant drying end point will be called leatherhard point here. The drying of all samples was carried out at the constant lab conditions. After drying for 282 hours, all samples are close to the leatherhard point, and a portion of the drying material from each sample was taken out and prepared for SEM observation according to the same procedure as mentioned in Section 3.2.3. It is necessary to point out that some minor extent of shrinkage for all samples was observed after 282 hours.

Experiment 3   pH and FeCl₃ concentration effect

This experiment was conducted on 0.5% SWy-1 montmorillonite model suspensions. Four initial suspension pH values were investigated: 2.0, 4.0, 9.4 (no pH adjustment) and 10.0, corresponding to four groups of samples. At each pH, six different FeCl₃ concentrations

were examined: 0, 0.5, 1, 2, 5 and 10 mM. When a gel point was reached, a part of the gel was taken out and dried using the hypercritical drying technique for observation under the SEM. In this study, the gel point was considered to be passed when the sample did not flow upon tilting its dish.

For each pH, this has been done with three FeCl₃ concentrations: respectively 0, 0.5 and 5 mM. Duplicate samples were used to record the complete drying curve. The time for each sample to reach the gel point and the mass at the gel point were recorded. In order that the fluctuations of the drying environment could be calibrated, an additional dish containing only distilled water for each group sample was prepared. Therefore, 10 dishes were used for each pH (see Table 3.2), that is, 40 crystallizing dishes with 70 mm (outside diameter) by 50 mm (height). Each dish (except those containing only distilled water) contained 100 g 0.5% montmorillonite suspensions including the FeCl₃ solution added. The evolution of the sample mass with time was recorded.

Table 3.2 List of samples on which drying was studied for each pH (2, 4, 9.4 and 10)

Sample No.	1	1"	2	2"	3	4	5	5"	6	7
FeCl₃ conc.(mM)	0	0	0.5	0.5	1	2	5	5	10	water

The mass was measured at regular time lapses. For each sample, the gel point was therefore not determined exactly, but was bracketed between two data point.

3.2.5 Swelling of montmorillonite

Experiment 1   Electrolyte concentration effect

Six 100 mL graduated cylinders numbered from #1 to #6 were used. The sample characteristics were different not only for their content but also for their preparation procedures, as illustrated in Fig.3.2 and described in **Table 3.3**.

The clay volume at the bottom of cylinders was recorded as a function of time. The swelling of sample #1 and #2 was performed twice. When the first swelling test was finished, these two samples were dried in the humidity cabinet at the same condition as sample #3 to #6, then 99.5 g distilled water was added to each sample. The second swelling test of these two samples began simultaneously with the swelling test of samples #3 to #6.

Table 3.3   Description of sample preparation for the electrolyte effect on swelling

Sample #1 (#1 cylinder)	0.5 g SWy-1montmorillonite dry powder was placed to the bottom of the cylinder and shaken gently so as to make the top surface flat. Then, 99.5 g distilled water was gently added along the wall of the cylinder to minimize the dispersion cause by the water flow. The cylinder was covered with a parafilm to prevent evaporation.
Sample #2 (#2 cylinder)	Similar to #1 except that 99.5 g of freshly prepared 5 mM FeCl$_3$ solution was added instead of distilled water.
Sample #3 (#3 cylinder)	100 g 0.5% SWy-1 montmorillonite suspension with no FeCl$_3$ added was added to the cylinder and dried in the humidity cabinet at a set relative humidity (R.H. = 50% and T = 60°). When it was dried, a small amount of material that stuck to the wall was scratched down with a long spoon. Then 99.5 g distilled water was added in the above-mentioned way.
Sample #4 (#4 cylinder)	Similar to sample #3 except in the last step 99.5 g of freshly prepared 5 mM FeCl$_3$ solution was added.
Sample #5 (#5 cylinder)	Similar to sample #3 except that the FeCl$_3$ concentration of the initial 0.5% SWy-1 montmorillonite suspension was 5 mM.
Sample #6 (#6 cylinder)	Similar to sample #5 except that later 99.5 g of freshly prepared 5 mM FeCl$_3$ solution was added.

Experiment 2   Solid content effect

Two groups of samples were prepared. Two 100 mL graduated cylinders were used for each group. The sample preparation is given as follows:

Group 1 (sample #1 and #2) - 0.5 g SWy-1 montmorillonite powder was placed at the bottom of each cylinder. Then, 99.5 g distilled water was added gently along the wall of the cylinder.

Group 2 (sample #3 and #4) - 1 g SWy-1 montmorillonite powder was placed at the bottom of each cylinder. Then, 99 g distilled water was added gently along the wall of the cylinder.

Experiment 3 Medium effect

In this experiment, the swelling behavior of montmorillonite in different media was studied. Two polar media, ethanol (C_2H_5OH) and acetone (CH_3COCH_3), were used. Two series of tests were conducted. For each series, 8 samples were prepared. The sample preparation is given below:

Series 1 Ethanol

Sample #1 - 0.5 g SWy-1 montmorillonite powder was placed at the bottom of a 100 mL graduated cylinder, then 99.5 g of 100% ethanol (close to 100%) was added gently along the wall of the cylinder.

Sample #2 to #8 - similar to sample #1 except the concentration of the ethanol added decreased progressively from #2 to #8 being respectively; 95%, 90%, 80%, 65%, 50%, 25% and 5%.

Series 2 Acetone

Exactly the same as that of series 1 except that acetone was used instead of ethanol.

Sample #1

Mt. Powder

Add distilled water

Parafilm

Sample #2   Mt. Powder

Add 5 mM FeCl3

Parafilm

Sample #3

0.5% Mt. suspension

No FeCl3

Drying

Scratching

Parafilm

Distilled water added
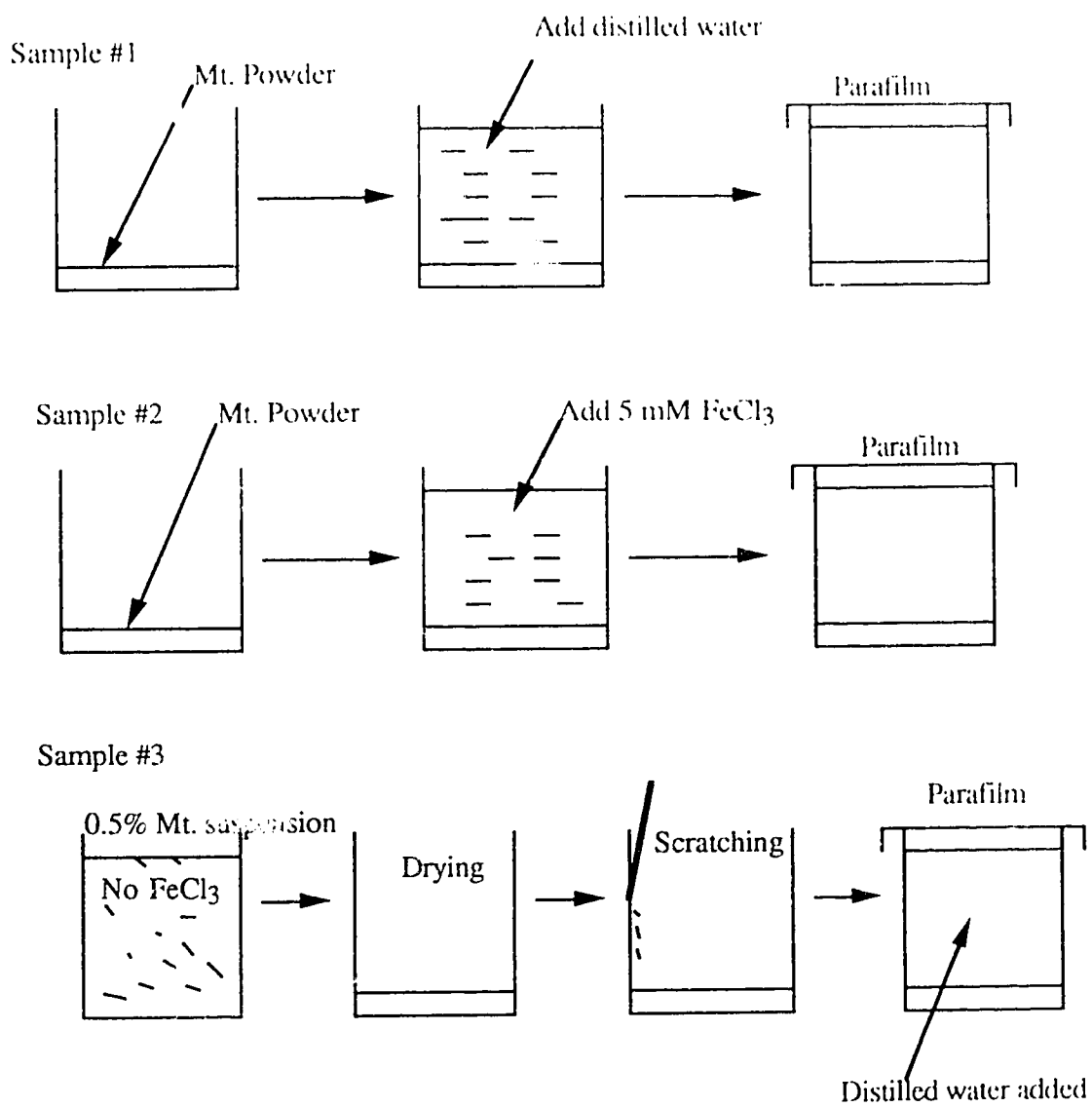
Fig.3.2   Illustration of the sample preparation for the effect of electrolyte on the swelling of montmorillonite (Mt.).

Sample #4

0.5% Mt. suspension

5 mM FeCl$_3$ added

Sample #5

0.5% Mt. suspension

Distilled water added

Sample #6

0.5% Mt. suspension

5 mM FeCl$_3$ added
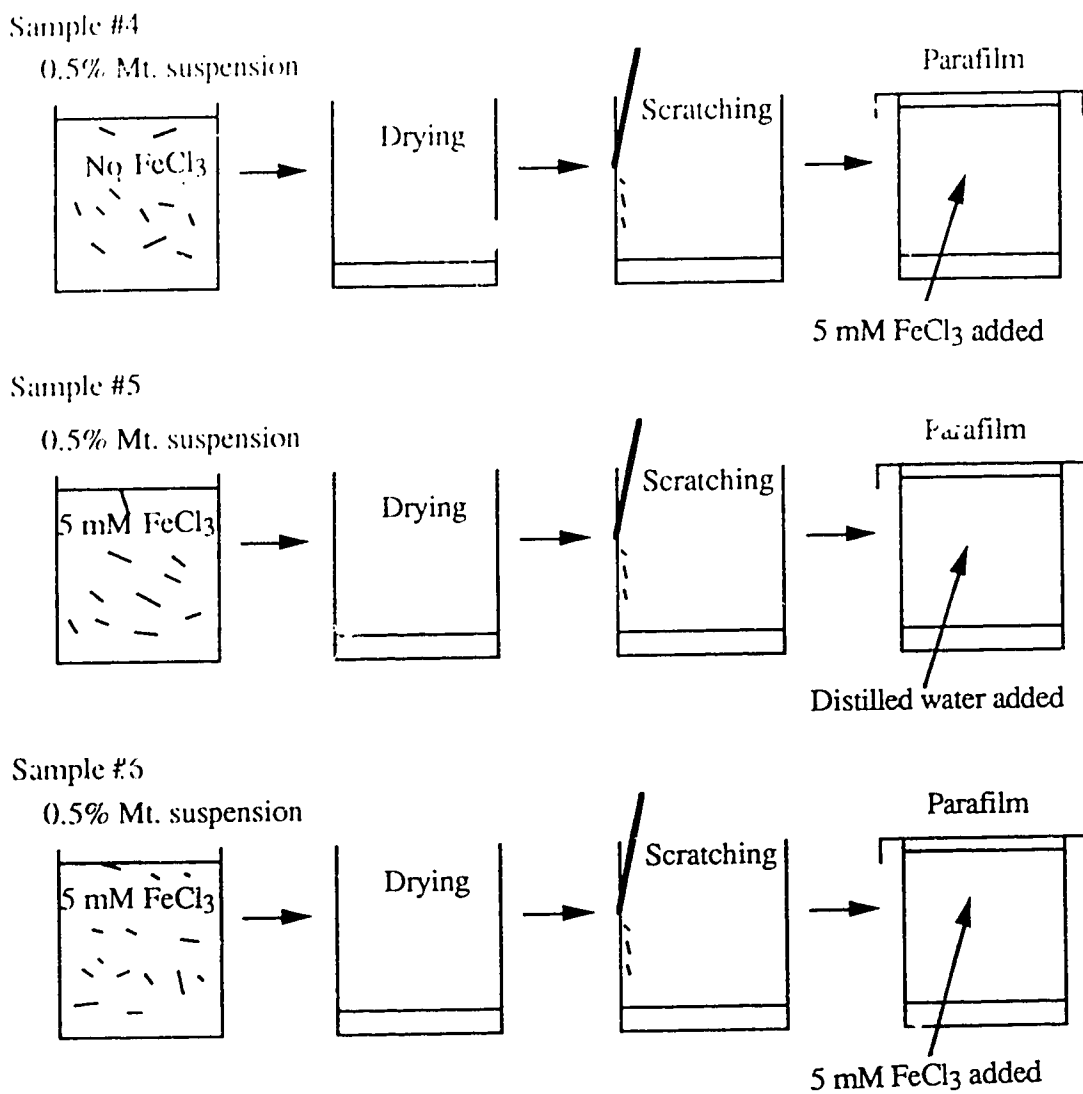
Fig.3.2 (Continued)

CHAPTER 4   EXPERIMENTAL RESULTS

4.1 SAMPLE ANALYSIS

4.1.1 X-ray diffraction

The X-ray diffraction pattern of a reference sludge sample is shown in Fig.4.1a. The broadening of X-ray diffraction peaks is inversely proportional to the grain size according to Scherrer's formula. It begins to be noticeable for a grain size smaller than 3 nm, and is largest with amorphous materials where the grain is of the order of a few molecules, and hence a crystal has no more meaning. Amorphous structures can be obtained by extensive shearing, for instance with platelike materials like clays (83). Here, the diffraction peaks are sharp; therefore, one can consider this tailings sludge is composed of a high portion of well crystallized quartz particles and less well-defined clay particles. Note that some peaks are shared by two types of clays. Given the high portion of well crystallized materials in this tailings sludge sample, the presence of amorphous materials, or of clay platelets with a dimension less than 3 nm would be expected to be difficult to notice. Quartz gives high intensity diffraction peaks. A moderate portion is therefore sufficient to observe it in a mixture. The major components of reference 1 sludge are therefore actually kaolinite and possibly illite and chlorite-montmorillonite. However, the X-ray diffraction pattern does not give a quantitative description of the components.

The results of the particle size distribution of two 0.5% (by mass) reference 1 sludge suspensions show that the size of 25% of the particles is less than 1 μm (see table 4.1). That is, 25% of the particles are colloidal while the rest are non-colloidal. In summary, the major solid component of this reference 1 sludge is non-colloidal, crystalline.

The X-ray diffraction pattern of a reference 2 sludge sample is shown in Fig.4.1b. It is basically the same as that of the reference 1 sludge except that a new component, siderite, is detected.

The X-ray diffraction pattern of SWy-1 montmorillonite and montmorillonite K10 are similar, as shown in Fig.4.2a and b; respectively. Although, SWy-1 montmorillonite is used as a reference clay, it still contains some impurities: here quartz and illite. As for montmorillonite K10, it is a mixture of illite and montmorillonite with a higher content of quartz impurity.

Table 4.1 The particle size distribution of reference 1 sludge

Particle size (μm)	Percentage, % (by count) sample #1	Percentage, % (by count) sample #2
<1	25	25
1	14	14
2	20	20
4	21	21
8	15	15
15	5	5
30	0	0
60	0	0

4.1.2 SEM and EDX

The dried reference 1 sludge sample appears under the SEM as being composed of aggregates or particles linked by a continuous cement (Fig.4.3). The size of the aggregates or particles ranges from a few μm up to 50 μm.

The EDX examination of one reference 1 sludge sample under the SEM shows that Fe is an important constituent element as well as Si and Al (Fig.4.3). However, Fe itself could come from two sources: structural Fe and impurity Fe. The portion of structural Fe (such as Fe in the illite layer structure) and impurity Fe cannot be determined by EDX. Nonetheless, its distribution is far from being uniform. Fe is found in abundance in local spots while it is missing in others, within the precision of EDX (a few % in mass). Very often, but not always, Fe is also present altogether with S, and when S is present, the amount of Fe present increases dramatically (point 1 and 4), suggesting pyrite FeS_2 as a non-negligible compound in actual sludges. A portion of the Fe may come from iron oxide which is often associated with clays. Unfortunately the EDX equipment used cannot detect the presence of oxygen. The EDX examination confirms the X-ray diffraction pattern of the tailings sludge for the presence of Si, Al, Fe, Ca and K in kaolinite, illite and quartz.

The SEM and EDX of a reference 2 sludge, SWy-1 montmorillonite and montmorillonite K10 sample are shown in Fig.4.4, Fig.4.5 and Fig.4.6, respectively. The SEM of these
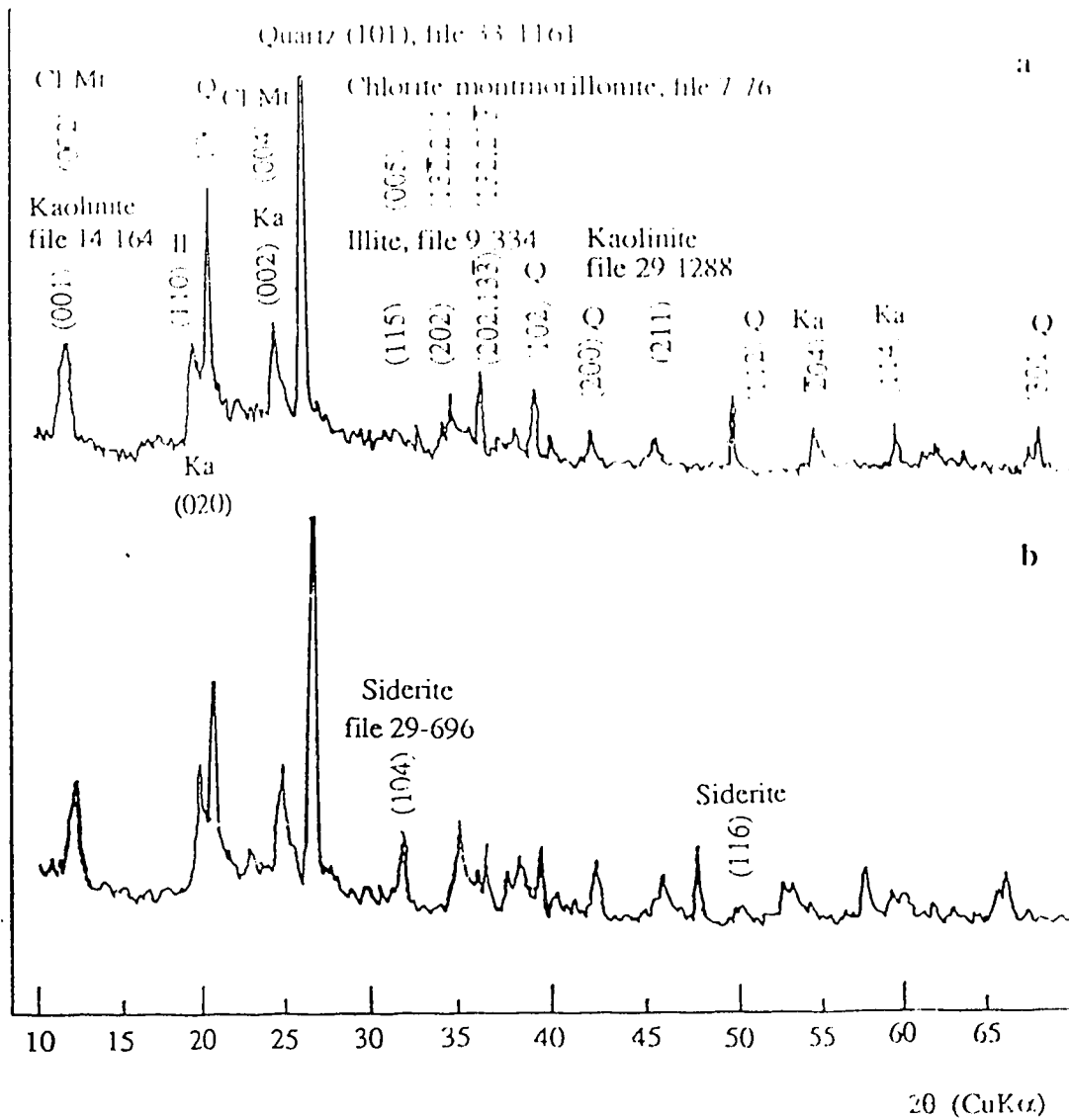
Fig.4.1 X-ray diffraction patterns of tailings sludge samples: (a) reference 1 sludge; (b) reference 2 sludge.
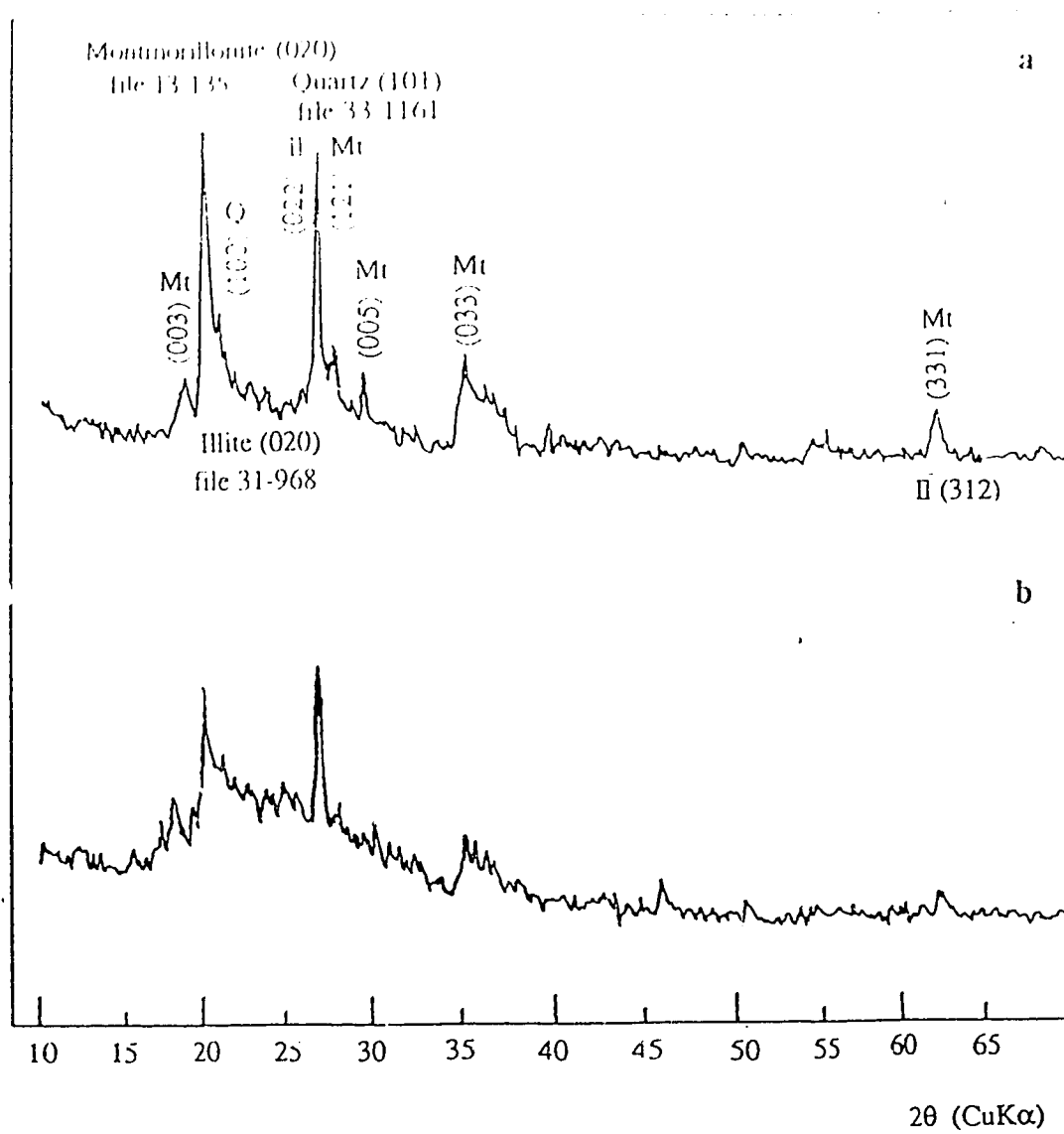
Fig.4.2 X-ray diffraction patterns of montmorillonites: (a) SWy-1 montmorillonite;
(b) montmorillonite K10.
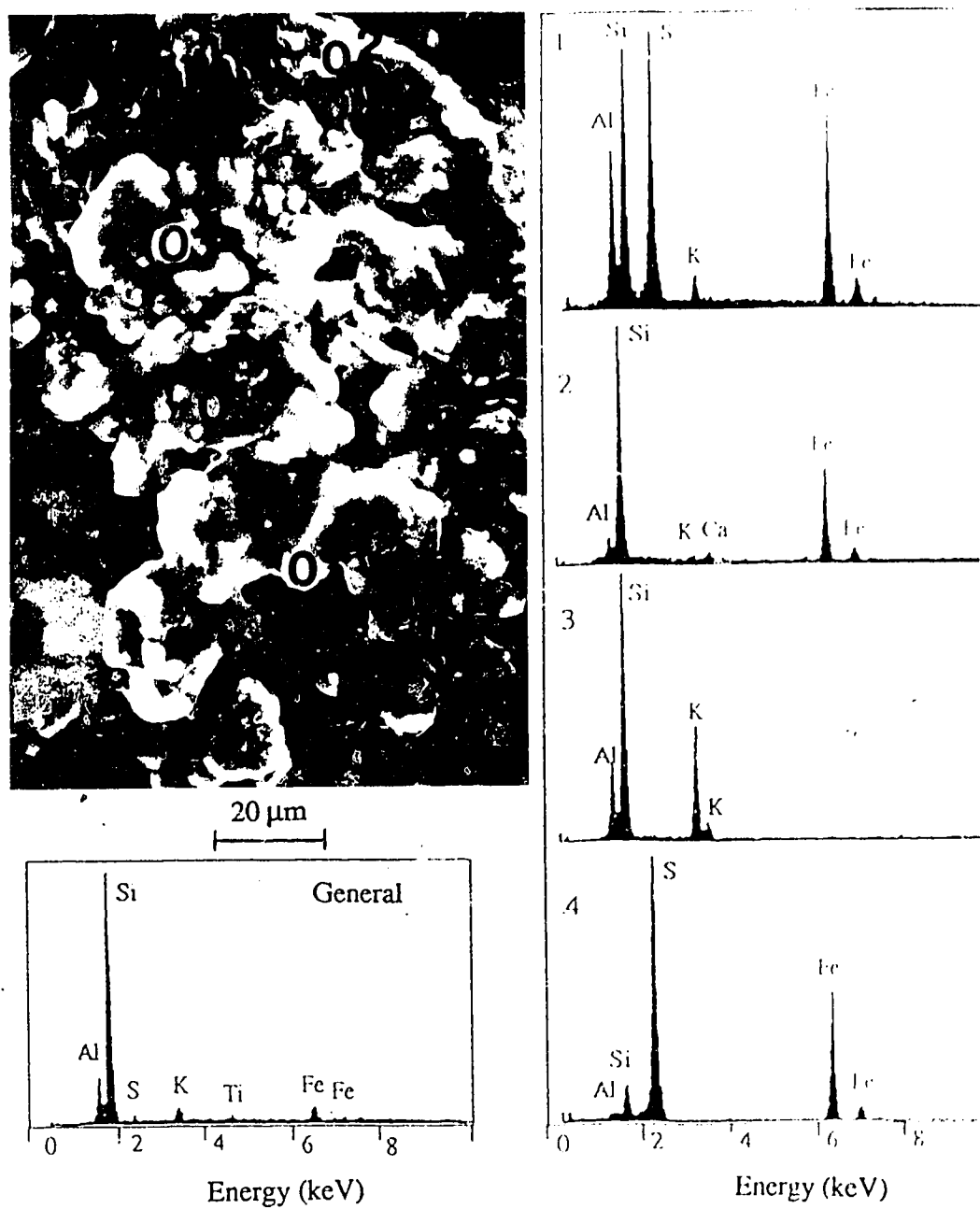
Fig.4.3 SEM and EDX of one reference 1 sludge sample.
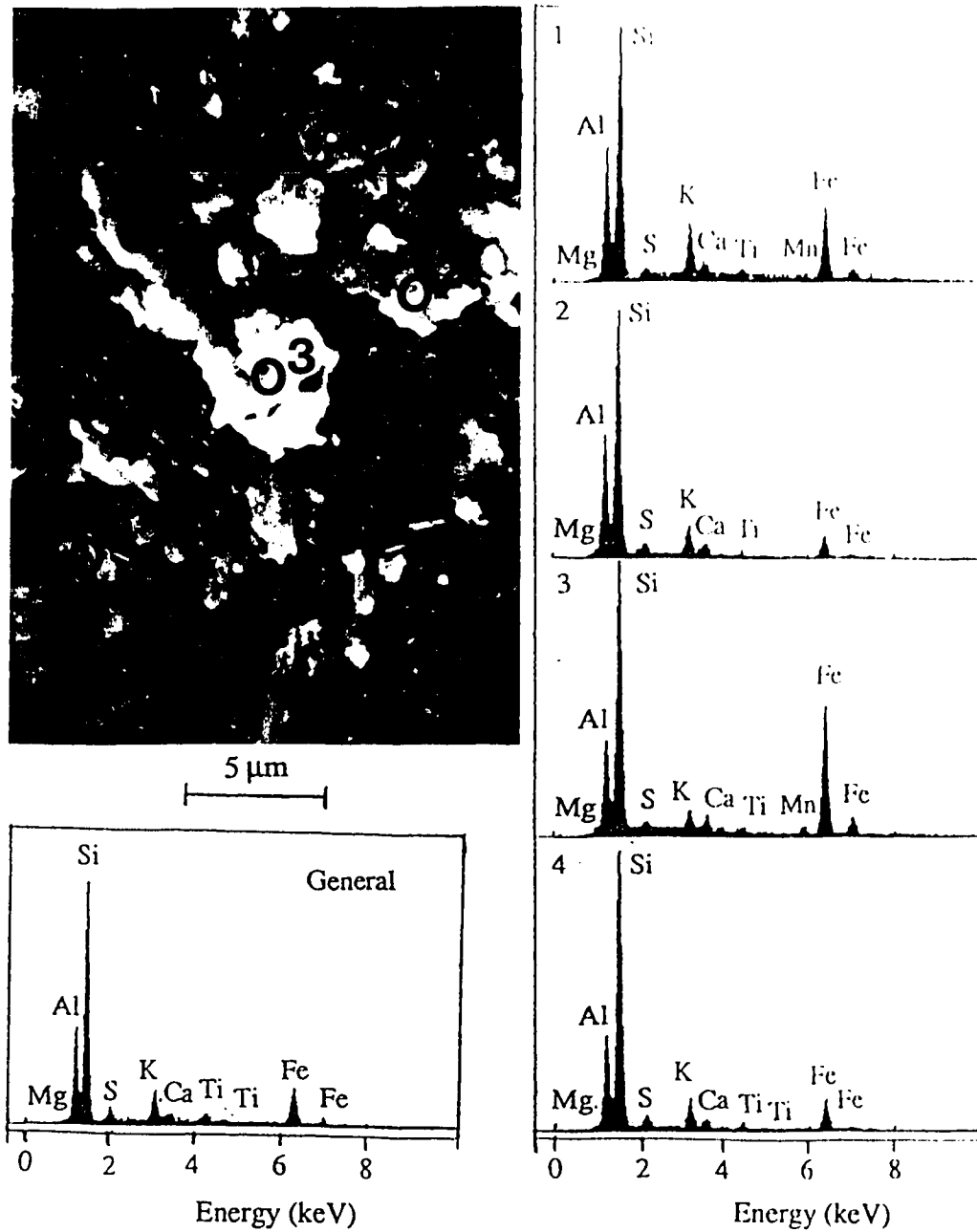
Fig.4.4   SEM and EDX of one reference 2 sludge sample.
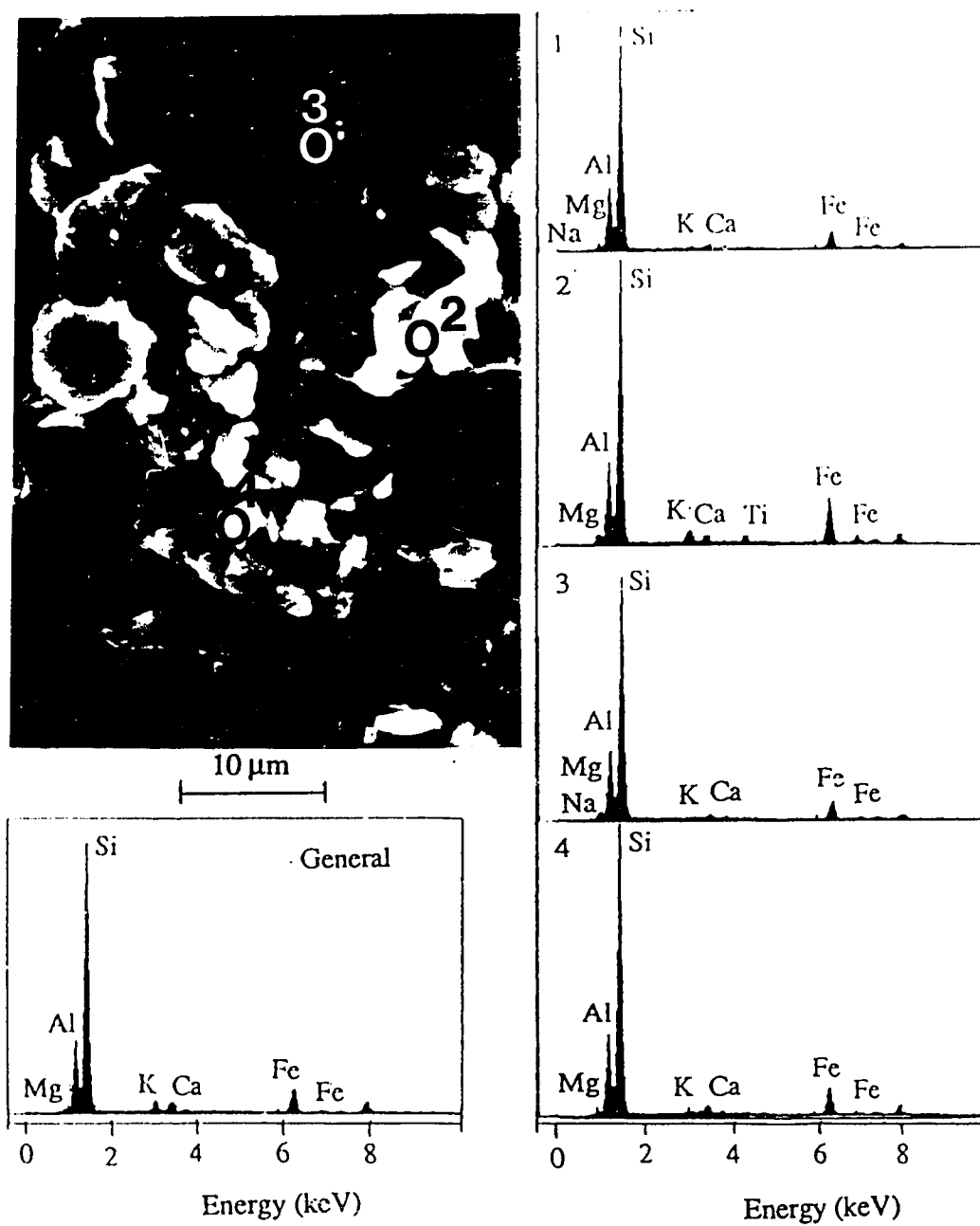
Fig.4.5   SEM and EDX of one SWy-1 montmorillonite sample.
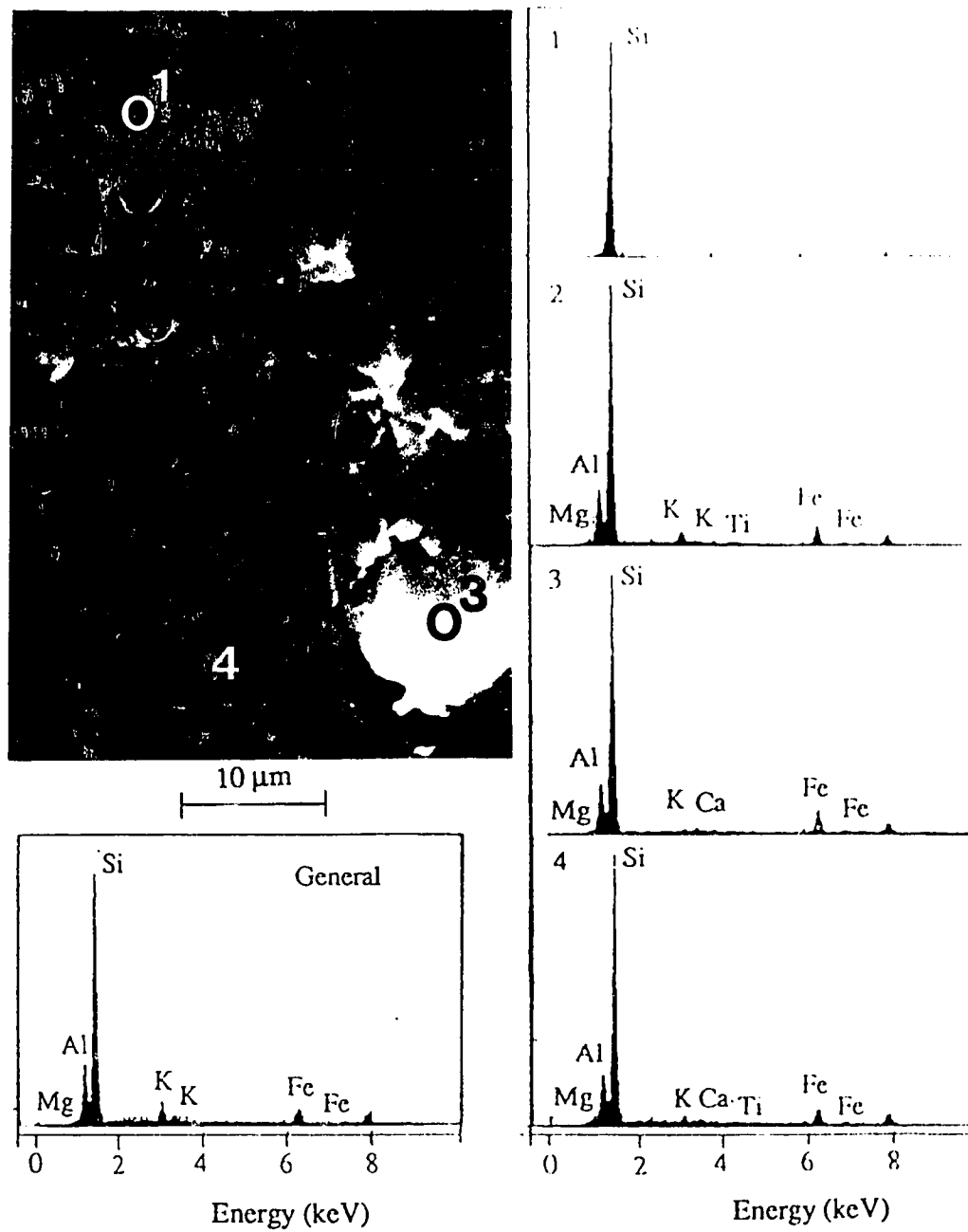
Fig.4.6   SEM and EDX of one montmorillonite K10 sample.

samples shows that all samples are composed of particles or aggregates with a wide size range. For the reference 2 sludge, more elements, Mg, Ti and Mn, are detected.

In a first approximation, the dry raw aspect and the element composition of SWy-1 montmorillonite is very close to that of the reference 1 and 2 sludge samples. Some secondary difference concerning Fe and S exists. No detectable amount of S is observed in SWy-1, and the Fe amount present is significantly less than in the reference sludges. FeS_2 is therefore possibly a secondary component not taken into account in our model compared to the reference sludges. The same difference is maintained between montmorillonite K10 and the reference sludges. Montmorillonite K10 also contains big silica (point 1 in Fig.4.6).

4.1.3 BET

The specific surface area of reference 1 sludge samples, the average of three samples, is 6.7 m^2/g, while the average pore size is 22.6 nm. The specific surface area and the average pore size of reference 1 sludge, SWy-1 montmorillonite and montmorillonite K10 are summarized in **Table 4.2**.

Table 4.2 Summary of surface area and average pore size for samples from different sources

Sample description	Specific surface area (m^2/g)	Average pore size (radius in nm)
Reference 1 Sludge	6.7 ± 0.8	22±2
SWy-1 montmorillonite	25±4	8.5±0.5
Montmorillonite K10	256±7	3.15±0.05

Note: ± error on different samples.

4.2 FLOCCULATION AND SEDIMENTATION

4.2.1 Montmorillonite-Fe(III)-Water model system

Types of qualitative behaviors

Depending on the electrolyte concentration and the pH of the montmorillonite suspensions, two types of segregation are observed: two-layer or three layer segregation, as illustrated on Fig.4.7, 4.8 and 4.9. Each layer corresponds to a different solid content.
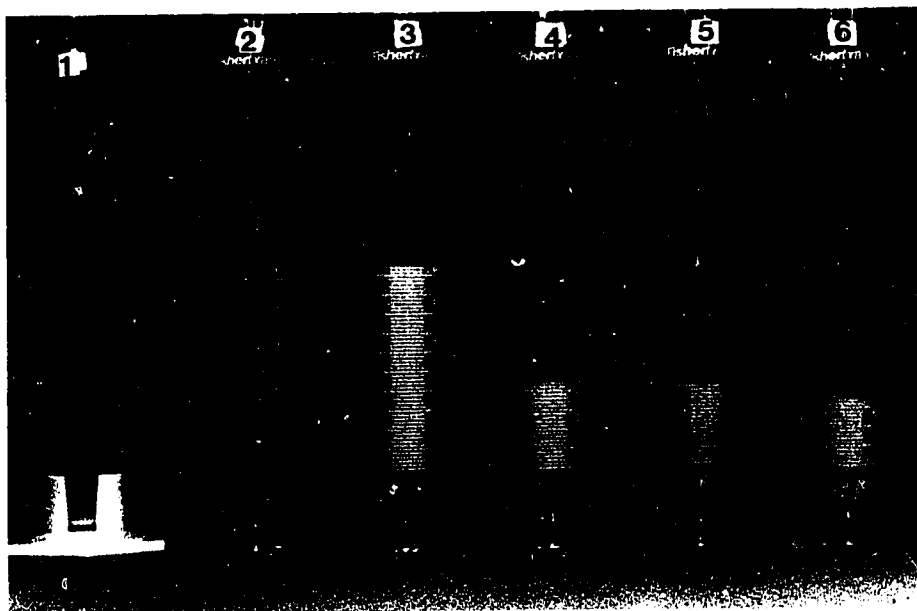
Fig.4.7 Three layer (#1 and #2) and two layer segregation (#3-#6) of 0.5% SWy-1
montmorillonite suspensions with different FeSO$_4$ concentrations at pH 9.4
after standing for 52 hours, FeSO$_4$ concentration in mM from sample #1
to sample #6: 0, 0.5, 1, 2, 5 and 10.

Fig.4.8   Three layer (#1) and two layer segregation (#2-#6) of 0.5% SWy-1
montmorillonite suspensions with different FeCl3 concentrations at pH 9.4
after standing for 240 hours, FeCl3 concentration in mM from sample #1
to sample #6: 0, 0.5, 1, 2, 5 and 10.
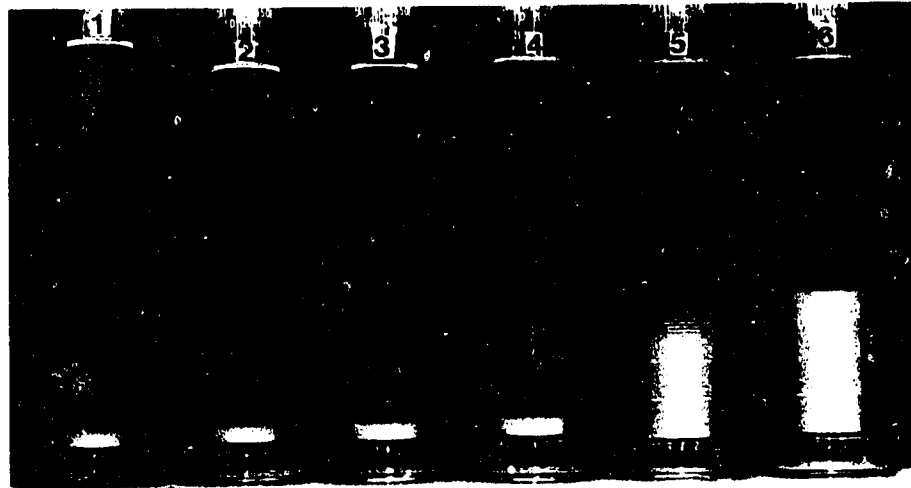
Fig.4.9　Three layer (#1-#4) and two layer segregation (#5 and #6) of 0.5% SWy-1
montmorillonite suspensions with different NaCl concentrations at pH 9.4
after standing for 240 hours, NaCl concentration in mM from sample #1
to sample #6: 0, 0.5, 1, 2, 5 and 10.

When two layers are formed, flocculation occurred (for example, samples 3 to 6 in
Fig.4.7), the flocs settling in a layer (or zone settling) with a sharp flat interface between
the upper clear liquid and the lower sediment layer. Note that the lower sediment layer
looks like a montmorillonite gel. This sediment has a solid content varying between 1% and
5% depe.:ding on conditions and time. However, it is still a fluid : if the cylinder is tilted, it

flows easily. It is therefore not a gel. It is called here **liquid-like sediment**. Most probably, each floc is the beginning of a gel network, but sedimentation occurred before complete gelation could be achieved. Its slow consolidation, nonetheless, could be considered as a typical syneresis of a gel. That is, a slow shrinkage upon ageing. The upper clear liquid is referred as **supernatant liquid**. It does not seem to contain any solid. The transition between the two layers is sharp.

When three layers are present, the suspension is relatively stable with respect to flocculation (for example, samples 1 and 2 on Fig.4.7); the bottom layer does not seem to flow when the cylinder is tilted. It is called **solid-like sediment**. At the upper part of the cylinder is the supernatant liquid. A new layer called **colloidal suspension**, however, emerges between the solid-like sediment and the supernatant liquid. The solid content of this colloidal suspension is much lower than that of the solid-like sediment. Its transition is sharp with the solid-like sediment layer, but gradual with the supernatant liquid.
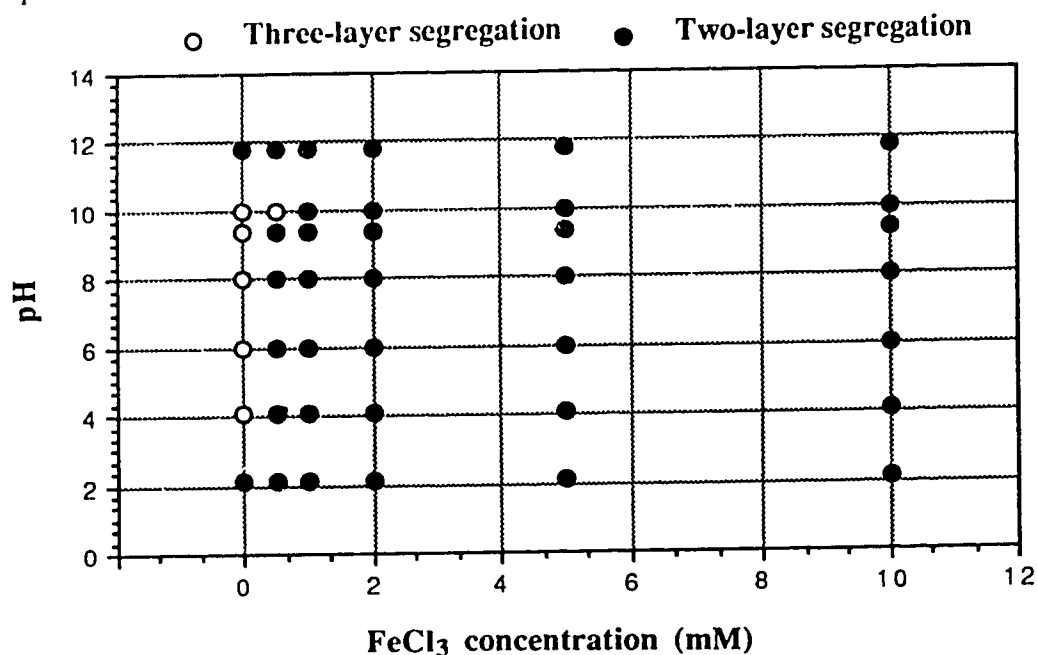
Fig.4.10 State diagram of 0.5% SWy-1 suspensions at different FeCl3 concentrations and suspension pH.

A state diagram of our model system gathering the pH and FeCl3 concentrations where three layers, or two layers occur, is shown on Fig.4.10.

Effect of the non-potential determining electrolytes

Fig.4.10 shows that the stability of the 0.5% SWy-1 montmorillonite suspension is very sensitive to the addition of FeCl₃. The suspension remains relatively stable only if no FeCl₃ is added except at pH=10.0 when 0.5 mM FeCl₃ is present. In term of the critical flocculation concentration (CFC), the CFC for FeCl₃ lies between 0 and 0.5 mM for all the initial pH values of the suspensions with the exception that the CFC is between 0.5 and 1 mM at pH 10.0.

When flocculation occurs, i.e. two layers are formed, the interface between the liquid-like sediment and the supernatant liquid moves downwards gradually from the surface of the initial suspension. That is to say, the liquid-like sediment has a volume which decreases with time. The settling kinetics can follow two types of evolutions, as noticed by Michaels and Bolger (71), and Smellie and La Mer (70) , and is illustrated on Fig.4. 13 at pH= 9.4 for the model system. **Type I** kinetics are observed for an FeCl₃ concentration of 0.5 mM when the time scale is short (Fig.4.11a). It is characterized by an **induction period** followed by a **constant settling rate period**. **Type II** kinetics are observed for FeCl₃ concentrations > 0.5 mM, and it is characterized by the immediate establishment of a constant settling rate period. Both kinetics are also observed for other electrolytes used. However, all the data seem to be type II when they are plotted on a long time scale (Fig.4.11b) since the induction period is short.

The data on the constant settling rate reported here are the slopes of the sediment volume versus time curves, at the beginning of the constant settling rate period. The final sediment volume is defined as the sediment volume after 240 hours' settling. With both kinetics, the constant settling rate period maintains for some time, until a progressive transition occurs towards a period during which the sediment volume decreases extremely slowly. This last period is called the **consolidation period** in which the constituent particles of the sediment rearrange themselves from a open structure to a denser one.
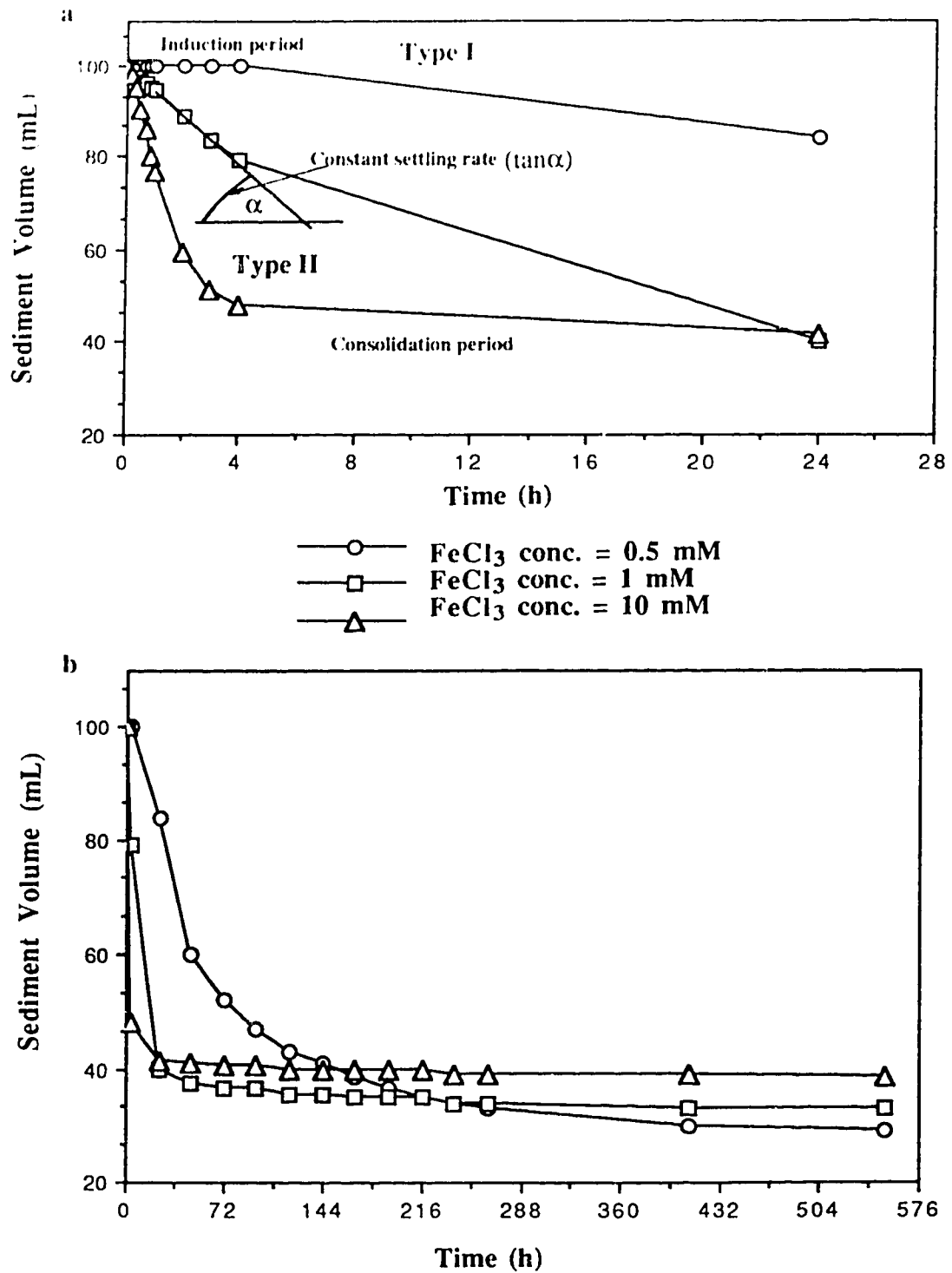
Fig.4.11 Settling kinetics of 0.5% SWy-1 montmorillonite suspensions with different FeCl₃ concentrations at suspension pH 9.4: (a) time scale = 24 hours; (b) time scale = 552 hours.

With FeCl₃ as the electrolyte, and for any given pH studied here, the constant settling rate increases with the FeCl₃ concentration, until it reaches a plateau (Fig.4.12) The plateau's constant settling rate decreases, and the time to reach this plateau increases, when the initial pH of the suspensions increases. It is very interesting to note that a lower settling rate (corresponding to lower FeCl₃ concentration) during the constant settling rate period results in a higher sediment volume before consolidation (Fig.4.11). However, the opposite occurs during the consolidation such that the liquid-like sediments settling with a lower constant settling rate end up with a lower final sediment volume. It shows that lower electrolyte concentration leads to a higher packing efficiency during the consolidation period. The final liquid-like sediment volume reaches a maximum for an FeCl₃ concentration of about 5 mM, independent of the pH, then it decreases again (Fig.4.13).
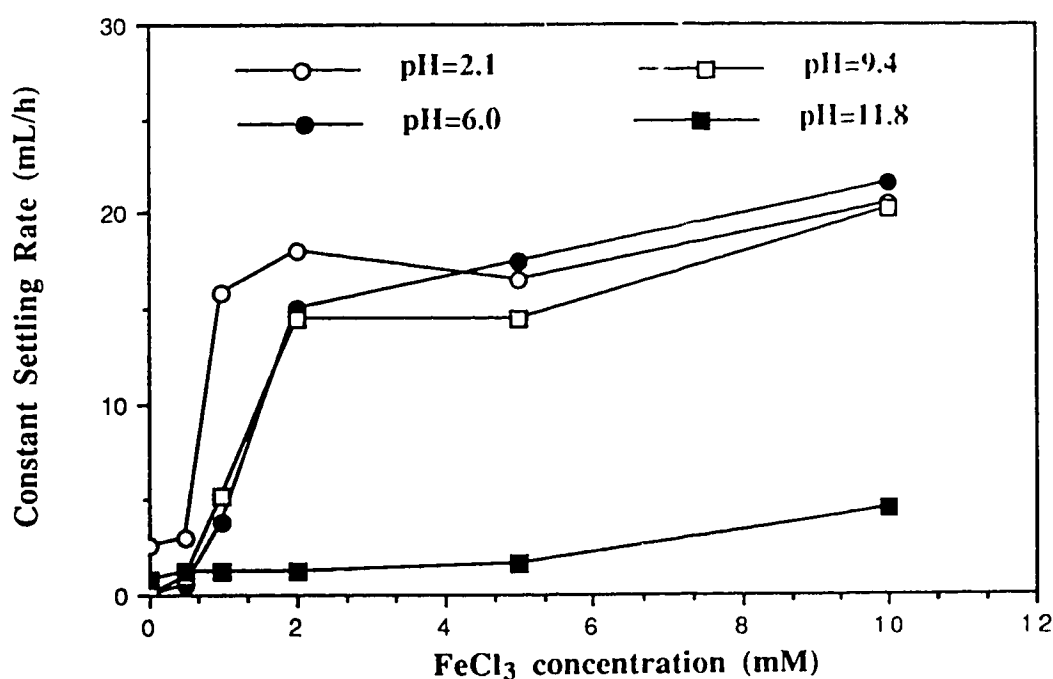
Fig.4.12 Constant settling rate of 0.5% SWy-1 montmorillonite suspensions as a function of FeCl₃ concentration.

When three layers are observed, the interface between the solid-like sediment and the colloidal suspension originates at the bottom of the cylinder, and moves upwards. That is to say, the solid-like sediment volume increases with time, in an accumulation process (Fig.4.14). We can also distinguish a constant rate for the bottom sediment accumulation followed by a progressive transition towards a final volume. It can be noticed that the

settling kinetics for other three layer segregations at different pH values are similar to the one shown on Fig.4.14. The turbidity of the colloidal suspension decreases very slowly over time, which indicates the fine particles in the colloidal suspension settle slowly. It takes at least a month for the colloidal suspension to become clear. The final volume of the solid-like sediment is much lower than that of the liquid-like sediments, in spite of an identical initial amount of clay.
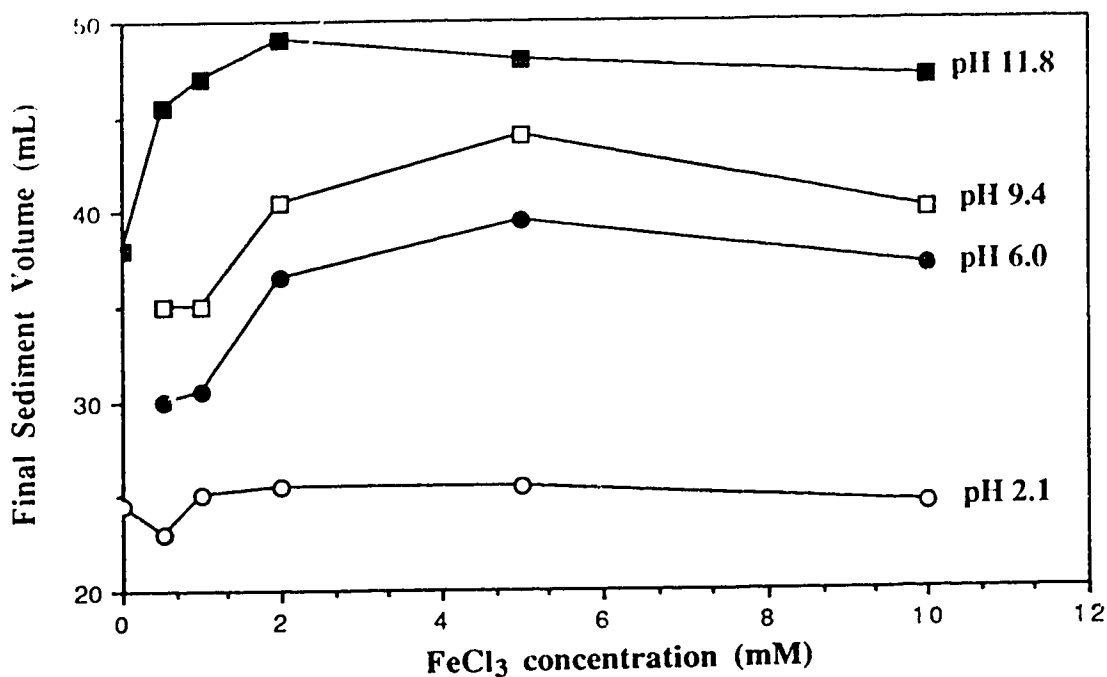
Fig.4.13 Final liquid-like sediment volume of 0.5% SWy-1 montmorillonite suspensions as a function of FeCl₃ concentrations.

Effect of the suspension initial pH

In the two layer segregation, the results show that, for any given $FeCl_3$ concentration, the constant settling rate, in general, decreases first up to pH 4.1, then remains relatively stable between pH 4.1 and 9.4, and finally decreases sharply at about pH 10.0 (Fig.4.15).

As for the final liquid-like sediment volume, it shows a variation just opposite to that of the constant settling rate. That is, it increases at first up to pH=4.1, then it remains relatively constant up to pH=9.4, and finally it increases sharply at higher pH (Fig.4.16).
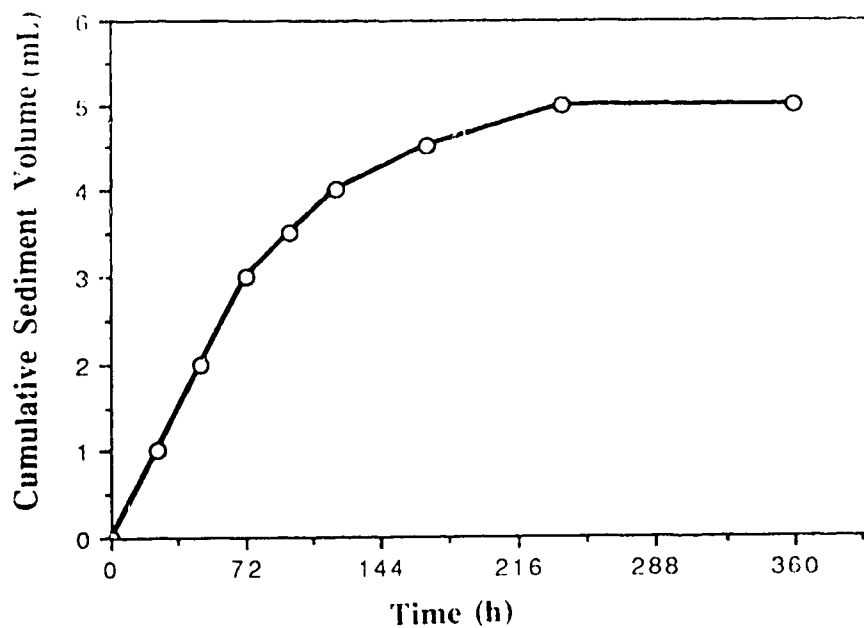
Fig. 4.14 Solid-like sediment volume of a 0.5% SWy-1 suspension as a function of time for three layer segregation (pH =9.4 and no electrolyte added).
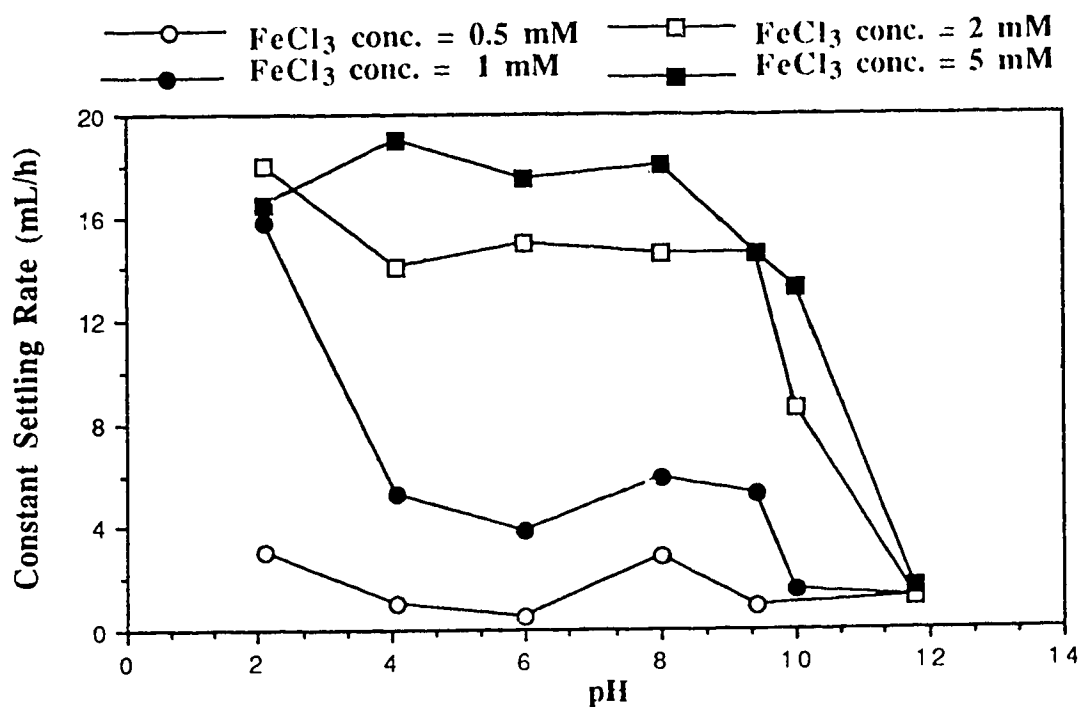
Fig. 4.15 Constant settling rate of 0.5% SWy-1 montmorillonite suspensions as a function of the suspension initial pH.
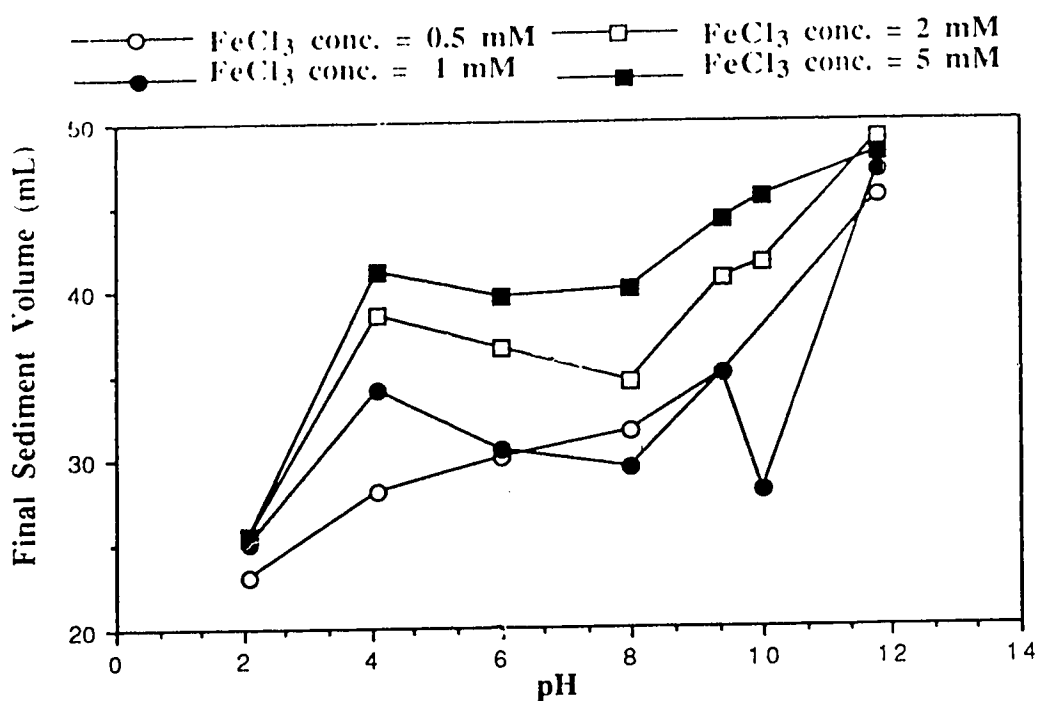
Fig.4.16 Final liquid-like sediment volume of 0.5% SWy-1 montmorillonite suspensions as a function of the suspension initial pH.

The addition of FeCl3 solution changes the pH of the suspensions considerably (see Table 4.3). However, as far as the pH effect is concerned, the settling rate and the final sediment volume are determined by the initial pH value of the suspensions. For example, for all different initial pH values, when the FeCl3 concentration reaches 10 mM, the pH values of the suspensions after addition of FeCl3 are the same, around 2.1. Yet, their constant settling rate and final sediment volume are very different. Table 4.3 also indicates that the initial pH values of the suspensions change with time. For example, the initial pH of 9.4 decreases to 8.2 after 10 days' standing. It is interesting to note the existence of a critical initial pH value at about 7. Below it, the suspension pH without addition of FeCl3 tends to increase with time. When the initial pH is above 7, the pH decreases with time.

The initial pH values of suspensions also have an effect on the color of the sediments. At pH 2.1, the color of sediments ranges from grey white, for the sediment without FeCl3, to grey with increasing FeCl3 concentration. When the initial pH reaches 4.1, the color of the sediment without FeCl3 is light yellow, while the color of other sediments ranges from deep yellow to reddish (similar to the color of FeCl3 solution). The sediment colors are summarized in Table 4.4.

Table 4.3   The pH values of suspensions after the addition of FeCl₃ for different FeCl₃ concentration after 10 days' standing

Initial pH	FeCl₃ concentration (mM)					
	0	0.5	1	2	5	10
2.1	2.1	2.2	2.2	2.2	2.1	2.1
4.1	5.8	3.7	3.0	2.7	2.3	2.1
6.0	6.8	5.8	3.4	2.8	2.3	2.1
8.0	7.3	5.9	2.9	2.5	2.2	2.1
9.4	8.2	5.0	2.7	2.3	2.2	2.0
10.0	9.2	6.9	6.2	2.6	2.3	2.1
11.8	11.6	11.6	11.5	11.4	10.3	2.3

Table 4.4   The color of sediments for different initial pH of suspensions and FeCl₃ concentration

Initial pH	FeCl₃ concentration 0 to 10 mM
2.1	Grey white to grey
4.1	light yellow to reddish yellow
9.4	light yellow to reddish yellow
10	light yellow to reddish

Effect of the nature of ions

The effects of $Fe_2(SO_4)_3$, $FeSO_4$ and $NaCl$ on the constant settling rate of 0.5% montmorillonite suspensions, at the initial suspension pH 9.4, are shown on Fig.4.17. The data indicate the constant settling rate increases with the valence state of both the anions and the cations, with a more drastic influence of the cation valence. With $NaCl$, the montmorillonite remains dispersed in a wider concentration range.

However, the final liquid-like sediment volume, after ageing, shows a major effect by the anions (Fig.4.18). With $Fe_2(SO_4)_3$ as the electrolyte, the final liquid-like sediment volume is notably lower than with $FeCl_3$, and it shows a maximum for a lower electrolyte concentration. By comparison, $NaCl$ and $FeCl_3$ which have the same anions, result in a similar sediment volume, regardless of a quite different valence state of their cations.
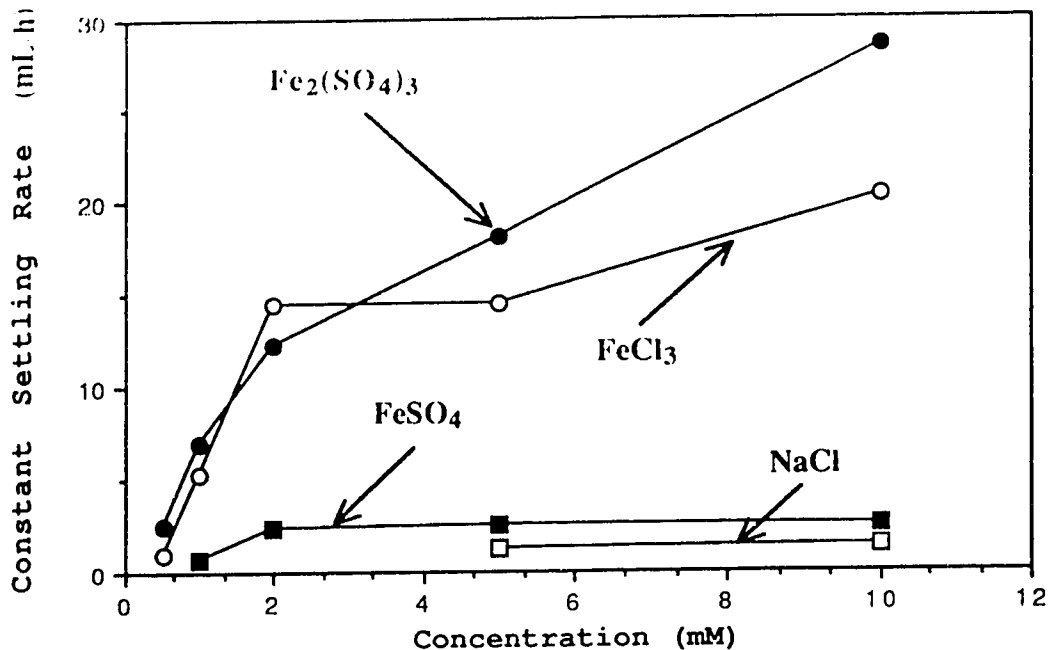
Fig.4. 17 Constant settling rate of 0.5% SWy-1 montmorillonite suspensions flocculated with different electrolytes as a function of electrolyte concentration.
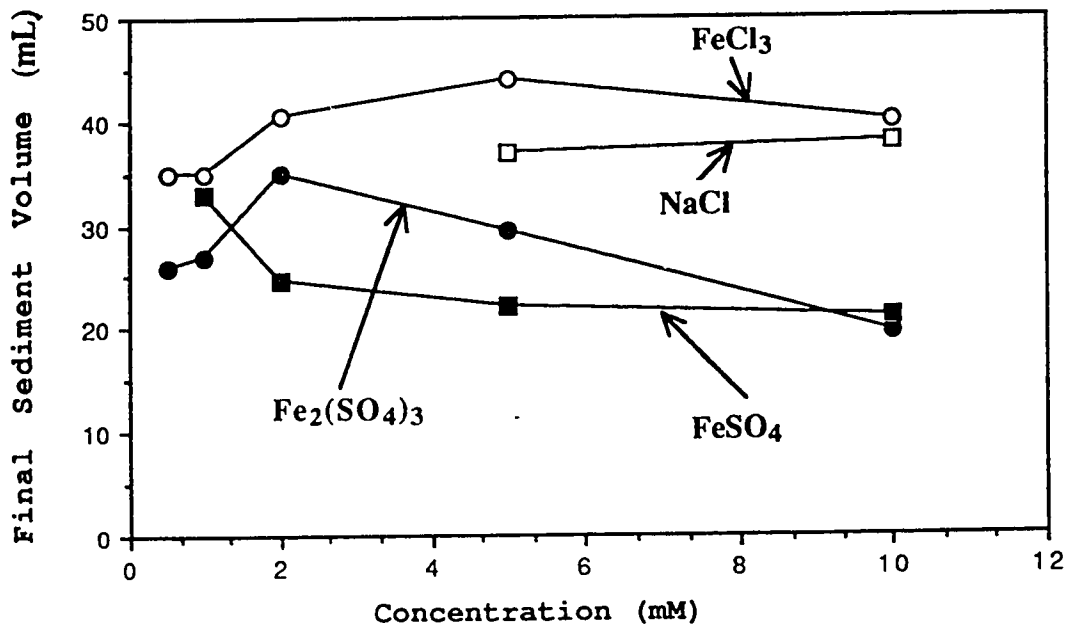
Fig.4.18 Final liquid-like sediment volume of 0.5% SWy-1 montmorillonite suspensions flocculated with different electrolytes as a function of electrolyte concentration.

4.2.2 Montmorillonite K10 suspensions

The behavior of montmorillonite K10 was very different from SWy-1 montmorillonite. The montmorillonite K10 suspensions were very unstable in the conditions no pH adjustment was made and no non-potential determining electrolyte was added, compared to SWy-1 montmorillonite suspensions. All its suspended solids settled within 24 hours. The sediment volume was close to the volume that the same amount of solids would occupy in powder state. That is, a very compact sediment was formed.

Both the pH adjustment and non-potential determining electrolytes had little effect on the stability of montmorillonite K10 suspensions although they had some effect on the settling rate of particles. In the 1.3 to 11.4 pH range studied, and the electrolyte concentration increasing progressively from 0 up to 2.1 M, no two-layer segregation was observed. That is, three layers were always observed. This indicated the kinetic units in montmorillonite K10 might be densely packed aggregates rather than the primary particles.

The time for all suspended solids to settle decreases somewhat with an increasing electrolyte concentration, including the acid or base added for pH adjustment. The settling rate also increases with the solid content. This also indicated montmorillonite K10 was contaminated. The settling rate is determined approximately by the change of turbidity over time since there is no sharp interface between the supernatant liquid and the colloidal suspensions. The montmorillonite contents (%, by mass) of the suspensions studied include 0.5, 1, 2, 5, 10 and 25%. The results for 2% montmorillonite suspensions are summarized in **Table 4.5**.

Table 4.5 Effects of pH and electrolyte concentration on the stability of 2% montmorillonite K10 suspensions

Electrolytes	Concentration range	pH range	Two-layer segregation
NH_4OH	0-2.1 M	3.7-11.4	No
H_2SO_4	0-240 mM	3.9-1.3	No
$Fe_2(SO_4)_3$	0-5 mM	3.9-2.1	No
$FeCl_3$	0-50 mM	3.9-1.8	No
HCl	0-160 mM	3.8-1.2	No

These results shows that montmorillonite K10 contains a significant amount of impurities, and/or the chemical processing through which this material has gone may have changed the colloidal properties of montmorillonite K10. As a result, montmorillonite K10 has been abandoned for any later experiments.

4.2.3 Oil sands tailings sludge references

Electrolyte concentration effect

The 0.5% reference 1 sludge suspensions also show two layer or three layer segregation depending on the electrolyte concentration. When no FeCl3 solution is added, three layer segregation is observed. It takes 10 days for the colloidal suspension to become clear. Fig.4.19 shows the final sediment volume after 10 days' standing.

Table 4.6 The reference 1 sludge sediment volume as a function of time for different FeCl3 concentration

Time (h)	FeCl3 concentration (mM)					
	0*	0.5	1	2	5	10
0	0	100	100	100	100	100
1	0	13	14.5	15	14	13
2	0	9.5	11.0	12	11	11
4	0	8	9.5	11	10	10
24	1	6.5	8	10	10	10
48	2	6.5	7	10	10	10
96	4	6	7	10	10	10
120	4.2	5.5	7	9.5	9.5	9.5
144	4.3	5.5	7	9.5	9.5	9.5
192	4.5	5	7	9.5	9.5	9.5
240	4.5	5	7	9.5	9.5	9.5

* Three layer segregation.

When the FeCl3 concentration reaches 0.5 mM, flocculation occurs. The flocs settle in such a manner that the interface between the supernatant liquid and the sediment is clear but not flat in the initial stage of settling, contrary to what is observed with 0.5% SWy-1 montmorillonite suspensions. This can be related to the different settling rate of individual flocs, and a different fractal structure in SWy-1 and the reference sludges. However, the sludge flocs settle rapidly, the settling process for the two layer segregation being

completed in one hour, regardless of the FeCl₃ concentration (See Table 4.6). That is, the FeCl3 concentration has little effect on the constant settling rate for the concentration range studied, which is different from the montmorillonite model system. Once all flocs have settled to the bottom, a sharp and clear flat interface occurs (see Fig.4.19) and the slow consolidation begins.
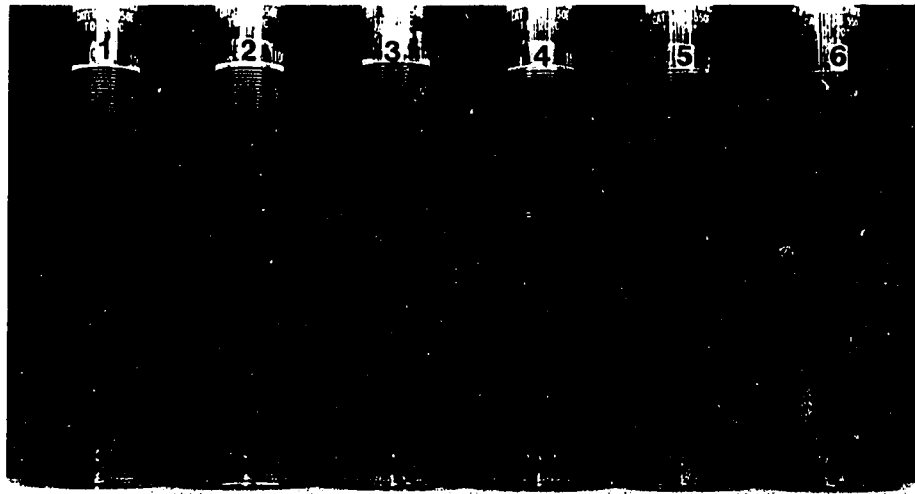
Fig.4.19 State of 0.5% reference 1 sludge suspensions with different FeCl3 concentration at pH 7.4 after standing for 240 hours, FeCl3 concentrations in mM from sample #1 to sample #6: 0, 0.5, 1, 2, 5 and 10.

The final sediment volume (shown on Fig.4.19) increases with the FeCl3 concentration and reaches a maximum at 2 mM. This is very similar to the model system except that it requires a lower electrolyte concentration (5 mM in the model system). Also at pH 7.4, the maximum sediment volume for 0.5% reference 1 sludge suspension is 9.5 mL instead of 40 mL for the model system at pH 8.

pH effect

The pH of the reference 1 sludge suspensions without any pH adjustment varied between 7.4 and 8.0, according to the results of four samples. The results indicate that a very small amount of the concentrated acids or bases modify the suspension pH to a large extent, inducing flocculation. The dilute ones modify the suspension pH progressively.

When the pH of the reference 1 sludge suspensions is approximately above 10 or approximately below 6, flocculation occurs. The type of acid or base added doesn't have a significant influence. Some of the results are given in Fig.4.20. It can be seen that the stability of sludge suspensions also increases with the suspension pH. 1.5 mM NH_4OH is required to induce flocculation (the suspension pH in the 8 to 10 range, Fig.4.20a), while 0.24 mM H_2SO_4 is needed to cause flocculation since it decreases the suspension pH (Fig.4.20 b).

The CFC of $Fe_2(SO_4)_3$ for the 0.5% reference 1 sludge suspensions is 0.033 mM, which is very low compared to 0.5 mM for $FeCl_3$ with a 0.5% SWy-1 montmorillonite suspension. This is mainly because sludge itself contains various ions, and the kinetic units of sludge suspensions are flocs rather than the primary particles. The kinetic units in SWy-1 montmorillonite suspensions are the primary particles. Therefore, lower electrolyte concentrations can induce flocculation in the sludge suspensions. The kinetic units of both the model and real sludge are examined in the next sections. At CFC with $Fe_2(SO_4)_3$, the reference 1 sludge suspension pH is 7.2 (Fig.4.20c).

Solid content effect

At a solid content of 15%, which is of the same order as the solid content in the final sediments of reference 1 sludge in Fig.2.19, settling does not occur in the suspension for the selected standing time (24 hours) even with an electrolyte concentration as high as 60 mM. It means that when the solid content reaches a sufficient level, settling and consolidation does not proceed any further. This is consistent with the real sludge problem: when the solid content reaches a certain value, the consolidation process virtually stops.
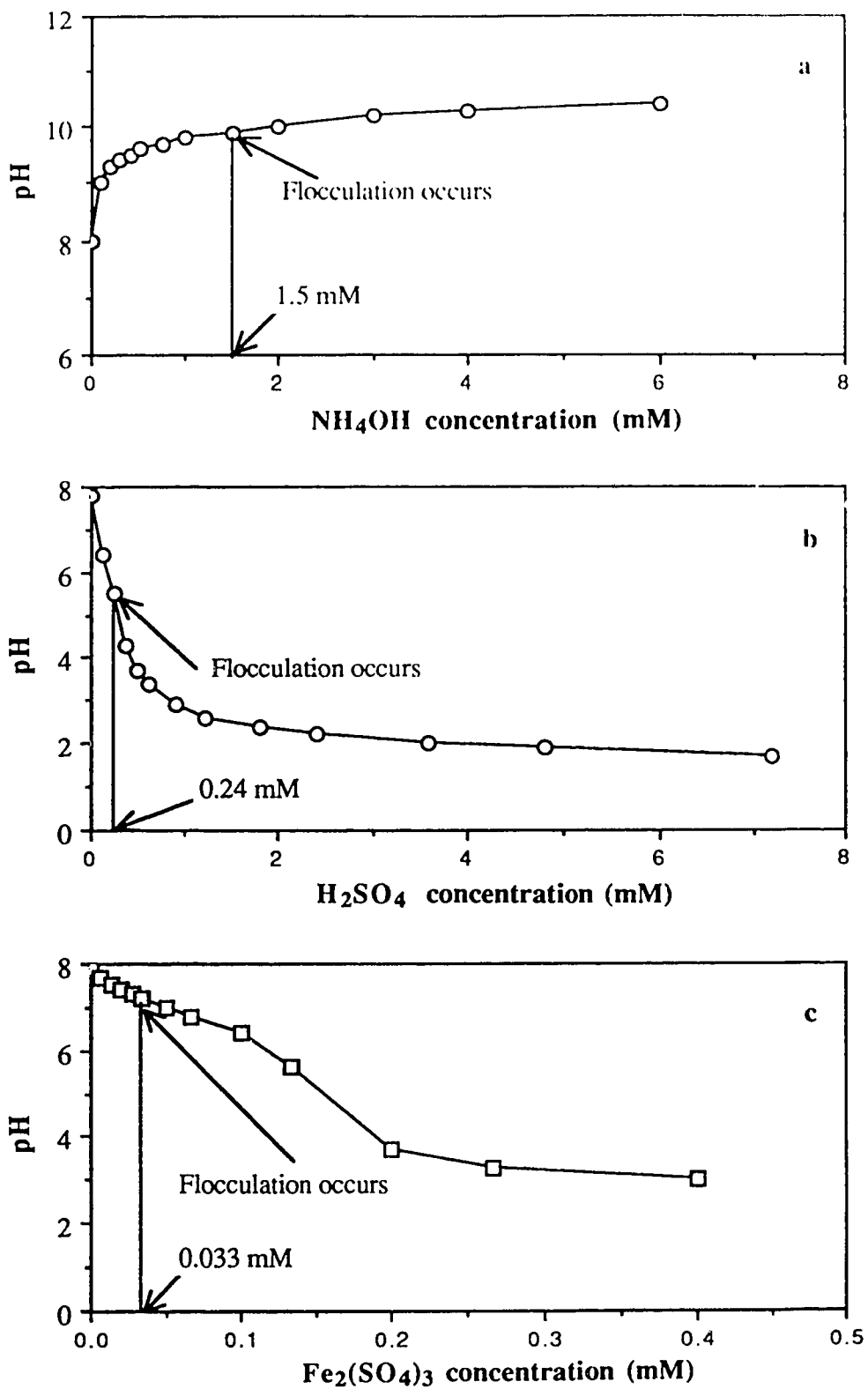
Fig.4.20. Stability of the 0.5% reference 1 sludge suspension with different electrolytes.

4.3 SEM STRUCTURE OF SEDIMENTS DRIED HYPERCRITICALLY

4.3.1 Reference 1 sludge

The SEM observations of all reference 1 sludge samples dried hypercritically show that the constituent particles have a wide size distribution, with linear dimensions ranging from below 0.1 micron to larger than 10 micron (Fig.4.21a, b and c and Fig.4.22a, b and c). This is consistent with the previous results of the particle size analysis. In general, the particles are plate-like. The thickness of the plate-like particles also shows a wide distribution, but is most often below 0.1 μm. That is to say in the colloidal range. Some particles are very fine and fluffy, and their shape is difficult to define at the highest useful magnification. It can also be observed that some quite large particles are trapped in the sediment fine network.

The particle association follows a random card house network pattern. Referring to the literature review concerning FF, FE and EE platelet association, it seems that the EE association dominates. The EE association seems rather to be 3 particle EEE association (Fig.4.24a). Or it could be EF linkage occurring at a place of distortion of 1 platelike particle (Fig.4.24b). These combinations of particle associations lead to the formation of flocs of different size. It can been seen that the boundaries of flocs are not well defined. These flocs aggregate to form a grid throughout the sediment. Apparently, the packing of particles inside the flocs forms a rather open but uniform platelet grid.

The structure of the sediments is a result of two-level hierarchical flocculation. At the highest magnification, (2 μm, Fig.4.21a, b and c), the electrolyte concentration seems not to have much effect on the structure of the sediments. At the lower magnification (Fig.4.22a, b and c and 4.23a and b), the electrolyte concentration seems to have an effect on the packing efficiency of the flocs. As the $FeCl_3$ concentration increases from 0 to 5 mM, the packing efficiency of the flocs decreases somewhat. However, the packing efficiency between individual particles inside flocs seems to be independent of the electrolyte concentration. This well explains the sediment volume increases with the increasing electrolyte concentration. That is to say, the final sediment volume is mainly determined by the packing efficiency between flocs rather than the packing efficiency between individual particles inside flocs. The estimated solid contents of sediments with 0, 1 and 5 mM $FeCl_3$ are around 10%, 7% and 5%, respectively.
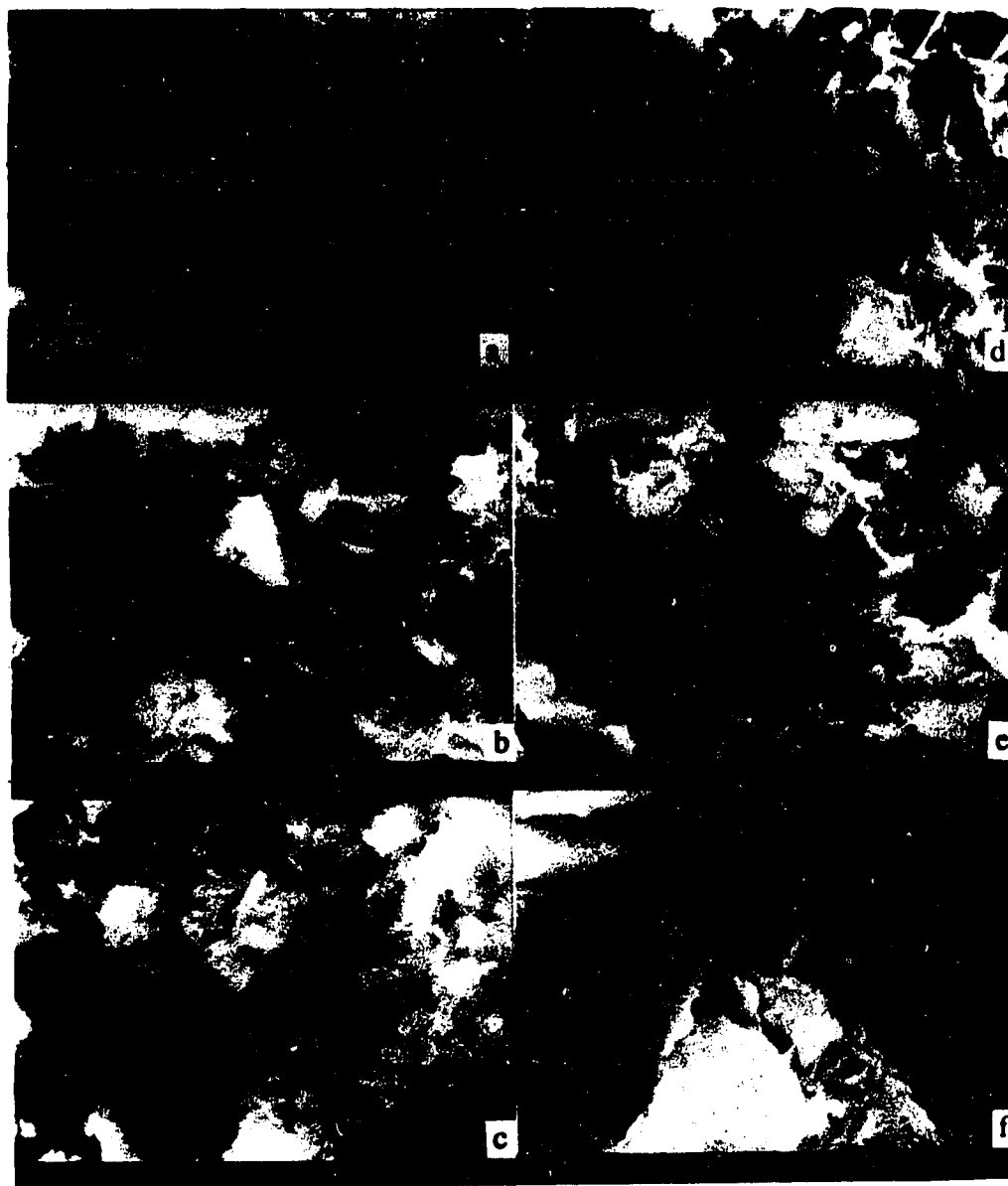
Fig. 4.21   SEM structure of sludge sediments after hypercritical drying, on a 2 μm scale:
(a) reference 1 sludge without electrolytes; (b) reference 1 sludge with 1 mM
FeCl₃; (c) reference 1 sludge with 5 mM FeCl₃; (d) reference 2 sludge without
electrolytes; (e) reference 2 sludge diluted with 60% acetone without
electrolytes; (f) reference 2 sludge with 5 mM FeCl₃.
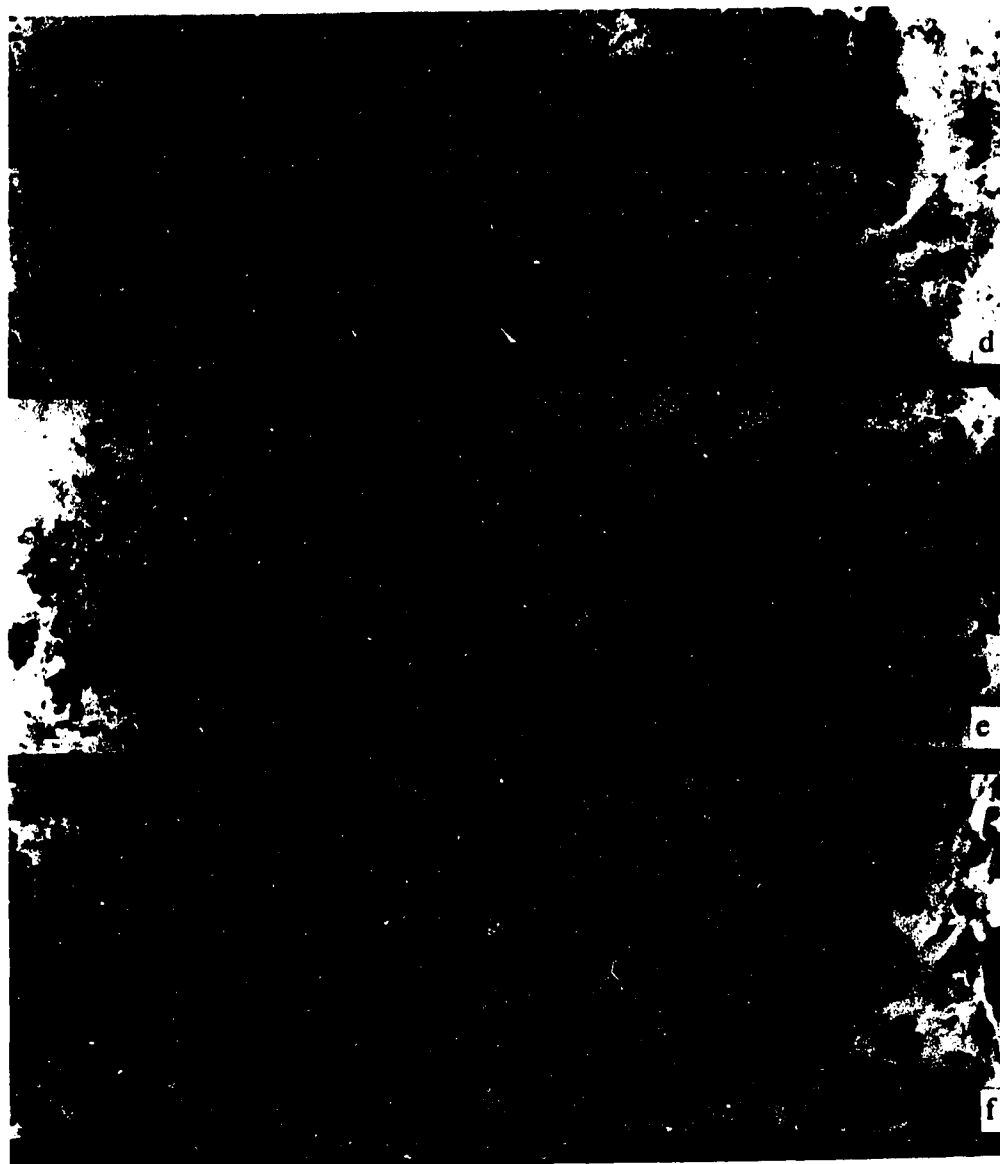
Fig. 4.22 SEM structure of sludge sediments after hypercritical drying, on a 10 μm scale:
(a) reference 1 sludge without electrolytes; (b) reference 1 sludge with 1 mM
FeCl₃; (c) reference 1 sludge with 5 mM FeCl₃; (d) reference 2 sludge without
electrolytes; (e) reference 2 sludge diluted with 60% acetone without
electrolytes; (f) reference 2 sludge with 5 mM FeCl₃.
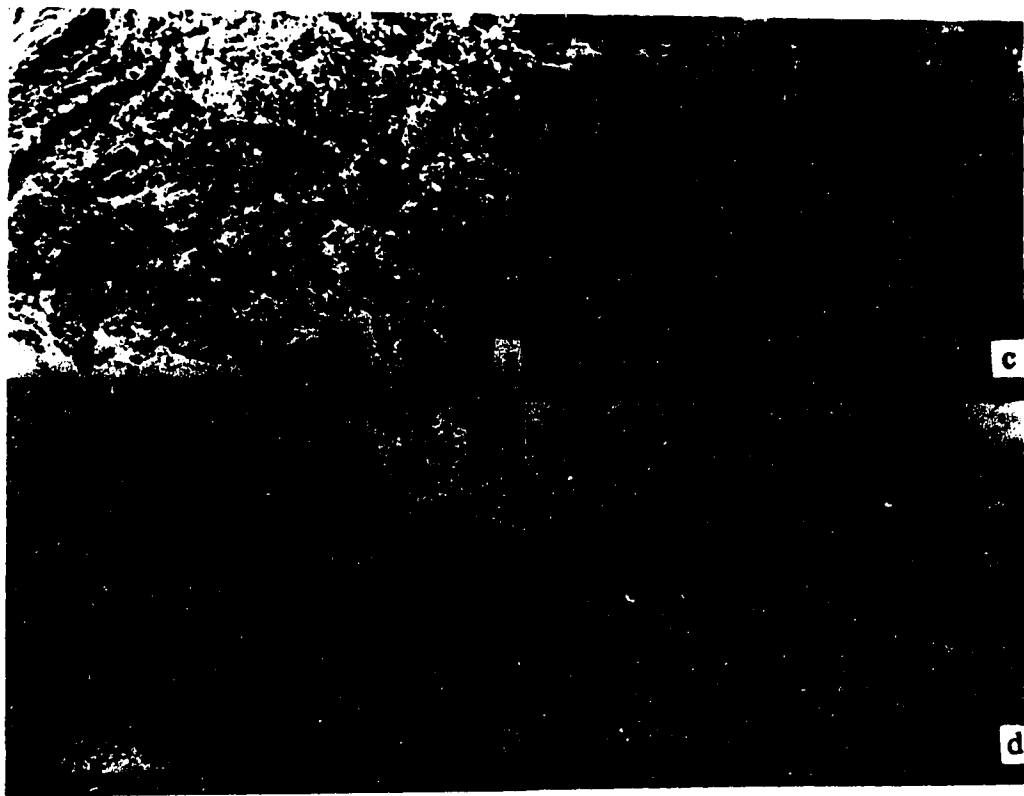
Fig. 4.23   SEM structure of sludge sediments after hypercritical drying, on 40 and 100
μm scales: (a) reference 1 sludge without electrolytes; (b) reference 1 sludge
with 5 mM FeCl₃; (c) reference 2 sludge without electrolytes; (d) reference 2
sludge with 5 mM FeCl₃.
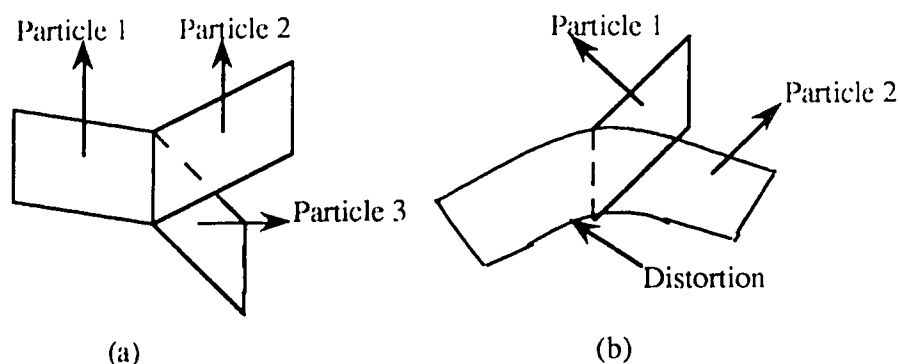
Fig.4.24 Structures built by different linkage of plate-like particles: (a) EEE linkage of three particles; (b) EF linkage at the distortion of one plate-like particle.

The specific surface area of the 0.5% reference 1 sludge sediment with 5 mM FeCl$_3$ (after hypercritical drying) has been found to be 39 ± 5 m^2/g, and the corresponding average pore size is 11.8 ± 0.3 nm, respectively. The data for the same suspension after conventional drying are 9 ± 2 m^2/g and 24 ± 1.5 nm (data reported here were results of several runs on the sample). These data indicate that FF association of the platelets occurs when the wet sediments are dried by conventional drying. This FF collapse is well illustrated by a comparison of the SEM picture of reference 1 sludge powder after conventional drying (Fig.4.3) with the present SEM picture after hypercritical drying (Fig.4.21).

4.3.2 Reference 2 sludge

There is a difference between the flocculation by FeCl$_3$ and by 60% acetone (see **Section 3.2.3** for the sample preparation of each sample). With acetone (and no Fe), a very flexible floc network formed very slowly at first, then the floc settled slowly to the bottom. The liquid-sediment interface was not flat initially, then changed to a flat one gradually. It was found that dilution of reference 2 sludge to a 0.5% suspension in 100% acetone resulted in rapid flocculation and settling, similar to the settling behavior of 0.5% suspension flocculated with 5 mM FeCl$_3$.

The structure under the SEM after hypercritical drying of the reference 2 sludge sediment as received (Fig.4.21d) is very similar to that of reference 1 sludge where no electrolyte is added (Fig.4.21a). The main difference is that the packing efficiency of flocs with reference 2 as received is higher, in relation with a higher solid content (25% versus 10%).

0.5% reference 2 sludge suspension in a 60% acetone medium, before liquid CO_2 exchange, shows somewhat the same type of structure, with a higher packing efficiency between particles inside flocs and lower packing efficiency between flocs (Fig.4.21e and 4.22e) by comparison with reference 2 sludge as received (Fig.4.21d and 4.22d). When 5 mM $FeCl_3$ is added, densely packed larger flocs comprising much coarser platelets are formed (Fig.4.21f and 4.22f). When mounting these two samples for observation under the SEM, it could be felt that the sample from the sediment flocculated by 5 mM $FeCl_3$ was strongly bonded and had a certain mechanical strength, while the sample diluted in 60% acetone without $FeCl_3$ was very soft, and could be easily broken up. It seems therefore that $FeCl_3$ had acted not only as a flocculant but also as a cement. Because of the different bonding nature , the sediment with 5 mM $FeCl_3$ had a higher sediment volume than that without $FeCl_3$ (8 mL vs 5 mL). The solid contents (by volume) were respectively about 6 % and 10 %.

4.3.3 Montmorillonite

The montmorillonite sediments studied after hypercritical drying have been made with the SWy-1 montmorillonite. Both samples show that the clay particles are plate-like and very thin (Fig.4.25). However, the packing pattern of the sample without $FeCl_3$ is different from the sample with $FeCl_3$. A three level hierarchic flocculation can be observed for the sediment flocculated with 5 mM $FeCl_3$. The first level flocculation is the association of the primary particles inside the flocs by EE linkage in a relatively dense way (Fig.4.25d, the highest magnification). At the second level flocculation, linear fractal branches establish a three-dimensional network between the first level flocs, leading to the formation of larger but loosely packed second level flocs (Fig.4.25e). At the third level, the second level flocs have themselves assembled in a loose fashion, producing a very porous floc network (Fig.4.25f, the lowest magnification). The overall picture is roughly coherent with the so-called hierarchical-DLA (Diffusion-Limited-Aggregation) model (86), and explains the high liquid-like sediment volume. The specific surface area of this sample is 420 m^2/g (the average of two runs), which is about 20 time higher than that of the sample dried by evaporation. And the average pore size is 9.1 nm (radius), being the same order as that of the sample dried by evaporation (see **Table 4.2**).

The sediment without the addition of any electrolytes has a quite uniform packing (Fig4.25a, b and c). At the highest magnification, the structure is the same as that observed with $FeCl_3$; the plate-like particles form a network through EE linkage, constituting a

rather uniform grid. No face sharing can be observed. Only, without FeCl3, the structure is uniform throughout the sediment. One does not observe the second- and third-level hierarchy typical of DLA aggregates (Fig.4.25b and c compared to Fig.4. 25e and f).
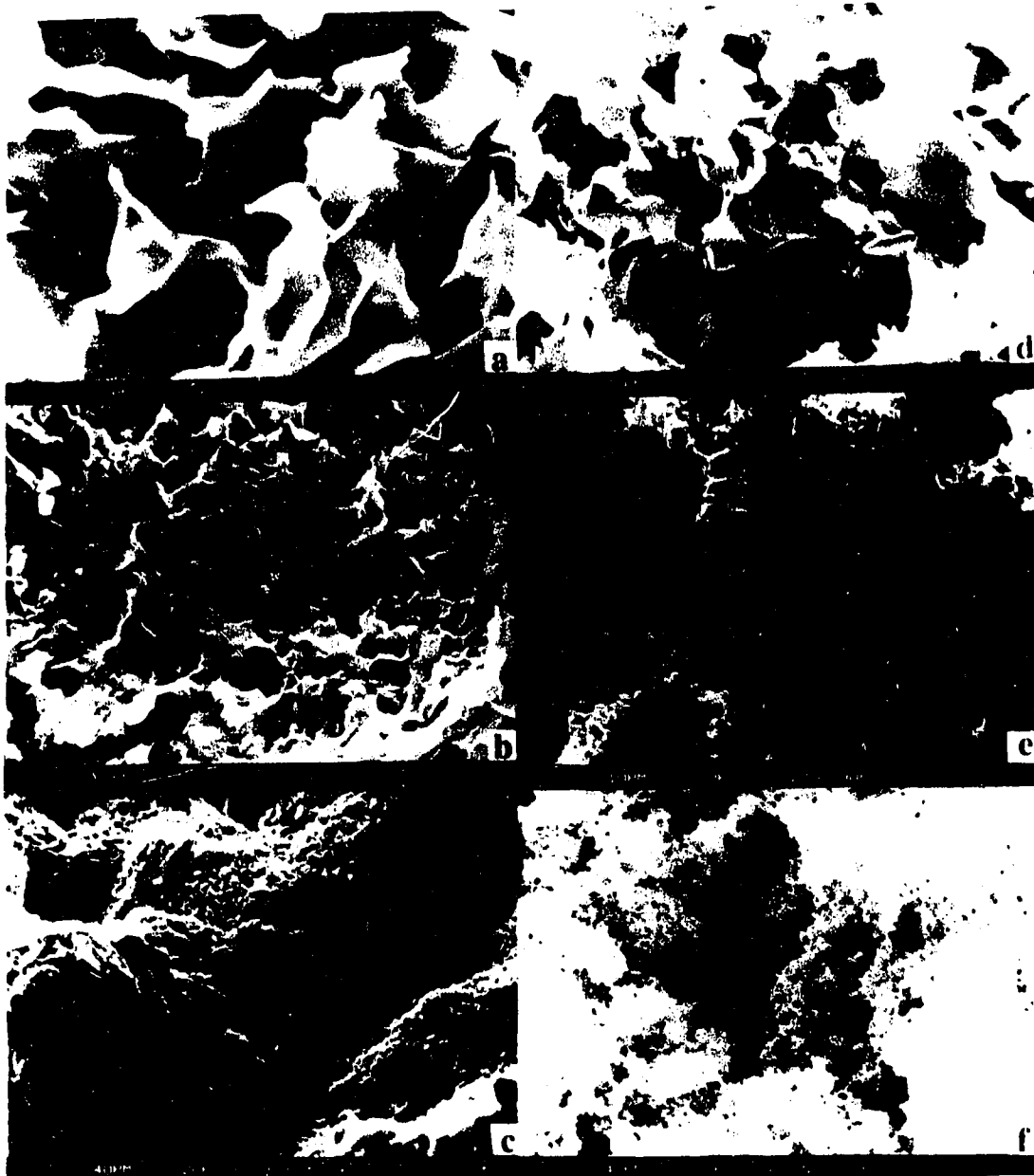
Fig.4.25 SEM structure of SWy-1 montmorillonite sediment after hypercritical drying:
(a) to (c) without electrolytes; (d) to (e) with 5 mM FeCl3.

4.4 DRYING BEHAVIOR

4.4.1 Drying kinetics

The drying kinetics of 5% SWy-1 montmorillonite gels in dishes of different size at constant lab temperature with $FeCl_3$ as the electrolyte are reported on Fig.4.26 and 4.27. For all samples, a constant drying rate period was observed, which ended at a critical point where shrinkage virtually stopped. On Fig.4.26a, the drying rate falls so rapidly that it seems that the sample stops drying after the constant drying rate period. This is somewhat different from the classical drying behavior of clays (see Fig.2.18 in **Section 2.4.6**).

The relative constant drying rate for each sample, defined as the quotient of the constant drying rate of the samples divided by the drying rate of distilled water under the same conditions, is reported on Fig.4.26b and 4.27b as a function of $FeCl_3$ concentrations. It can been seen that the relative constant drying rate shows fluctuation, and the fluctuation observed would have to be clarified in further experiments. It is necessary to point out that the constant drying rate was expressed in mass loss per unit time (g/h) rather than mass loss per unit time and per unit area ($g/h\cdot cm^2$). This is mainly because the surface area exposed to air changes during drying. In the drying process, warping and then cracking occurs before the end of the constant drying rate (see Fig.4.39). The surface available for water evaporation first increases moderately with cracking and then decreases when shrinkage becomes significant. If the drying rate is expressed in $g/h\cdot cm^2$, the drying rate may change with time after drying for some time.

For the samples prepared in dishes of 70 mm x 50 mm, the highest constant drying rate (sample without $FeCl_3$) is 25.5% higher than the lowest constant drying rate (sample with 5 mM $FeCl_3$) (see Fig.4.27b and **Table 4.7**), which cannot be attributed to the small size difference of the dishes.

After drying for 24 hours, warping occurs in all samples. When drying time reaches 48 hours, a crack occurs in samples of which the $FeCl_3$ concentration is 0, 0.5, 1 and 2 mM. The width and depth of cracks increases with drying time. After 90 hours' drying, a crack occurs in the sample with 5 mM $FeCl_3$. The sample with 10 mM $FeCl_3$ remained monolithic until the end of drying.
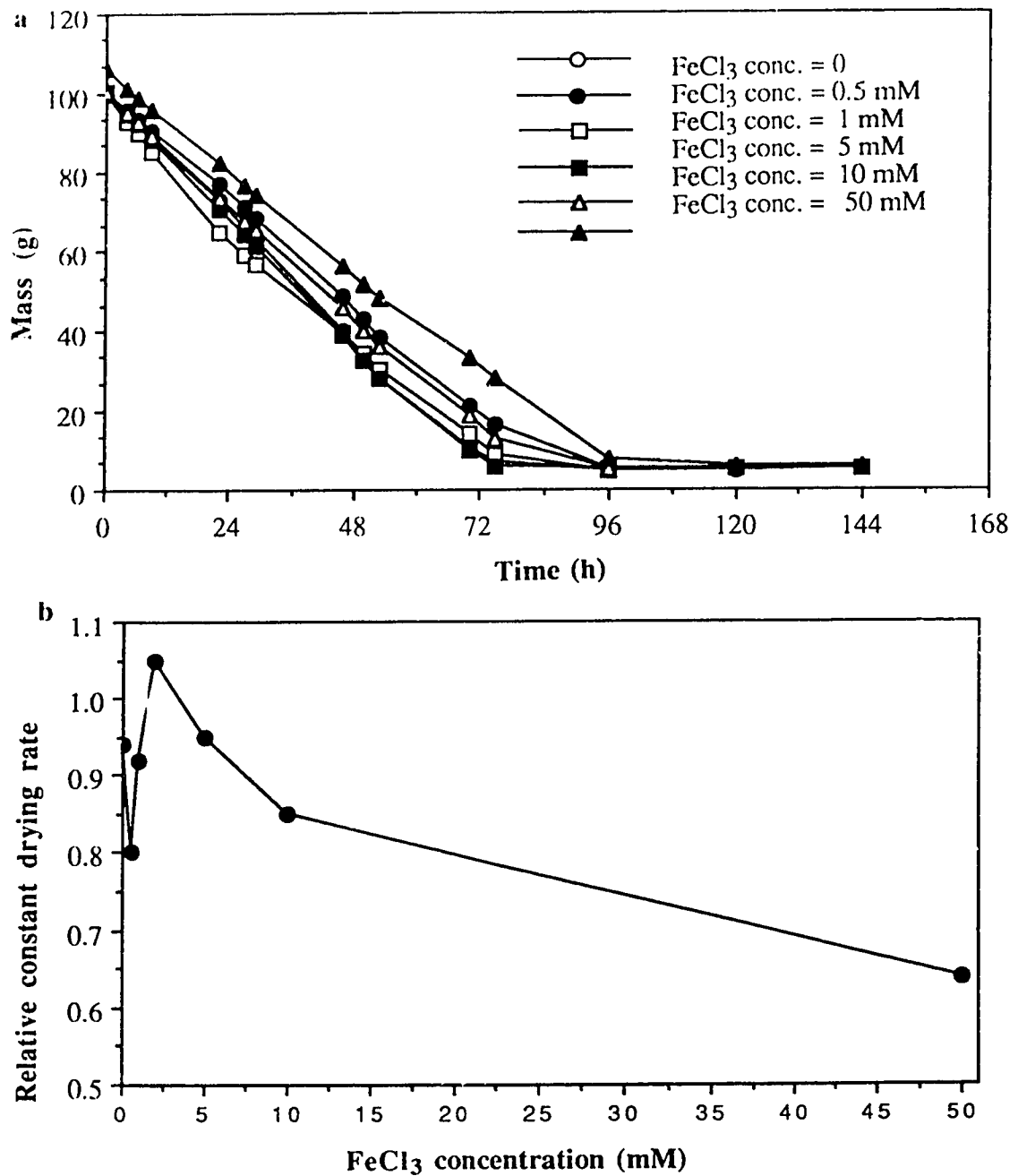
Fig.4.26 Drying kinetics of 5% SWy-1 montmorillonite gel with different FeCl₃
concentrations in 125 mm x 65 mm dishes (a), and the relative constant drying
rate as a function of FeCl₃ concentrations (b).
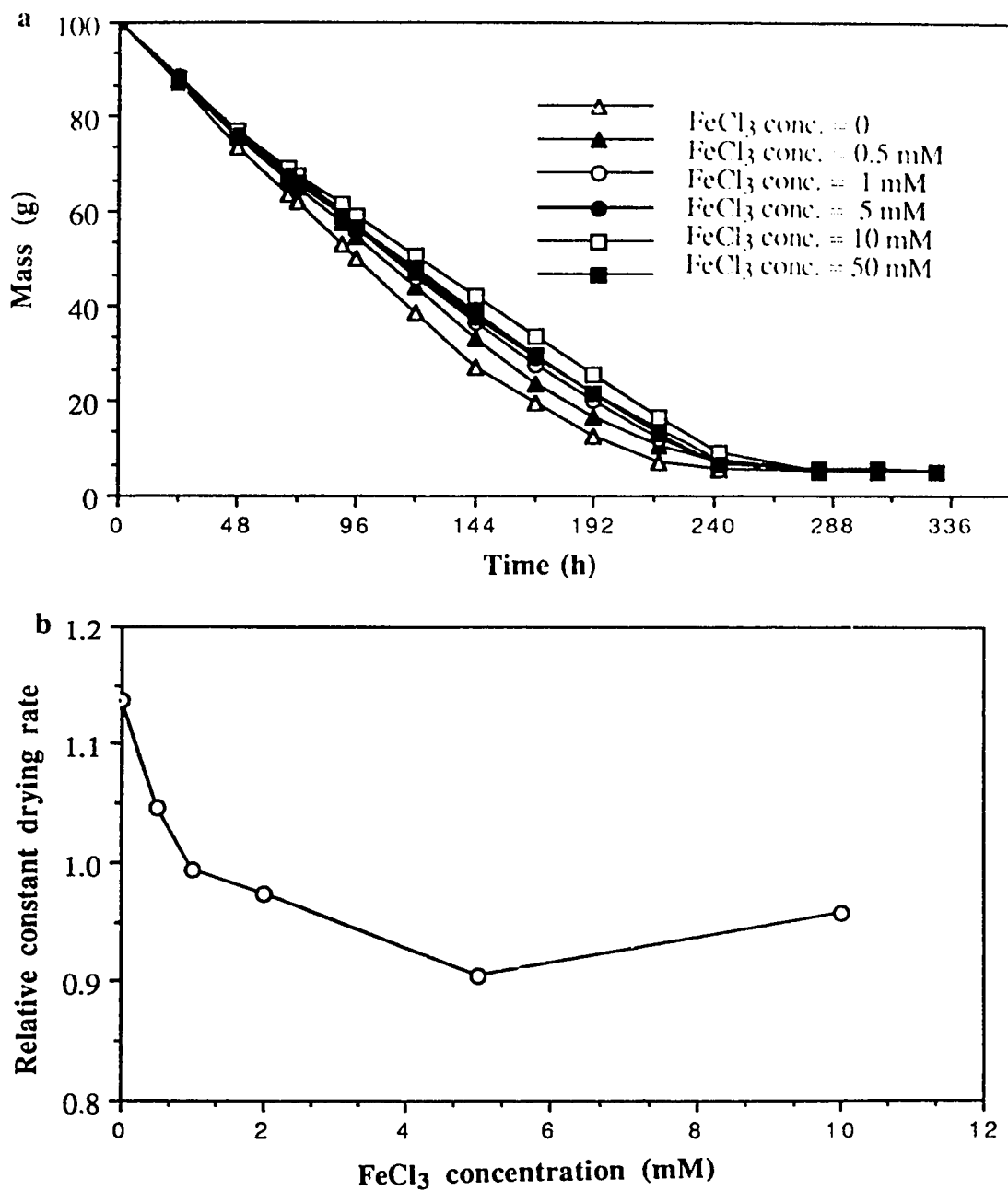
Fig.4.27   Drying kinetics of 5% SWy-1 montmorillonite gel with different FeCl3
concentrations in 70 mm x 50 mm dishes (a), and the relative constant drying
rate as a function of FeCl3 concentrations (b).

Table 4.7 Constant drying rate of 5% montmorillonite gel flocculated by different FeCl3 concentrations

FeCl3 Concentration, mM	0	0.5	1	2	5	10
Constant drying rate, g/h	0.506	0.466	0.442	0.433	0.403	0.426

Effects of pH and FeCl3 concentration

The effects of pH and FeCl3 concentration on the drying kinetics were assessed on 0.5% SWy-1 montmorillonite suspensions.

Depending on the FeCl3 concentration and the initial pH values of the suspensions, two-layer or three-layer segregation occurred. The segregation state of all samples was summarized in **Table 4.8**.

Table 4.8 Segregation state of 0.5% SWy-1 montmorillonite suspensions at different pH and FeCl3 concentrations

pH	FeCl3 Concentration (mM)					
	0	0.5	1	2	5	10
2.0	2l	2l	2l	2l	2l	2l
4.0	3l	2l	2l	2l	2l	2l
9.4	3l	2l	2l	2l	2l	2l
10.0	3l	3l	2l	2l	2l	2l

2l- Two-layer segregation; 3l - Three-layer segregation.

When two-layer segregation occurred, a liquid-like sediment formed. At the early stage of drying, the liquid-like sediment would flow when the dish containing the sample was tilted. As drying proceeded, the liquid-like sediment volume decreased and would not flow at some point of time, defined as gel point.

For all samples, a constant drying rate is observed (Fig.4.28, 4.29, 4.30 and 4.31). Both the FeCl3 concentration and the initial suspension pH affect the relative constant drying rate (Fig.4.32). At pH 2.0 and pH 4.0, the relative constant drying rate first increases to a maximum at 0.5 mM FeCl3, then decrease to a minimum at 5 mM FeCl3, finally increases again with a higher FeCl3 concentration. At pH 10.0, the relative constant drying rate shows a clear trend of decreasing with the increasing FeCl3 concentration. At pH 9.4, an opposite trend to pH 2.0 and pH 4.0 is observed, that is, the relative constant drying rate first decreases up to 0.5 mM FeCl3, then increases to a maximum at 5 mM FeCl3, finally

decreases again with higher FeCl₃ concentration. Most samples have a higher constant drying rate than the distilled water under the same conditions.

Drying experiments have been made when the settling rate of sediments is faster than the drying rate. That is, a supernatant liquid layer exists. For two layer segregation, the sediment volume decreases with time, while the supernatant layer also undergoes evaporation. When the sediment stops settling, the supernatant liquid layer decreases in thickness until it disappears. The drying time necessary for the supernatant layer to disappear increases when the sediment volume decreases. The supernatant layer disappearance time in hour for all samples with two-layer segregation is given in **Table 4.9**. It can be seen that this time decreases considerably with an increasing FeCl₃ content for an initial pH of 9.4. These results are consistent with the results of the kinetics of sedimentation in **Section 4.2.1**.

Once the supernatant layer has disappeared, the sediment alone keeps drying. At first it is liquid-like. Then it reaches a gel point, when it does not flow any more upon tilting the container. The gel point and the mass at the gel point for all samples are summarized in **Table 4.10**. All samples reach the gel point before reaching the end of the constant drying rate. Overall, the samples with a higher sediment volume reach the gel point earlier than the samples with a lower sediment volume. The data are reported on Fig.4.33 as a function of FeCl₃ concentration. The mass at the gel point overall increases with FeCl₃ concentration for a given pH, and increases with the initial pH value of the suspension for a given FeCl₃ concentration.

Table 4.9 Supernatant layer disappearance time for different FeCl₃ concentrations at different initial pH values for 0.5 % montmorillonite suspensions

pH	FeCl₃ Concentration (mM)					
	0	0.5	1	2	5	10
2.0	120	120	120	120	120	72
4.0	31	120	12C	90	66	72
9.4	31	90	90	66	66	72
10.0	31	31	120	90	66	66

3l- Three-layer segregation
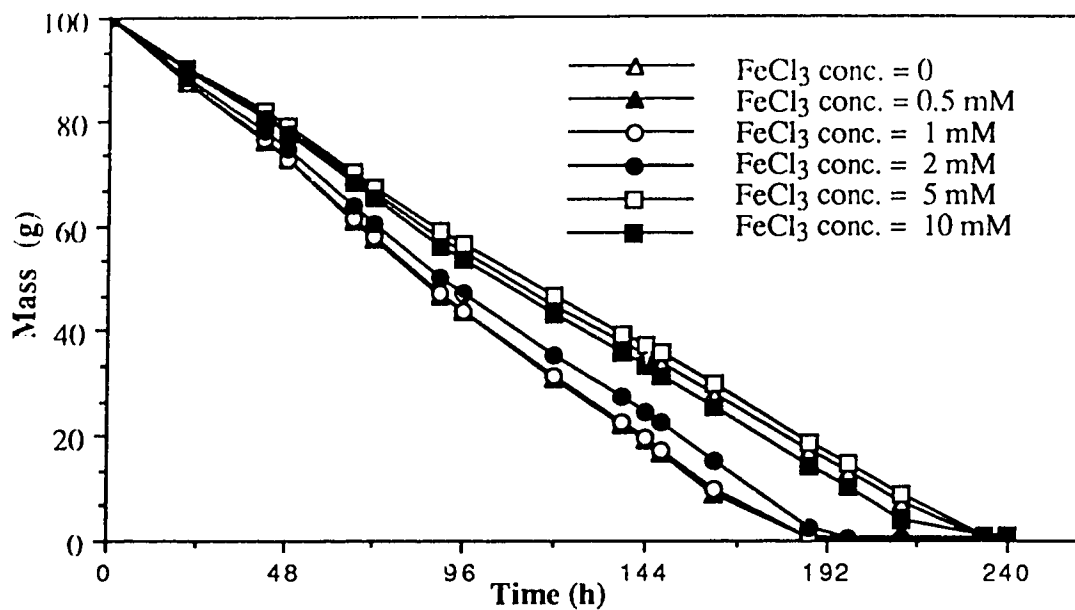
Fig.4.28   Drying kinetics of 0.5% SWy-1 montmorillonite suspensions with different
FeCl₃ concentrations at pH = 2.0.
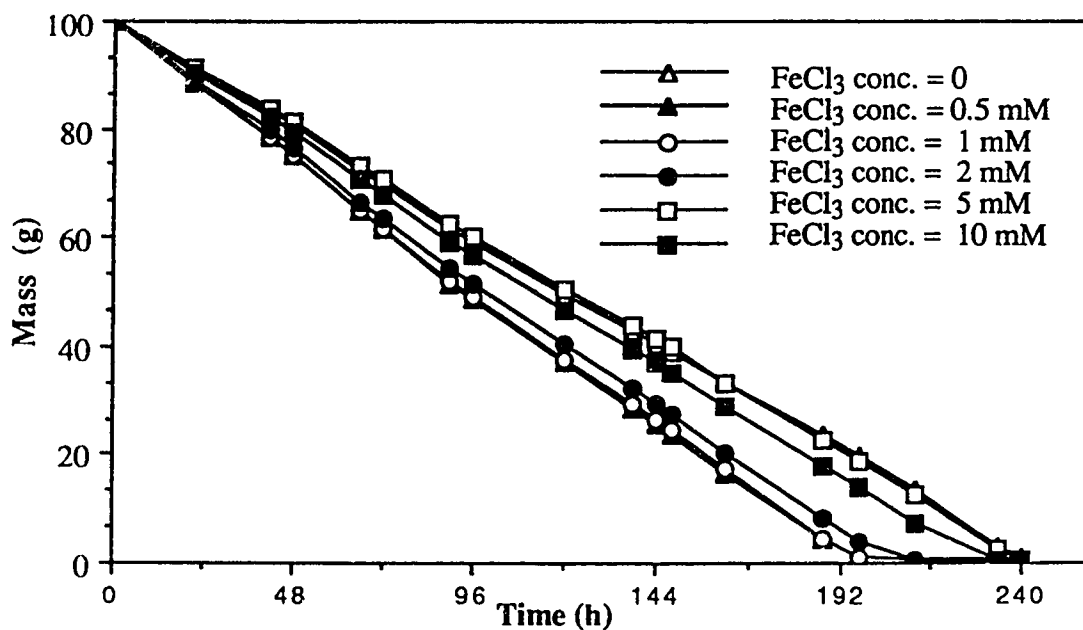
Fig.4.29   Drying kinetics of 0.5% SWy-1 montmorillonite suspensions with different
FeCl₃ concentrations at pH = 4.0.
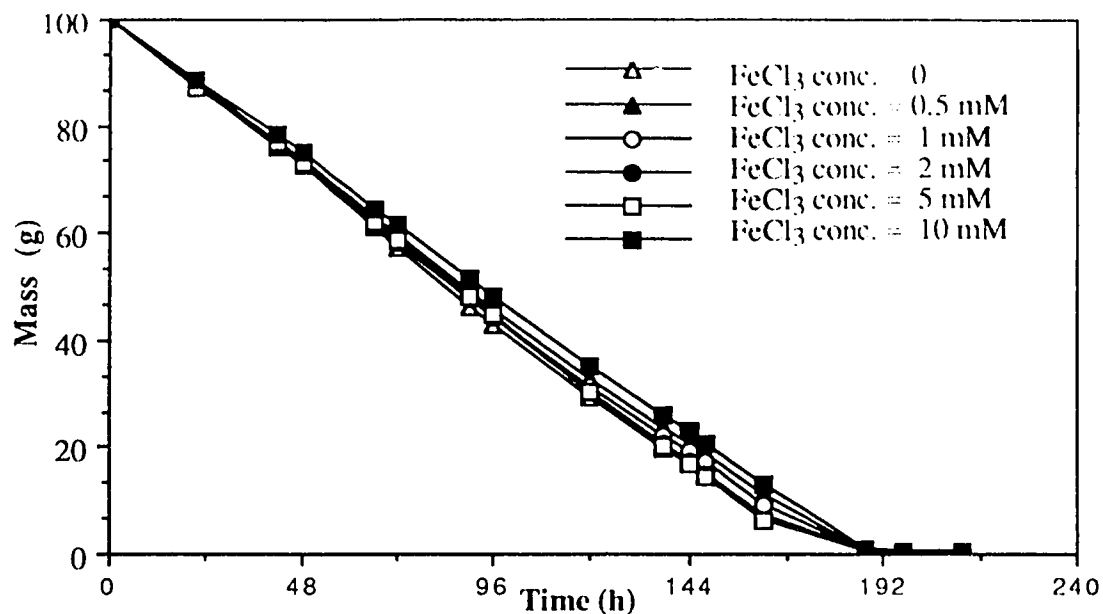
Fig.4.30   Drying kinetics of 0.5% SWy-1 montmorillonite suspensions with different
           FeCl₃ concentrations at pH = 9.4.
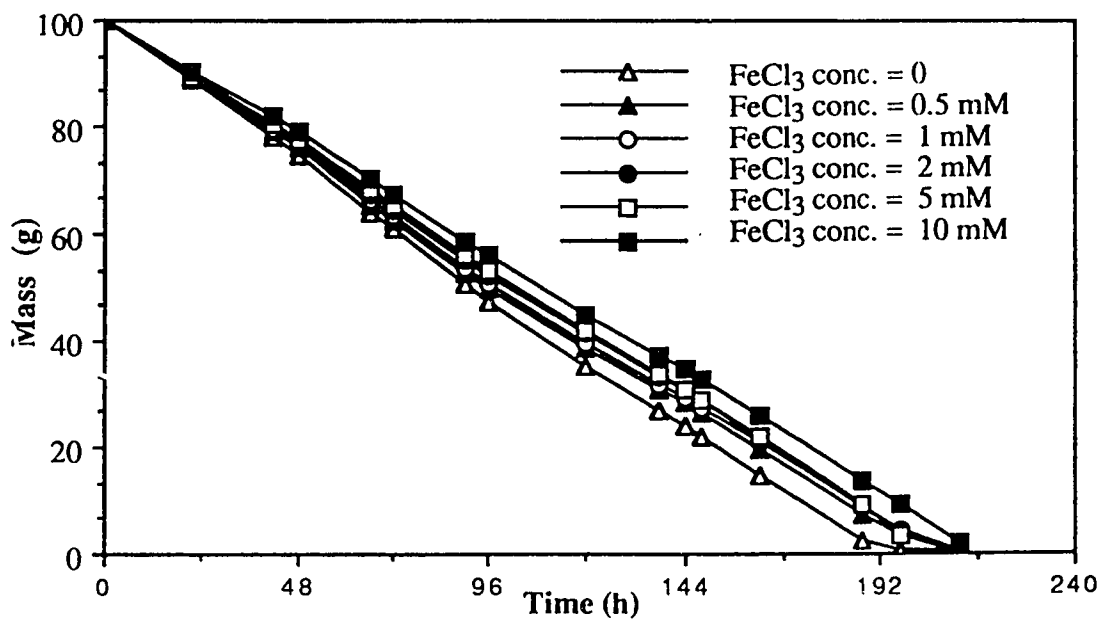
Fig.4.31   Drying kinetics of 0.5% SWy-1 montmorillonite suspensions with different
           FeCl₃ concentrations at pH = 10.0.
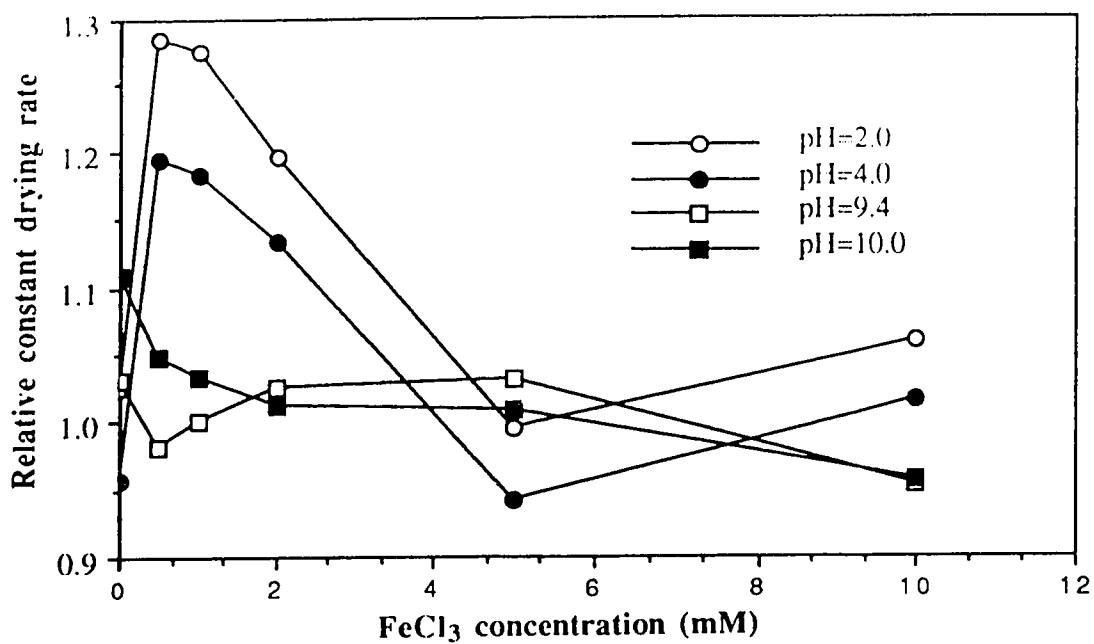
Fig.4.32   The relative constant drying rate of 0.5% SWy-1 montmorillonite suspensions
as a function of FeCl₃ concentration at different pH.
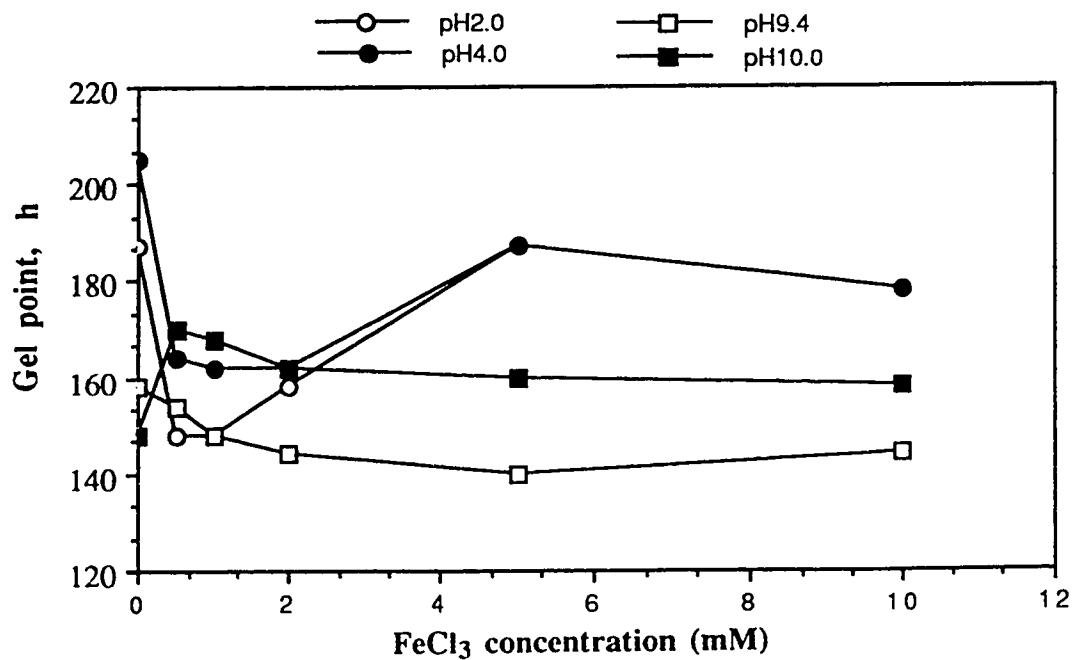
Fig.4.33   The gel point of 0.5% SWy-1 montmorillonite suspensions as a function of
FeCl₃ concentration at different pH.

Table 4.10 Gel point and the mass at the gel point of 0.5% montmorillonite suspensions at different FeCl₃ concentrations and the initial pH values of the suspensions

	FeCl₃ Concentration (mM)					
	0	0.5	1	2	5	10
pH 2.0						
Gel point, h	187	148	148	158	187	178
Mass, g	17.24	16.84	17.4	17.4	18.76	18.23
pH 4.0						
Gel point, h	205	164	162	162	187	178
Mass, g	16.46	15.43	17.25	20.42	22.53	21.78
pH 9.4						
Gel point, h	158	154	148	144	140	144
Mass, g	9.23	15.30	17.10	17.20	18.90	22.90
pH 10.0						
Gel point, h	148	170	168	162	160	158
Mass, g	22.10	15.55	18.1	21.53	23.17	26.84

4.4.2 Aspects near leatherhard point

Under the SEM after hypercritical drying, the structure near the leatherhard point of 5% montmorillonite suspensions does not show a clear trend regarding the effect of FeCl₃ concentration (Fig.4.34 and Fig.4.35). This indicates that the capillary stresses have compacted the structure of the gel to a uniform grid – the same structure observed on the clay without FeCl₃. Between the gel point and the leatherhard point, the capillaries have to shear the EE bonds in order to obtain FF packings. This will depend on the strength of the EE bonds, hence on Fe(III) concentration.

4.4.3 Aspects of samples hypercritically dried at gel point

The structures after hypercritical drying under the SEM of the samples at the gel point for different FeCl₃ concentrations and initial pH values of the suspensions are shown in Fig.4.36 to Fig.4.41. Each time two identical samples were prepared with each FeCl₃ concentration of 0, 0.5 and 5 mM and for each pH. One of these two samples was prepared using the hypercritical drying technique for SEM observation of the structure when reaching the gel point time.
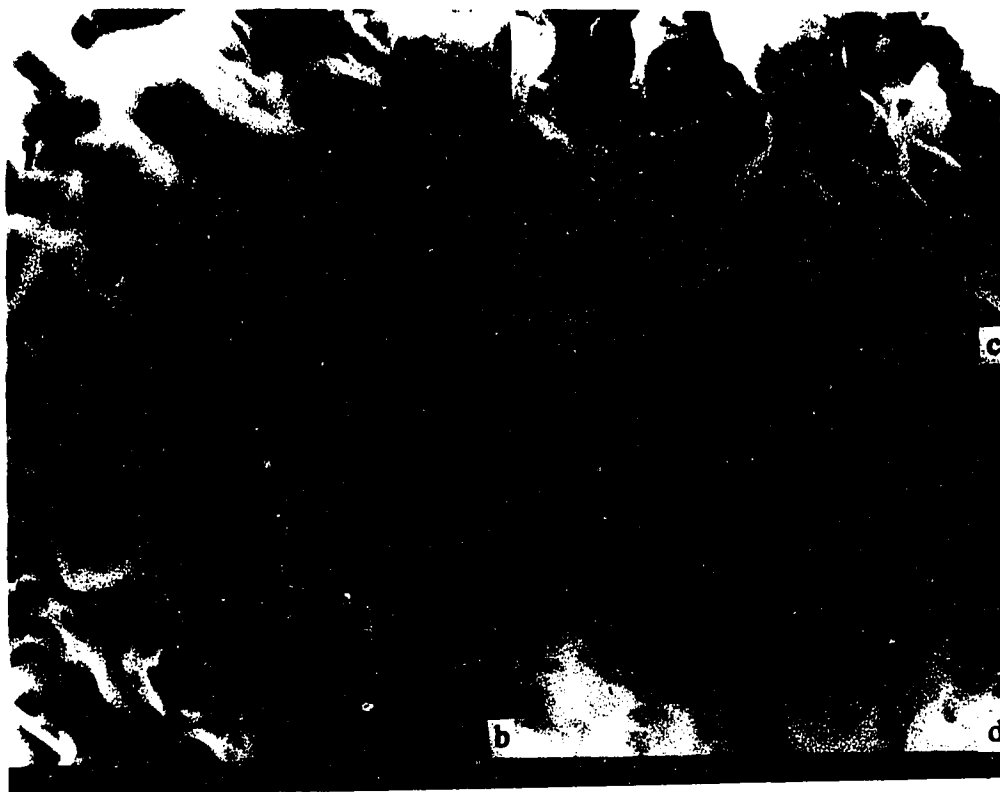
Fig.4.34 SEM structure on a 2 μm scale of 5% SWy-1 montmorillonite gel near
leatherhard point after hypercritical drying: (a) FeCl₃ Conc. = 0 ; (b) FeCl₃
Conc. = 1 mM; (c) FeCl₃ Conc. = 2 mM; (d) FeCl₃ Conc. = 10 mM.
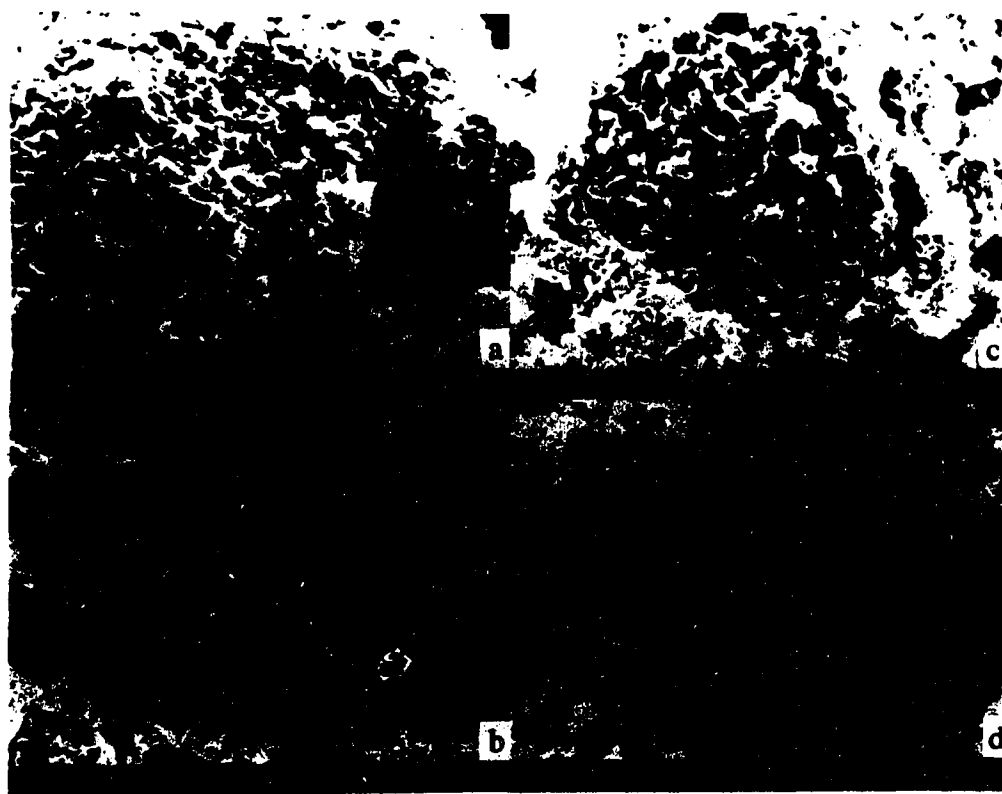
Fig.4.35 SEM structure on a 10 μm scale of 5% SWy-1 montmorillonite gel near
leatherhard point after hypercritical drying: (a) FeCl₃ Conc. = 0 ; (b) FeCl₃
Conc. = 1 mM; (c) FeCl₃ Conc. = 2 mM; (d) FeCl₃ Conc. = 10 mM.

On a smaller scale (10 μm), the packing of the clay particles is basically the same. The main differences are on larger scale (100 μm). We observe structures ranging from very uniform ones (Fig.4.36f, Fig.4.37h and Fig.4.38h) to more or less dense flocs clearly identified (Fig.4.36g, Fig.37e and f and Fig.4.38g). This is somewhat coherent with the uniformity observed at the leatherhard point. It seems to indicate that capillary stresses have forced linkage between the flocs by deforming them.

4.4.4 Aspects of samples dried by evaporation

For SWy-1 montmorillonite samples with $Fe_2(SO_4)_3$ as the electrolyte, the electrolyte concentration has an important effect on the behavior of montmorillonite during drying. At concentrations of 0, 0.1 and 0.5 mM, warping occurred after drying for 48 hours in the controlled humidity cabinet. After 72 hours, several cracks appeared in these samples, and kept opening with further drying. Consequently, the drying process accelerated and the volume of drying materials decreased quickly. On the contrary, no cracks occurred in other samples with higher electrolyte concentrations until 408 hours, and the volume of these samples kept decreasing very slowly (Fig.4.39a). After 552 hours, one single crack occurred in samples with electrolyte concentrations of 2 and 5 mM. The only sample to remain perfectly monolithic without cracking contained 1 mM electrolyte (Fig.4.39b). It also has the highest volume.

The structures of dried samples observed under the SEM shows that the packing of the dried samples changed abruptly from a laminar structure to a random and more open one when $Fe_2(SO_4)_3$ concentration increases from 0.5 mM to 1 mM (Fig.4.40).

The cracking behavior during drying and the structure aspect after drying prove that Fe strengthens considerably the clay network.

Like with $Fe_2(SO_4)_3$, the addition of $FeCl_3$ also has an effect on the aspects of the dried samples. For all samples, a relatively small extent of radial shrinkage occurs by comparison with thickness shrinkage (Fig.4.41). However, for the sample without $FeCl_3$, cracks occur and the thin plate-like material can be easily peeled off (Fig.4.41a). When the $FeCl_3$ concentration is above 1 mM, no cracks occur and the dried materials cannot be peeled off even with the help of a sharp tool (Fig.4.44b and c). These indicates $FeCl_3$ also acts as a strong bonding agent with the glass container.
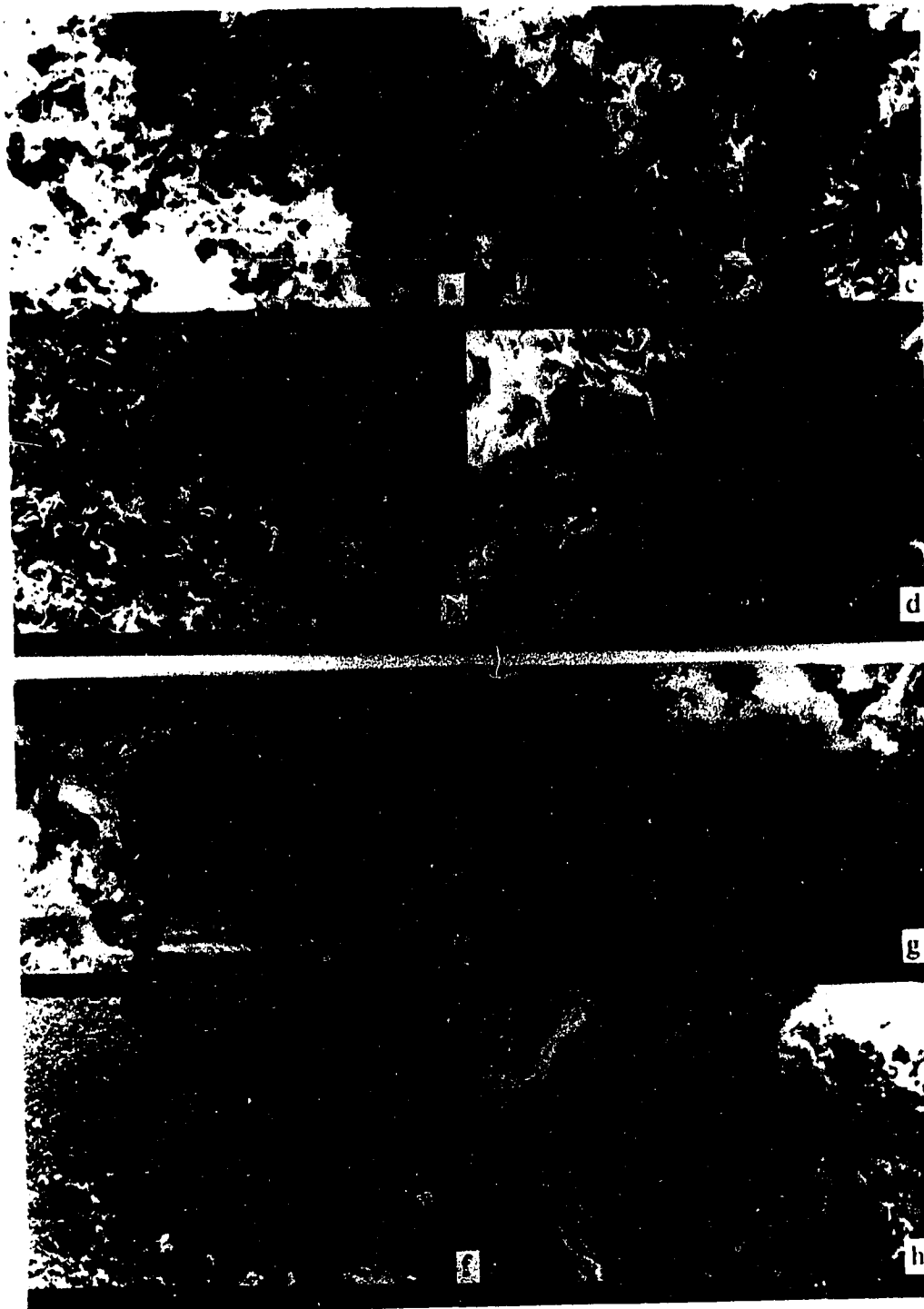
Fig.4.36 SEM structure after hypercritical drying on 10 and 100 µm scales of 0.5% SWy-1 montmorillonite suspensions at gel point without FeCl₃ at different pH: (a) and (e) pH 2.0; (b) and (f) pH 4.0; (c) and (g) pH 9.4; and (d) and (h) pH 10.0.
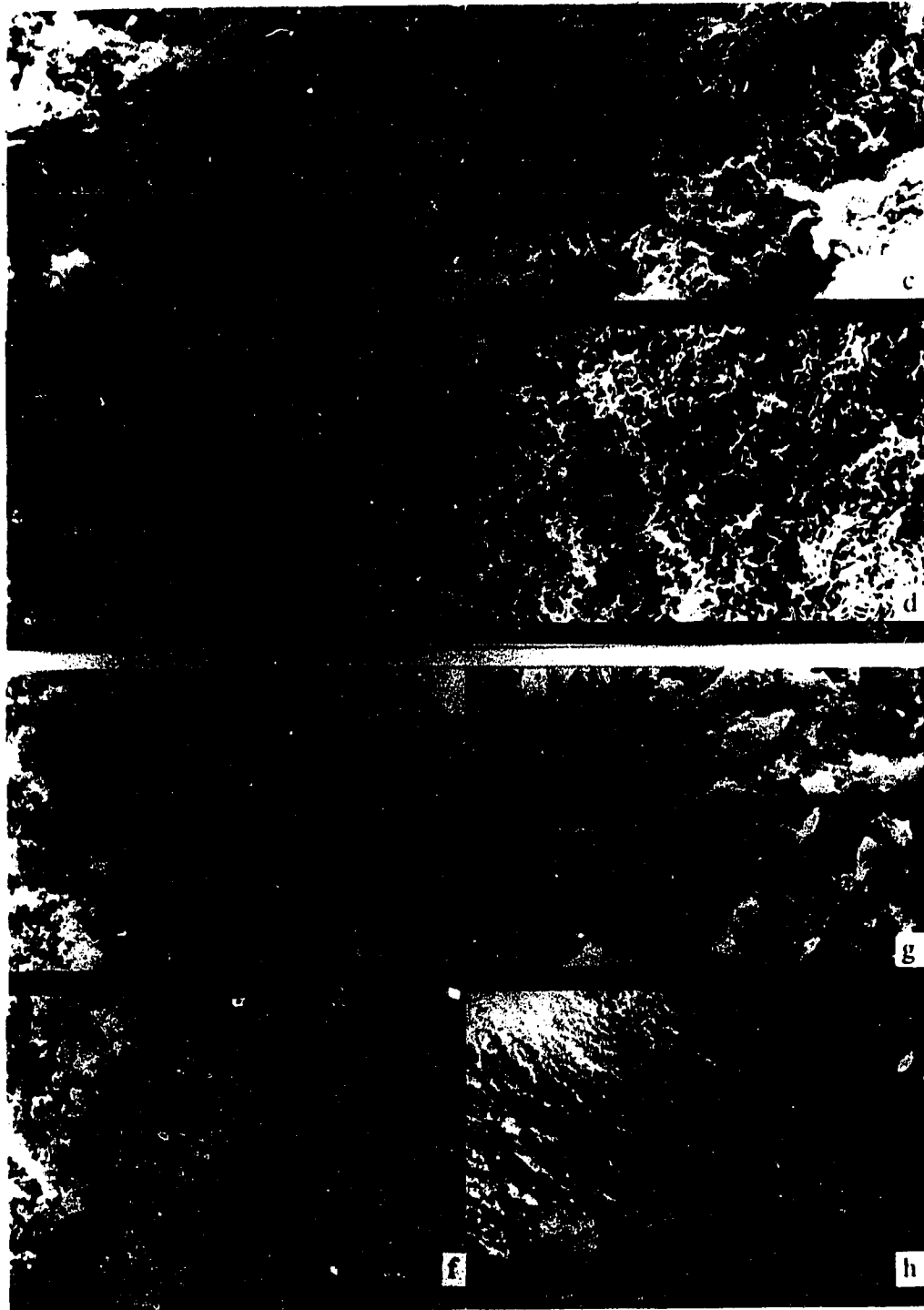
Fig.4.37 SEM structure after hypercritical drying on 10 and 100 μm scales of 0.5% SWy-1
montmorillonite suspensions at gel point with 0.5 mM $FeCl_3$ at different pH:
(a) and (e) pH 2.0; (b) and (f) pH 4.0; (c) and (g) pH 9.4; and (d) and (h) pH
10.0.
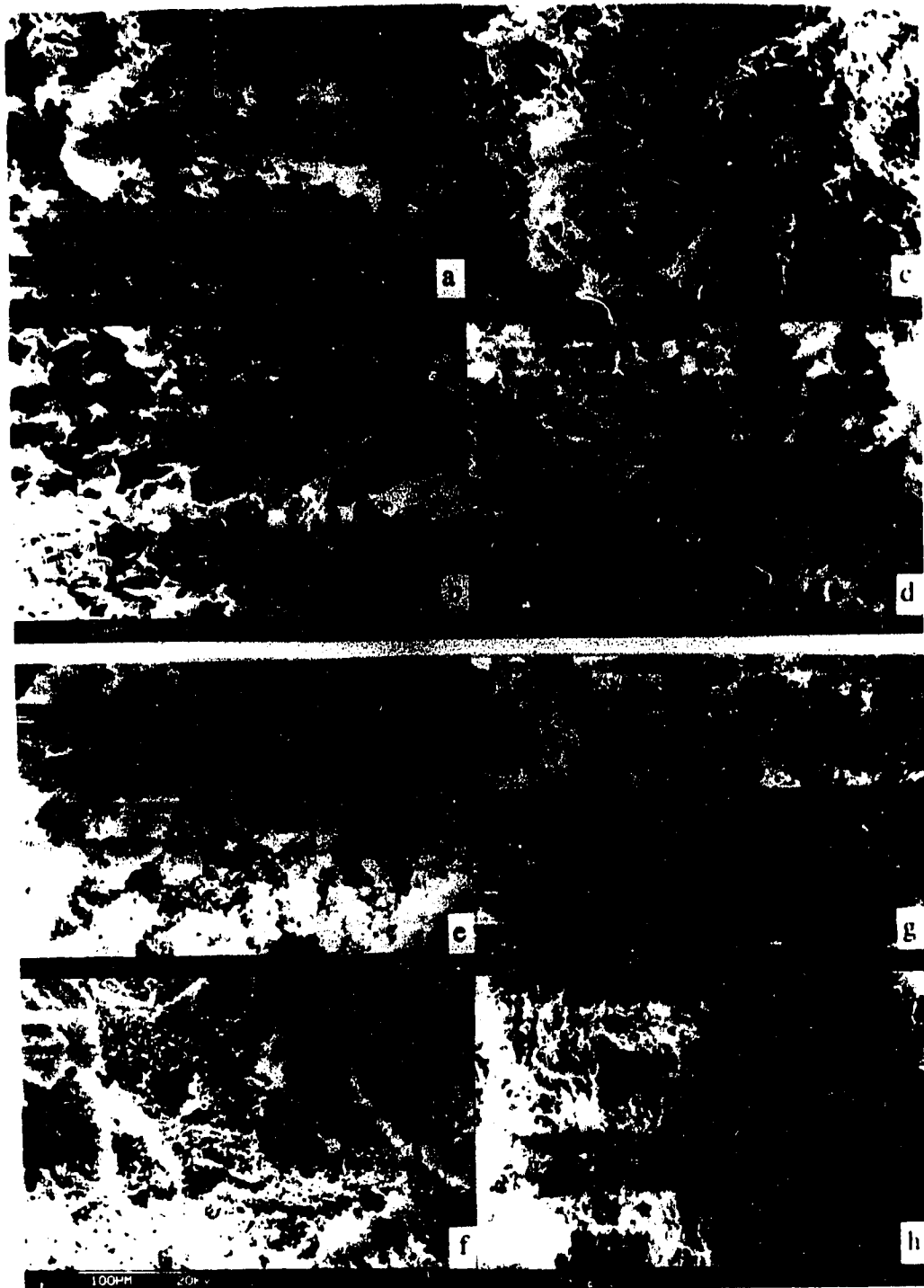
Fig.4.38 SEM structure after hypercritical drying on 10 and 100 μm scales of 0.5% SWy-1
montmorillonite suspensions at gel point with 5 mM FeCl3 at different pH:
(a) and (e) pH 2.0; (b) and (f) pH 4.0; (c) and (g) pH 9.4; and (d) and (h) pH
10.0.

The moisture content at the leatherhard point increases with the $FeCl_3$ concentration (Fig.4.42), indicating an increase in the sediment volume. That is to say the flocs are stronger and can resist more to collapse by the capillary stress.
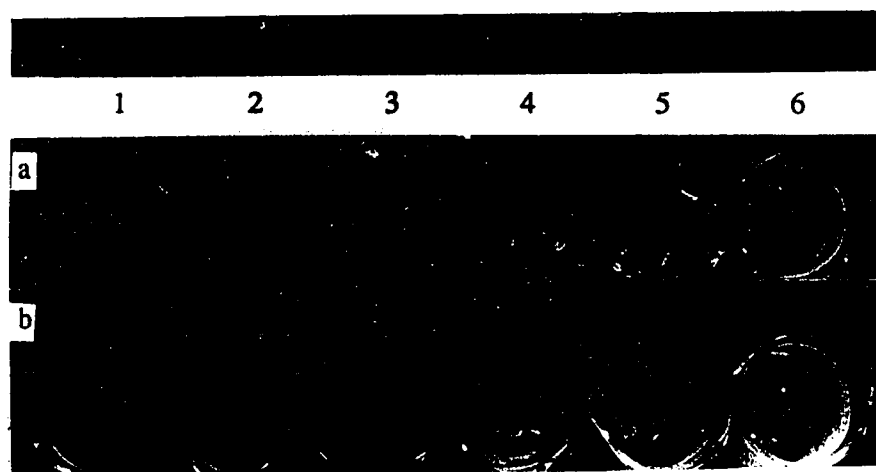
Fig.4.39 Volume and shape of 5% SWy-1 montmorillonite gel with different $Fe_2(SO_4)_3$ concentrations after drying for : (a) 408 hours; (b) 552 hours (R.H. =95%, T=25°C; $Fe_2(SO_4)_3$ concentration in mM from #1 to #6: 0, 0.1, 0.5, 1, 2 and 5 respectively).

Fig.4.40 SEM structure of conventionally dried sediments of 5% SWy-1 montmorillonite gel with different $Fe_2(SO_4)_3$ concentrations in mM: (a) 0; (b) 0.1; (c) 0.5; (d) 1; (e) 2 and (f) 5.
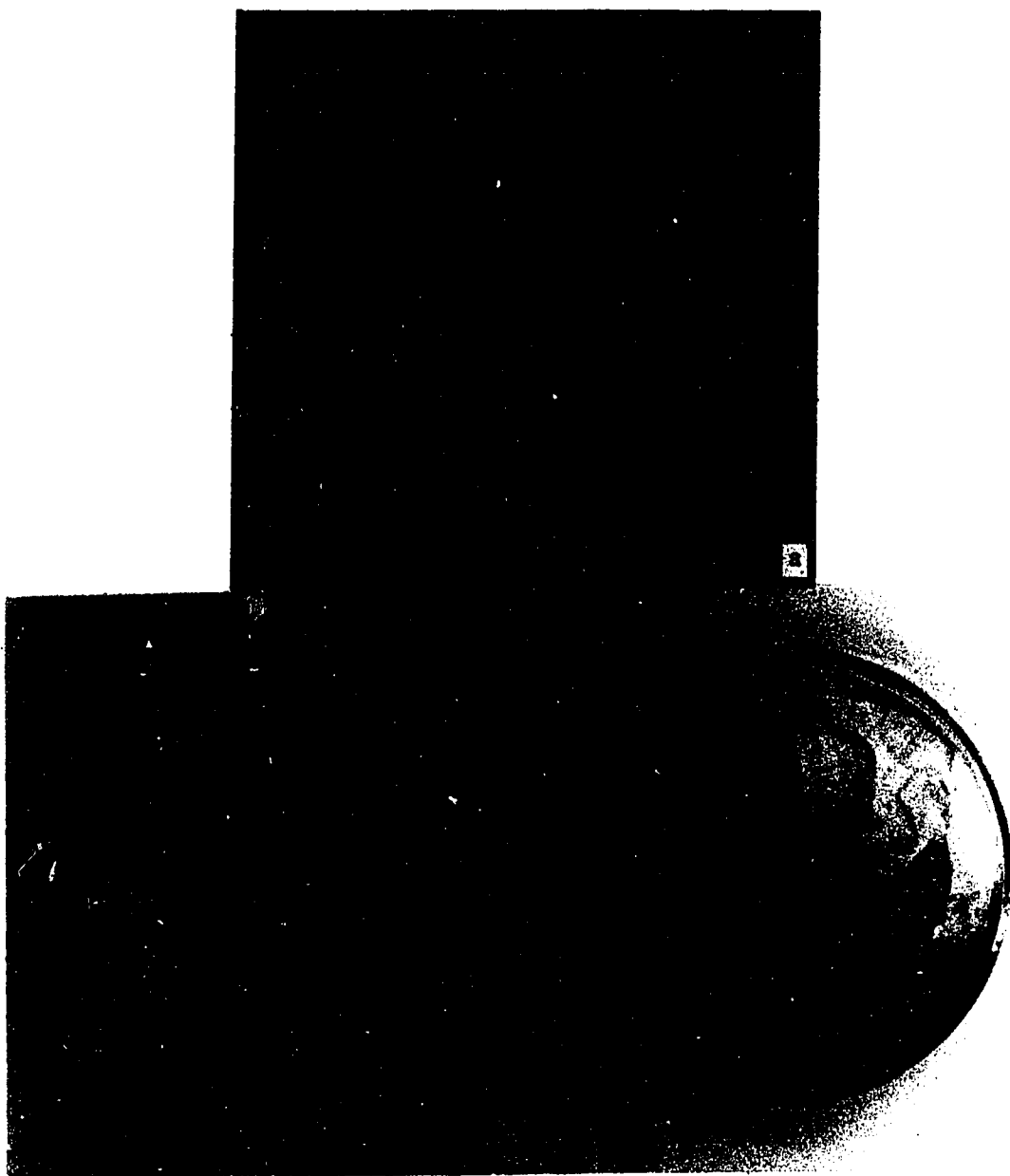
Fig.4.41 Aspects of 5% SWy-1 montmorillonite gel after complete drying with different FeCl₃ concentration in mM : (a) 0; (b) 2 mM; and (c) 50 mM.
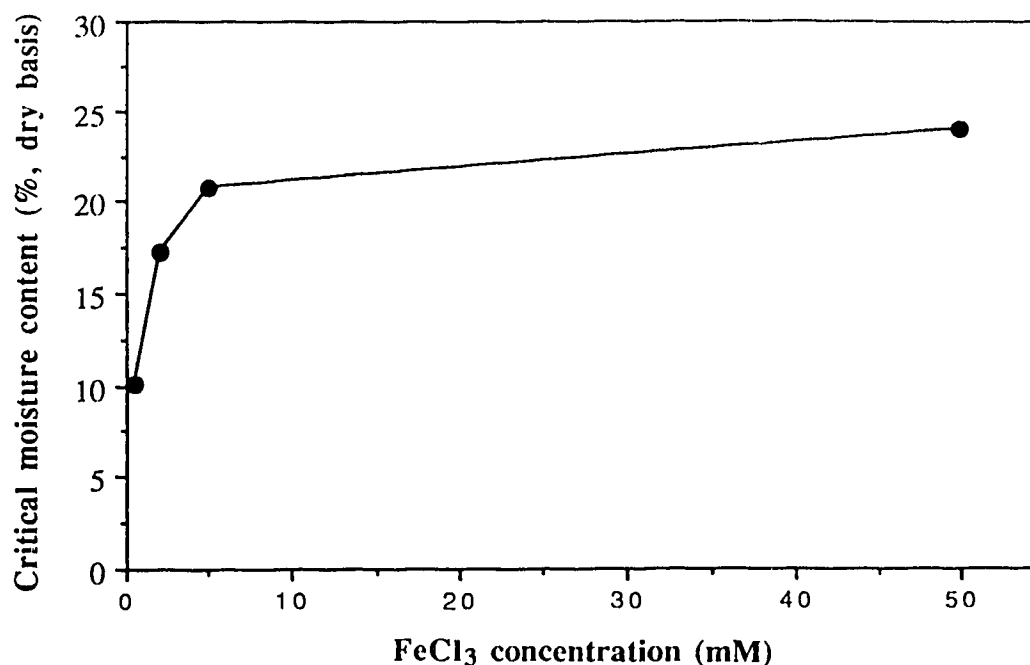
Fig.4.42 Moisture content of 5% SWy-1 montmorillonite gel at leatherhard point as a function of $FeCl_3$ concentration.

4.5 SWELLING OF MONTMORILLONITE

A certain extent of swelling is observed for all samples in spite of their difference in electrolyte concentration, nature of the medium and the sample preparation procedure. However, the extent of swelling is mainly determined by the electrolyte concentration and the nature of the medium.

4.5.1 Electrolyte effect

For a first-time test on fresh SWy-1 montmorillonite, without adding any electrolytes, the clay volume increases dramatically from 0.5 mL to 5 mL in the first half hour (sample #1B in Fig.4.43). Then it increases more and more slowly to 9 mL in 48 hours, where it remains constant up to 144 hours. Finally it resumes swelling after 144 hours to reach a final stable volume of 13 mL after 360 hours (Fig.4.43 #1B). For the second time swelling test after a preliminary swelling followed by drying, the swelling kinetics is faster than the first time. It also follows a more regular route (Fig.4.43 #1A). However, the asymptotic

swelling after a long time is the same. The same asymptotic value of swelling is done from a montmorillonite suspension which had been dried previously (#3A).

In a 5 mM FeCl$_3$ solution (sample #2B), the first swelling of fresh montmorillonite powder proceeds to 5.5 mL in the first half hour, then stops completely. After drying, the second time swelling is very limited, reaching 1.5 mL in the first half hour, then stopping (#2A).
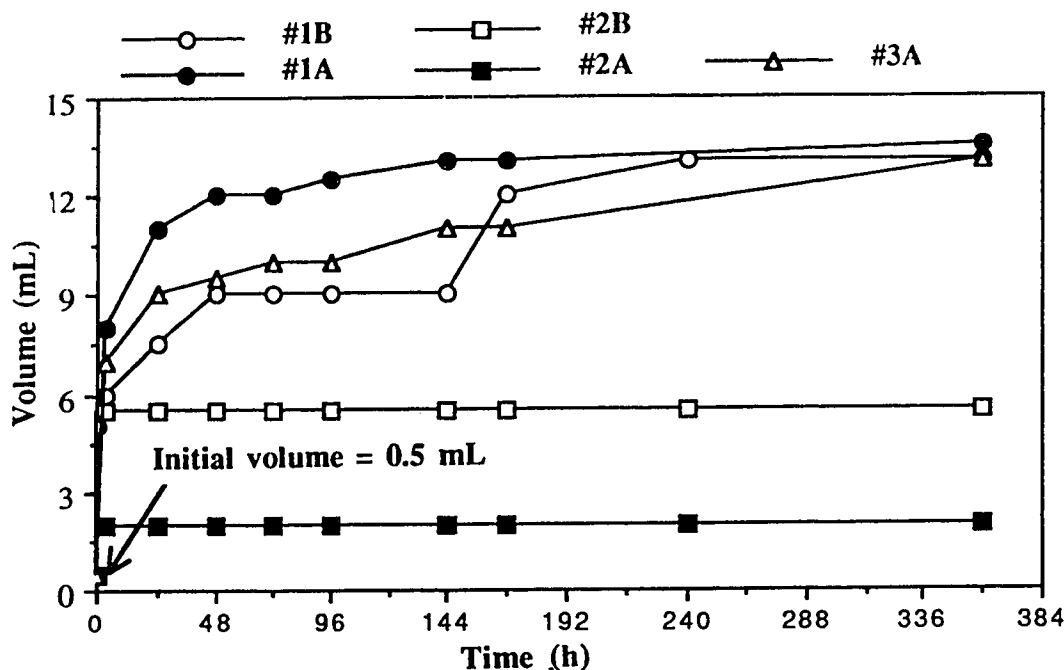
Fig.4.43 Swelling kinetics of sample #1 to #3. B- not preceded by drying; A- preceded by drying.

For sample #4 to #6, after a preliminary drying, very limited swelling occurs in the first half hour (see Section 3.2.5 for the detail of each sample). They follow the same pattern as sample #2 in the second time test (Fig. 4.43 #2A). The final swelling volume for sample #4, #5 and #6 is the same as in the first half hour, being 2.5mL, 2 mL and 2 mL; respectively.

If the swelling in the first half hour is defined as the initial swelling, and the swelling after initial swelling is defined as second stage swelling, then, the above results can be summarized as follows: the initial swelling exist for all samples and the second stage swelling is observed for the samples without any electrolytes. In fact, the initial swelling is

the interlayer swelling, while the second stage swelling is physical swelling. With electrolytes, the driving force responsible for the physical swelling, double layer repulsion, decreases. In the meantime, the attraction between particles predominates.

We also observed that the swelling begins from the top. When extensive swelling occurs in the upper part, the material in the bottom is still in the powder form while the upper part of the swelling sample consists of diffusive layer after some time.

In addition, swelling experiment at the end of drying a group of 5% SWy-1 montmorillonite gel (see **Section 3.2.4** for detail) shows the extent of swelling decreases with $FeCl_3$ concentrations. Without electrolytes, the clay sheet (see Fig.4.41) swells considerably in two directions: radially and vertically. When $FeCl_3$ reaches 1 mM, only interlayer swelling is observed. No physical swelling is observed for montmorillonite K10 without adding any electrolytes. Dried reference 1 and reference 2 sludge samples do not show any tangible swelling in distilled water.

4.5.2 Solid content effect

The result of the experiment shows that the volume of montmorillonite after swelling does not double when the amount of montmorillonite added doubles (see **Table 4.11**). The swelling volume for 1 g SWy-1 montmorillonite after 60 days' swelling is about 30% higher than that of 0.5 g SWy-1 montmorillonite (16.5 mL versus 13 mL).

Table 4.11 Volume of montmorillonite after 60 days' swelling vs. initial solid content without any electrolytes

Sample No.	Solid content (g)	Volume (mL)
#1	0.5	17
#2	0.5	16
#3	1	21
#4	1	22

4.5.3 Medium effect

The extent of swelling has been also found to depend on the liquid composition where it is performed. We report the effect of the medium on the swelling of fresh montmorillonite after 10 days.

Ethanol

The volume of montmorillonite after 10 days' swelling in various mixed distilled water-ethanol solutions is shown in **Table 4.12**. When the water content increases above 35 %, the extent of swelling increases dramatically. Above a 75 % water content, the swelling volume is almost the same as that in 100 % distilled water.

At the end of the swelling test, the cylinders containing the samples were shaken forcefully by hand and each sample became a suspension. It was found the the stability of these suspensions increases with the water content. After standing for 24 hours, all particles in samples 1 and 2 had settled to the bottom, and their sediment volume was 1 mL. When the water content increased from 20% to 50% (sample 3 to 6), the turbidity of the suspension decreased. When the water content reached 75%, a very stable suspension formed. That is, the extent of swelling as a function of water content is consistent with the stability of the suspensions as a function of water content.

Acetone

The swelling of montmorillonite in a water-acetone solution is similar to the swelling in a water-ethanol solution (see **Table 4.13**). The only difference is that obtaining full swelling is much easier with the former than with the latter (35% water content versus 75% water content).

Table 4.12 Volume of montmorillonite after 10 days' swelling in the water-ethanol solution

Sample	1	2	3	4	5	6	7	8
Water, %	0	5	10	20	35	50	75	95
Ethanol, %	100	95	90	80	65	50	25	5
Volume, mL	1	1	1	1.5	2	8	12	12

Table 4.13 Volume of montmorillonite after 10 days' swelling in the water-acetone solution

Sample	1	2	3	4	5	6	7	8
Water, %	0	5	10	20	35	50	75	95
Acetone, %	100	95	90	80	65	50	25	5
Volume, mL	1.5	1.5	1.5	4	11	12	12	13

CHAPTER 5   DISCUSSION

The aim of the present research is to design a simple experimental model for oil sands sludge. This model has three components: clay (mostly montmorillonite), Fe(III) and water. Results are discussed below under two main subjects: (1) the properties and behavior of the selected ternary model, and (2) the validity of the model system in describing actual oil sands sludge. Finally, some possible clues are offered to solve the oil sands sludge disposal problem.

5.1 PROPERTIES AND BEHAVIOR OF THE MODEL SYSTEM

Clay particles tend to aggregate in a fashion which depends on the conditions in the aqueous medium where they have been dispersed. Their behavior during sedimentation, drying and swelling is a consequence of the structure of aggregates which are created.

5.1.1 The structure of aggregates

The way in which the montmorillonite plate-like particles are linked in aqueous medium has been the subject of much discussion. The model most often advocated is the card-house structure with three possible modes of particle association (49): FF, EF and EE. It appears that the structure of aggregates in our model is well illustrated by the photographs taken after drying hypercritically. However, the FF linkage is not observed, which can be explained by the relatively strong double layer repulsion between negatively charged faces. The FF linkage occurs only with forced shrinkage by capillary stresses when dried by evaporation as indicated by Fig.4.40. The EF linkage, which is often considered as the mechanism for the gelation of montmorillonites, is also absent. As a matter of fact, only EE linkage seems to prevail. This is consistent with the DLVO theory of gelation, since it is well known that the electric double layer is less thick near the edges of plates, and, hence, favors linear flocculation. Fe (III) has a triple role in the system: (1) as a counterion favoring EE approach; (2) as a former of Fe polymeric chemical complexes (when freshly prepared) which acts as bonding agents; and (3) as an exchange cation anchoring the Fe complexes in the clay plates.

The main difference between the various types of aggregates is a difference of the packing efficiency between the solid-like sediment (sample without Fe (III)) and the liquid-like sediment (the sample with 5 mM FeCl$_3$). For the sample without Fe (III), the double layer

repulsion between montmorillonite particles is strong, and flocculation does not occur. These particles settle as individual units, the separation between these settled platelets is mainly determined by the magnitude of the double layer repulsion between the faces. Because the double layer repulsion is basically the same for all particles and the double layer repulsion only predominates at very small separation, the packing shows a uniform and relatively dense grid with many 3-edge branching, where one edge is shared by three platelets.

Flocculation occurs in the sample with 5 mM $FeCl_3$. The packing efficiency is determined by the nature of fractal branches, rather than the packing pattern inside the first level flocs in which the primary particles are always densely packed together (12), as indicated in Fig. 4.25a and d. Since the repulsion between edges is lower than that between faces, edge-to-edge linkage occurs. The linkage in these branches is strong because of the hydrolysis of Fe(III), which glues two neighbor platelets by an iron-gel bond.This creates a fractal flocs network. The overall picture is consistent with the structures built by colloidal sols through diffusion-limited aggregation (DLA) (86).

In summary, these SEM observations show that the structure of the liquid-like sediment of montmorillonites is similar to the hierarchical structure usually considered for colloidal silica gel (87), except that the spherical silica particles are replaced by plate-like montmorillonite particles. The addition of fresh Fe(III) has a very important effect on the structure of sediments, by strengthening their fractal branches.

5.1.2 Settling and consolidation behavior

Most of the results found in the flocculation and sedimentation experiments can be qualitatively interpreted in agreement with the D.L.V.O. theory and the description of clays as platelike particles with their faces charged negatively.

With the SWy-1 montmorillonite suspensions, Fe^{3+} constitutes what is called the counterion. When its concentration is low and pH>4, the electrostatic repulsion between particles is strong. Those colloidal particles remain dispersed, while the non-colloidal particles fall under gravity. Hence, a three-layer segregation is observed, with the non-colloidal particles packing tightly in a solid-like sediment at the bottom of the cylinder, while the colloidal particles remain dispersed for a long period of time in the sol (Fig.5.1a). Since the time required for the non-colloidal particles to settle is directly proportional to the

distance between the particles and the bottom of the container, the sediment volume increases linearly with time. For those particles with a size close to the upper limit of the colloid, their thermal energy begins to slow down their settling rate. For those colloidal particles in the lower limit of colloid, settling occurs extremely slowly as a result of aging of these particles. Because of the wide particle size range, we observe the type of settling curve in Fig.4.14, that is, the sediment volume increases linearly with time for some time, then increases at a decreasing rate and finally virtually stops.

As the $FeCl_3$ concentration increases, the electrical double layer around each clay particle becomes thinner and the repulsion between particles decreases to such an extent that collisions between particles can lead to the formation of flocs. These flocs have a very open structure. They hinder each other in the settling process even when the solid content of suspensions is low (0.5%); that is, a floc can move downwards only when the floc below it moves downwards. Therefore, the flocculated suspension seems to settle as a single kinetic unit. Consequently, a two-layer segregation can be observed: the liquid-like sediment and the supernatant liquid (Fig.5.1b). As the $FeCl_3$ concentration keeps increasing, the electrical double layer becomes even thinner and the flocs become denser. As a result, the settling rate of these flocs increases, and thus the overall settling rate of the sediment. The liquid-like sediment volume before consolidation decreases.
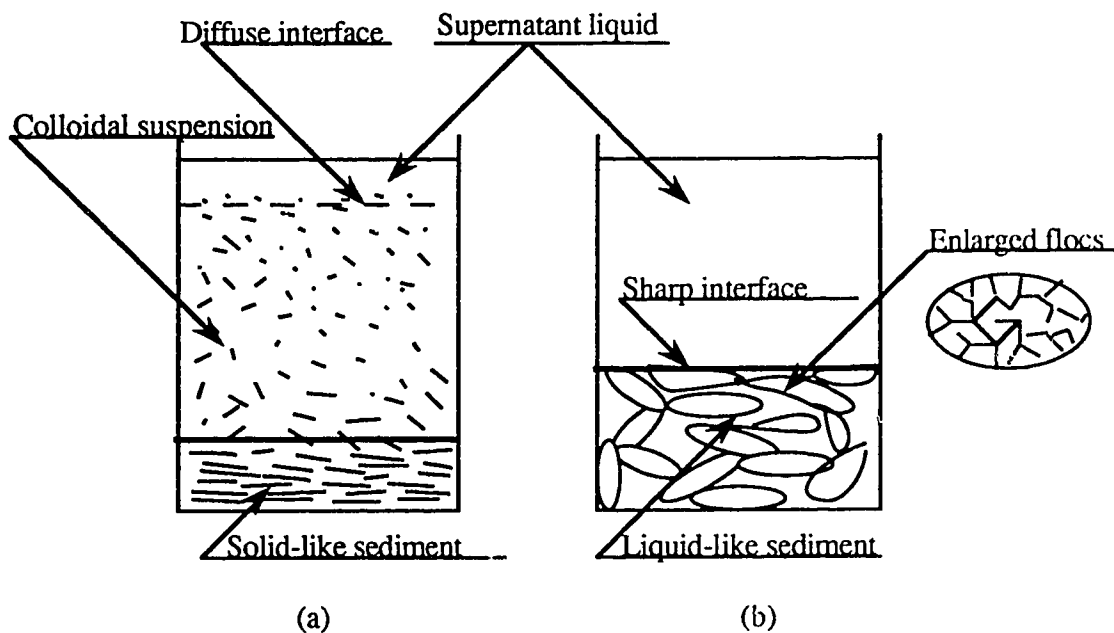
Fig. 5.1 Mechanisms of layer segregation for suspensions made with plate-like clay particles: (a) three-layer segregation; (b) two-layer segregation.

The fractal chains formed by the primary particles in the flocs are flexible and can be slowly compressed during consolidation. The flexibility of these chains increases with the fractal character of these colloidal chains. Consequently, while a low Fe^{3+} concentration results in a lower constant settling rate together with a higher liquid-like sediment volume before consolidation, the sediment volume ends up being lower during consolidation due to the formation of more fractal flocs.

The effect of the suspension pH is similar. As the pH increases, it is well known that the magnitude of the negative zeta potential of montmorillonite increases. That is to say, the repulsion between particles increases, and the flocs become, on average, more fractal. Therefore, the constant settling rate decreases with the suspension pH, while the liquid-like sediment volume before consolidation increases. In details, the zeta potential of montmorillonite changes moderately between pH 4 and pH 10, and abruptly around pH 10 (62); so do the constant settling rate and the final sediment volume.

With Fe(III) as the counterion, the hydrolysis of Fe(III) also has an effect on the linkage between clay particles. It is well known that the earlier hydrolysis products of freshly prepared Fe(III) solutions act as bonding agents, and the final product after aging, iron oxide, is present as discrete particles with little bonding effect (65, 67, 88). Actually, Fe(III) is well known to undertake its own hydrolysis upon aging, and to form pH-dependent hydrolysis products. When the freshly prepared $FeCl_3$ concentration increases, more hydrolysis products are formed. The bonding between clay particles increases and offers more resistance to the shearing of the bond between particles. Therefore, the final sediment volume increases with $FeCl_3$ concentration.

The hydrolysis products known to form with Fe(III) go from α-FeOOH (goethite) at pH >10 to α-Fe_2O_3 (haematite) at pH<4, with a mixture of both materials in the pH range 4 to 10 (79). It is very interesting to note that these two pH values correspond to the two end points of a plateau in the constant settling rate vs. pH curve and the final sediment volume vs. pH curve. In addition, the color of the sediments remains basically the same between pH 4 and 10 for a given $FeCl_3$ concentration (see **Table 4.4**). This indicates that the same type of hydrolysis product of Fe(III) forms between pH 4 and 10.

Hence, Fe(III) does not only behave as a simple counterion for the negatively charged clay particles. It also surrounds them with its hydrolysis products, and changes the structure of

the sediment. Actually, at pH =11.8, a red hydrolysis product distributes itself over the liquid-like sediment.

It is also known that the hydrolysis of metal cations in aqueous solution depends largely on the anion (79, 81). This is mainly because the polymeric complexes which are built during hydrolysis incorporate the anions in their structure. The difference found between $FeCl_3$ and $Fe_2(SO_4)_3$ is, therefore, not surprising.

The nature of ions may affect the settling and consolidation behavior of the model system through the following two ways. First, the valence and the concentration of anions modify the double layer thickness (see eq.2.1), that is, the double layer repulsion between particles, thereby modifying the fractal nature of flocs. Second, the anions have marked effect on the hydrolysis and condensation reactions and therefore the hydrolysis products as mentioned in **Section 2.5.**

The very different behavior with montmorillonite K10 suspensions indicates that montmorillonite K10 has been severely contaminated. Since montmorillonite K10 has gone through chemical processing and was not purified before the experiments, the differences found between SWy-1 montmorillonite and montmorillonite K10 are not surprising. It shows the importance of sample source and purification. Generally speaking, differences regarding the colloidal behavior of clays, such as CFC and swelling behavior for the same type of clay, come partly from differences in sample sources and different purification procedures.

5.1.3 Drying behavior

In general, the drying behavior of all samples for the model system is roughly consistent with the classical drying behavior of clays. That is, a constant drying rate period is followed by a falling rate period. The surface area available for evaporation changes with time as a result of the warping and cracking. The change in surface area is often moderate , and may not have a major effect on the drying rate. Macey (89) found that a slight reduction of evaporation surface area in the shrinkage period, and only a slight correction had to be done when evaluating the drying rate per unit area.

The results of drying experiments show the constant drying rate is affected by both the $FeCl_3$ concentration and the suspension pH. This could be explained by the fact that both

the electrolyte concentration and the suspension pH modify the interactions between clay particles. Consequently, the structure of the drying mass are modified. However, it does not show a clear trend with respect to the $FeCl_3$ concentration and the suspension pH. Since some differences may exist in the size of drying dishes and the local air velocity around each dish, it is difficult to make a conclusion regarding the effect of electrolyte concentration and pH on the constant drying rate at this stage. Further controlled experiments are needed to reach a conclusive result.

Visual and SEM examinations on the model system dried by evaporation show that cracking is avoided or delayed in the drying process, while the laminar structure of dried materials changes to a more open one when the electrolyte concentration exceeds a certain value. It is well known that rapid and uneven drying result in moisture gradients which are responsible for the warping and cracking. The addition of electrolytes usually leads to the formation of a more open structure that enables the moisture to escape more readily from the interior, consequently avoiding cracking or reducing its extent (20,77). The observed moisture content at the leatherhard point increases with the electrolyte concentration. This can well be explained as follows. As the electrolyte concentration increases, a more open and stronger structure forms; consequently, more water is trapped inside the sediment at the leatherhard point.

By examining the structure of the model system by the hypercritical drying method at the gel point, near the leatherhard point, and after completely drying by evaporation (Fig.4.25, 4.36, 4.37, 4.38, 4.34, 4.35 and 4.40), it can be seen that the capillary stresses due to the liquid/air meniscus have compacted the structure of a liquid-like sediment from a very open to a very dense one. However, the shearing of EE bonds seems not to occur until the end of drying or even not occur at all. Normally, the leatherhard point is where the shrinkage stops, hence FF packing must be achieved between the gel point and the leatherhard point. This indicates therefore that the hydrolysis products of Fe(III) act as strong bonding agents between the edges of montmorillonite particles.

5.1.4 Swelling behavior

The results of swelling experiments show the driving force responsible for the swelling of montmorillonite, especially the physical swelling, is the double layer repulsion between particles.

In the absence of electrolytes (samples #1B and #3A), the double layer repulsion between montmorillonite is strong. First, water molecules penetrate the layer structure of montmorillonite, increasing the interlamellar distance inside one particle and the volume increases to a minor extent. Then, the double layer repulsion begins to operate and push particles as far away as possible in relation with a decreases in van der Waals attraction. This is consistent with the fact that the double layer repulsion only predominate at a certain separation range (see Fig.2.2). With the addition of electrolytes, the double layer repulsion decreases. Therefore, the extent of swelling decreases with the increasing electrolyte concentration.

We know from the flocculation and sedimentation experiments, that the CFC of $FeCl_3$ for 0.5% montmorillonite suspensions is 0.5 mM. When placed in 5 mM $FeCl_3$ solution, montmorillonite shows some extent of physical swelling in the first half hours, then swelling does not proceed any further (sample #2B). This is mainly because it takes some time for flocculation to occur. Before flocculation, the double layer repulsion is higher than the attraction; consequently, swelling occurs to a certain extent. Once flocculation begins, the attraction begins to dominate, therefore, no further swelling occurs. The same sample does not show any physical swelling after drying (sample #2A). This result and that of samples #4 to #6 all prove that once flocculation occurs, the physical swelling by the double layer repulsion is not possible. Besides, Fe (III) helps to form strong bonds between the clay particles.

The swelling volume of SWy-1 montmorillonite does not double when its amount doubles. This is mainly because SWy-1 montmorillonite may contains small amounts of ions. When the solid content increases, the amount of ions also increases. Consequently, the double layer repulsion decreases and so does the extent of swelling. Although when the amount of montmorillonite increases, the weight of overburden borne by the bottom particles increases, the weight difference between 0.5 g and 1 g cannot lead to the considerable difference in the swelling volume. Westman (90) found that a external pressure of about 5.5 MPa was required to reduce the volume of plastic clays to the normal dry volume.

The effect of liquid nature on the swelling of a montmorillonite and the stability of montmorillonite suspensions made with water-organic solution indicates the addition of organic liquids like ethanol and acetone reduces the repulsion between the particles.

From eq. 2.1, we know that the double layer thickness κ^{-1} is directly proportional to the square root of the dielectric constant ε of the medium, assuming all other parameters are not modified. That is:

$$\kappa^{-1} \propto \varepsilon^{1/2} \qquad\qquad\qquad (eq.5.1)$$

For a mixture of two components, water and a non-electrolyte, when the non-electrolyte concentration is low, the static dielectric constant of the mixture (ε_{sm}) is approximately a linear function of the concentration C_2 of the non-electrolyte in moles per litre of solution (91):

$$\varepsilon_{sm} = \varepsilon_{s1} + \delta C_2 \qquad\qquad\qquad (eq.5.2)$$

Where ε_{s1} is the static dielectric constant of pure water and δ is the dielectric increment.

Table 5.1 Dielectric constants of water-acetone or water-ethanol solutions (92)

Solvent, % by mass	ε, at 20°C, for water-acetone or water-ethanol mixture	
	Acetone	Ethanol
10	74.8	74.6
20	68.6	68.7
30	62.5	62.6
40	56.0	56.5
50	49.5	50.4
60	42.9	44.7
70	36.5	39.1
80	30.3	33.9
90	24.6	29.0

Note: Acetone or ethanol is the solvent here.

Table 5.2 Dielectric constant and dipole moment of water, acetone and ethanol at 20°C (93)

	Dielectric constant	Dipole moment, D
Water	80.10	1.84
Acetone	20.70	2.88
Ethanol	24.55	1.69

For both acetone and ethanol, δ is negative, which means the dielectric constant of the solution decreases with their concentration (see **Table 5.1**). Therefore, the double layer

repulsion decreases with the addition of acetone or ethanol. We observed that the swelling volume of montmorillonites decreases also. The observed minor difference between acetone and ethanol may be attributed to their difference in polarity. Acetone is more polar than water while ethanol is less polar than water (see Table 5.2). However, the dielectric properties of aqueous media is a very complicated topics (91). The addition of acetone or ethanol may modify the interactions between clay particles in a different way. The sediments of the suspensions made with montmorillonite in water-acetone or water-ethanol solutions are solid-like rather than liquid-like when the acetone or ethanol concentration exceeds a certain value. The mechanism explaining how organic liquids affect the interactions between clay particles in water-organics solutions requires further studies.

For montmorillonite K10 and reference sludges, no tangible swelling occurs. Since montmorillonite K10 is contaminated and the sludge system contains varying amounts of various cations, the repulsion between particles must be smaller than the attraction. In addition, bitumen in sludges may also act as a bonding agent, preventing them from swelling.

5.2 VALIDITY OF THE MODEL TERNARY SYSTEM TO DESCRIBE REAL OIL SANDS SLUDGE

5.2.1 Comparison of structures

The analysis of reference sludge samples shows that oil sands tailings sludge is a heterogeneous system composed of kaolinite, illite, montmorillonite, quartz and siderite, with particle sizes ranging from colloidal to non-colloidal. These results are consistent with previous published data (3,7,9,22).

However, the EDX of reference sludges shows that iron sulfide and iron oxide are also possibly present. Since the composition of oil sands deposit itself is complex, and the natural clays often contain iron oxide, this result is not surprising. The EDX also confirms the presence of metals like Ti, Fe, Mg, Mn and Al (4, 94-95), and inorganic cations like Na^+, K^+, Ca^{2+}, Mg^{2+}, Al^{3+} and Fe^{2+} and Fe^{3+} (4,6) in tailings sludge. Although the EDX technique can give information on the elemental composition of samples, it cannot provide any formation on the location of these elements in possible structural components such as Fe_2O_3, MnO, MgO, CaO, K_2O, inorganic cations and heavy metals.

It must be pointed out the SEM observations of samples dried by evaporation do not show the individual particles which can be observed after hypercritical drying. Evaporation inevitably leads to the densification of aggregates, where particles can no longer be distinguished.

SWy-1 montmorillonite and montmorillonite K10 have elemental compositions and dry aspects very close to the reference sludges, with some secondary composition differences concerning elements Fe, Ti and S.

After drying by evaporation, the SEM pictures in Fig.4.3, 4.5 and 4.6 show that montmorillonite K10 has the smallest average aggregate size while reference 1 sludge has the biggest. Consequently, K10 has the highest specific surface area and reference 1 has the lowest specific surface area, after drying by evaporation.

However, after hypercritical drying, the structure of reference sludge sediments is similar to that of the model system to a large extent. It shows card-house structure at the highest magnification. The reference sludges have a wide particle size distribution, but they comprise a high portion of colloidal platelets much smaller than in the model. Some differences concerning the packing efficiency exist. First, reference sludges do not show a uniform packing pattern when no $FeCl_3$ is added. Secondly, the first level flocs (observable at highest magnification) seem to be more densely packed than those of the model system. These difference could be explained as follows. A certain extent of flocculation for reference sludges has occurred before the addition of $FeCl_3$ solution. Consequently, the uniform packing pattern observed only on the well-dispersed systems in which the primary particles settle as individual particles is absent. In addition, it is more difficult for these previously formed flocs to diffuse; therefore the branches formed by sludge flocs are much less fractal than those of the model system.

The electrolyte concentration seems not to have an important effect on the structure of sludge sediments. Oil sands sludge has been contaminated with various ions. The highest sediment volume of reference 1 sludge is twice that of the lowest one, 9.5 mL vs 4.5 mL, while the highest sediment volume (with 5 mM $FeCl_3$) of the model system is about 9 times higher than the lowest one (without $FeCl_3$), 43 mL versus 4.5 mL. Therefore, the effect of electrolyte concentration on sludges is not as marked as with the model system, which is not surprising in view of the presence of Fe in the sludge. Nonetheless, the packing efficiency

between flocs seems to decrease somewhat with the increasing electrolyte concentration, which is consistent with the results by Aksay and Schilling (96).

Of course, the oil sands sludge is a very complex system and other factors may also contribute to the observed difference between real sludge and the model system. However, the similarities between the model and the real sludge are interesting.

5.2.2 Comparison of settling behavior

The settling and consolidation behavior of reference sludges are very similar to the model system in terms of the electrolyte concentration and suspension pH.

Some differences concerning the settling rate and the final sediment volume exist of course. The settling rate of reference sludges is considerably higher than that of the model system under similar electrolyte conditions. And the final sediment volume of reference sludges is much lower than that of the model system. For example, at pH 8.0 and 1 mM FeCl₃, the constant settling rate of the model system is 2.5 mL/h and the final sediment volume is 29.5 mL. At pH 7.4 and 1 mM FeCl₃, the constant settling rate of reference 1 sludge is 85.5 mL/h with the final sediment volume being 7 mL. This is obviously attributed to the difference in the fractal nature of flocs observed with reference sludges and the model system. For the model system, the constituent particles of flocs are thinner than those of reference sludges, and the flocs built by SWy-1 montmorillonite particles are considerably more open than those flocs by sludge particles, by comparing Fig.4.21, 4.22 and 4.23 with Fig 4.25. Therefore the reference sludge has a higher settling rate and a lower final sediment volume. These results are quite consistent with the microstructure observed.

5.3 TOWARDS A SOLUTION TO THE DISPOSAL OF OIL SANDS SLUDGE

Three approaches can be considered for solving oil sands tailings sludge problem: (1) reduction of toxicity to an acceptable level, then dumping into rivers or lakes, which is usually considered to be not realistic; (2) development of new processes to recover bitumen from oil sands without the production of sludges; and (3) transformation into a form that can be disposed of at an acceptable cost, or minimization of the amount of sludges produced. Here, we are only concerned with the last approach mainly because the Hot Water Process has been the only process with commercial success.

The results of the present study provide some useful clues for the disposal of oil sands tailings sludge. For any particular sludge treatment or disposal method, one must well define the objective or goal first. If the aim is to provide maximum amount of recycle water as quickly as possible, the addition of flocculants in sludges is one of the options. However, one must carefully select the type and concentration of flocculants used since the settling and consolidation rate are mainly determined by the fractal nature of flocs and the bonding strength between particles. In general, besides lower cost, lower flocculant concentration leads to the formation of very open and weakly-linked flocs, which settle slowly in the settling stage but can be compressed relatively easily in the consolidation stage. In any case, one must avoid using any flocculants such as ferric salts and some polyelectrolytes that will act as bonding agents between particles in order to increase the solid content of sediments. On the other hand, sludge water contains varying amount of various cations. The recycle of water from sludges without any purification or dilution inevitably increases the electrolyte concentration in the conditioned oil sands slurry, thereby decreasing the stability of slurry and the recovery rate of slurry. It is well known that a stable oil sands slurry results in a better recovery rate of bitumen.

The gel-like structure of sludges offers some very useful clues to the disposal of oil sands sludge (with solid content above 20%) after settling for a certain period. One can increase the solid content of the so called "mature sludge" by using any cost-effective methods that achieve shearing of the bonds between particles and flocs. A number of methods based on such a principle have increased the solid content of tailings sludges to a certain extent. These include freeze-thawing, dewatering with slowly moving screens, sand-clay mixing (accomplishing shearing and densification of aggregates) and sand spray technique.

The mature sludge transforms from liquid-like sediment into a gel with a certain shear strength when the solid content exceeds a certain value. A gel structure with a certain magnitude shear strength is much more easily handled than the liquid-like structure. The question is how to increase the solid content of sludges over the gel point in an economically acceptable way.

Based on the results of the present study and the nature of the Hot Water Process, the author proposes the following solution to the oil sands sludge disposal. The detail must be worked out after a pilot project. This proposed solution includes several steps described below:

(1) Separate the supernatant water (for recycle) and dilute sludge (transferred to another tailings pond) from mature sludge. At least two tailings ponds are needed, depending on the amount of sludge produced annually, the size of ponds and the extent of interference with the production schedule. One is for impounding the mature sludge. The other is for impounding fresh sludge and the separated dilute sludge. The mined-out open pit can used as a tailings pond.

(2) Increase the shear strength of the gel-like mature sludge. A combination of several currently available resources may accomplish this. First, freeze-thawing of the sludge by means of the turnaround of winter and summer. Secondly, the natural evaporation of water. Thirdly and the most important, the drying of the mature sludge by the thermal energy of fresh sludge produced continuously. This can be done in a specially designed facility in which the mature sludge is separated from the running fresh sludge by a layer material of a certain thickness which has a good thermal conductivity. One must find out the gel point for sludge first, then the drying time to reach the gel point.

(3) Transform the gel sludge into useful products. One of them would be construction materials. The gel sludge might be turned into bricks, facilities for agriculture purpose. One must be open-minded. It is well known that the raw material for making bricks is clay, why could it not be possible with sludge? Fly ash can be used as a major component for cement products and the construction of ski runs, why not with sludge? We must conduct some feasibility studies before eliminating these possibilities.

CHAPTER 6   CONCLUSIONS

The oil sands tailings sludge represents a heterogeneous system, comprising numerous substances, both inorganic and organic, with solid particle size ranging from below 0.1 μm to larger than 10 μm. The inorganic components include several types of clays with various cations and anions. While each component may have an effect on the system behavior, settling and consolidation are mainly determined by the interactions between two components: water and clays, and those factors affecting such interactions, mainly the electrolyte concentration, the suspension pH and the particle size as we observed on both the model system and reference sludges.

The selected oil sands sludge model system, Montmorillonite-Fe(III)-Water, fairly presents the real sludge system in terms of suspension stability, settling and consolidation behavior.

The results of sedimentation experiments show that stability with respect to flocculation of the model system increases with the suspension pH, as a result of the pH dependence of the double layer repulsion between plate-like clay particles. This is consistent with the fact that the pH of a water-oil sands mixture is raised to the range 8-8.5 with the addition of NaOH or other reagents in order to make a well dispersed suspension and thereby increasing the recovery rate of bitumen.

The settling and consolidation behavior of colloidal dispersions or suspensions of the mixture of colloidal and non-colloidal particles depends largely on the fractal nature of flocs and the strength of linkage between primary particles and flocs. With the increasing non-potential determining electrolyte concentration, the attraction between particles increases; the flocs become denser. The settling rate increases. On the other hand, these less fractal flocs offer more resistance to compression and to shearing of bonds between particles. This results in a slower consolidation process, that is, a higher final sediment volume. Therefore, the settling rate and the final sediment volume increase with the electrolyte concentration. The suspension pH has a similar effect by modifying the double layer repulsion between clay particles.

The flocs built by plate-like clays favor the EE linkage since the repulsion between edges is much smaller in comparison with the repulsion between faces. With Fe(III) as the counterion, the interactions between plate-like particles become more complex. First, Fe(III) undertakes hydrolysis. The hydrolysis products of Fe(III) are pH and time dependent.

Secondly, the Fe polymeric complexes act as a bonding agent between clay particles. Consequently, chain-like branches are observed, the EE linkage is strong, and the shearing of such bonds seems not to occur until the end of drying by evaporation. In order to increase the consolidation process, the linkage between particles and flocs must be broken slowly so that the entrapped water can be released before the particle linkage is recovered. To a certain extent, this can explain why a higher solid content of sludge can be achieved by using slowly moving screens or employing the freezing and thawing technique.

A direct observation of the reference sludges after hypercritically drying under SEM provides valuable information on the structure of oil sands sludge and the morphology of the constituent particles. It is clear now that the building blocks of oil sands sludges (after settling) are relatively densely packed chain-like flocs rather than primary particles. These flocs assemble themselves into a grid.

When flocculation occurs, the structures of liquid-like sediments of both the model system and oil sands sludge are basically consistent with the diffusion-limited aggregation (DLA) model. Flocculation is mainly a diffusion-controlled process. With smaller particles, more open flocs form. On average, the constituent particles of sludges are wider and thicker than those of montmorillonite. Therefore, the liquid-like sediments of the model system have a more open and more fractal structure than those of sludges.

The electrolyte concentration and the suspension pH seem to have an effect on the drying behavior of clay-water system, since they modify the structure of the drying mass. However, several other factors may also contribute to the observed fluctuations regarding drying rate, such as the drying environment.

The driving force responsible for the swelling of montmorillonite is the double layer repulsion. In addition to the electrolyte concentration and the suspension pH, the nature of the medium also has a major effect on the interactions between particles.

CHAPTER 7   SUGGESTIONS FOR FURTHER STUDIES

The present study has examined the effects of electrolyte concentration, suspension pH and the hydrolysis of a polyvalent cation Fe(III) on the settling and consolidation behavior in a relatively detailed way, and provided the first time **direct observation** of the structure of oil sands sludge. However, due to the time and financial constraints, it could not provide conclusive results with respect to the effects of the electrolyte concentration and suspension pH on drying behavior and on the mechanism by which the interactions can be modified by the nature of media, particularly, organic liquids.

Further studies should focus on the details of one or two selected areas in which the effects of the most important parameters can be evaluated on a sound basis. The following several topics are suggested for further studies.

(1) The SEM observation of the   the model system under different suspension pH, Fe (III) concentrations and   tents. The suspension pH range and Fe (III) concentration range studied in an.   s is recommended. However, since montmorillonite aqueous mixtures change from a suspension to a gel when the solid content is above 2%, and the solid content of liquid-like sediments observed in the present study is in the range 1% to 5%, three solid contents (0.5%, 2% without electrolytes and 5% without electrolytes) are recommended. They would allow the determination of the possible differences between the structure of the liquid-like sediments and that of the montmorillonite gels.

(2) A more detailed study of the effect of electrolyte concentrations and suspension pH on the drying behavior of clay-water systems under well-defined conditions. In addition, the structure evolution during drying should be studied under SEM.

(3) Study of a different model system, such as Kaolinite-Fe(III)-Water or a model system close to the oil sands sludge like Kaolinite-Montmorillonite-Illite-Fe(III)-water. The effect of electrolyte concentration and suspension pH on the settling/consolidation and the structure of sediments should be determined. The results should be compared with those of a real oil sands sludge system after purification, that is, when the various ions present in the sludge have been extracted, for instance, by using a semi-permeable membrane.

REFERENCES:

1. Syncrude Canada Ltd, " Syncrude: Mega-Bits," Promotion material, 1991.

2. Stone, J.A., and Clark, J.E.,"Oil Sands Extraction: A Dynamic Technology," Preprint of the Proceedings of Oil Sands 2000: Energy, Environment and Enterprise", AOSTRA, Edmonton, March, 1990.

3. Camp, F. W., " Processing Athabasca Tar Sands - Tailing Disposal ," 26th Canadian Chemical Engineering Conference , Toronto, October, 1976.

4. MacKinnon, M.D. and Retallack, J.T., " Preliminary Characterization and Detoxification of Tailings Pond Water at the Syncrude Canada Ltd. Oil Sands Plant," in "Land and Water Issues Related to Energy Development , 4th Conference, Denver, Colorado, 1981," Rand, P.J., Ed., Ann Arbor Science, 185, 1982.

5. Dusseault, M.B. and Scott, J.D., "Behavior of Oil Sands Tailings," Proceedings of the 33rd Canadian Geotechnical Conference, Calgary, Alberta, September, 1980.

6. Scott, J.D., Dusseault, M.B. and Carrier III, W.D., " Behavior of the Clay/Bitumen/Water Sludge System from Oil Sands Extraction Plants," *Applied Clay Sci.*, 1, 207, 1985.

7. C-H Synfuels Limited, " Dry Tailings Disposal from Oil Sands Mining," Unpublished report, Industrial Programs Branch, Environmental Protection Service, Environment Canada, 1984.

8. Kessick, M.A. and Jobson, A.M., " Clay Tailings from Alberta Oil Sands and Other Sources: A Review," Alberta Environment Peport, 1977.

9. Hardy Associates Ltd., "Athabasca Oil Sands Tailings Disposal Beyond Surface Mineable Limits," Alberta Environment Report, 1979.

10. Baes, C. F. Jr. and Mesmer, R. E., The Hydrolysis of Cations, Wiley, New York, 1976.

11. Hiemenz, H. C., Principles of Colloid and Surface Chemistry, Marcel Dekker, New York, 1977.

12. Pierre, A.C., Introduction aux procédés Sol-Gel, under publication, Septima, Paris, 1991.

13. Ives, K.J., "Introduction", in "The Scientific Basis of Flocculation Proceedings of the NATO Advanced Study Institute on the Scientific Basis of Flocculation, Cambridge, July, 1977," Ives, K.J., Ed., Sijthoff & Noordhoff, Alphen aan den Rijn, 1, 1978.

14. Lyklema, J., "Surface Chemistry of Colloids in Connection with Stability" in "The Scientific Basis of Flocculation-Proceedings of the NATO Advanced Study Institute on the Scientific Basis of Flocculation, Cambridge, July, 1977," Ives, K.J., Ed., Sijthoff & Noordhoff, Alphen aan den Rijn, 3, 1978.

15. van Oss, C. J., Giese, R.F., and Costanzo, P. M., "DLVO and Non-DLVO Interactions in Hectorite," *Clays and Clay Minerals*, 38, 151, 1990.

16. Riddick, T. M., Control of Colloid Stability through ZETA POTENTIAL, Livingston, Wynnewood, 1968.

17. Pierre, A. C., "Sol-Gel Processing of Ceramic Powders," *Ceramic Bulletin*, 70, 1281, 1991.

18. Gutcho, S., Waste Treatment with Polyelectrolytes and Other Flocculants, Noyes Data Corporation, Park Ridge, 1977.

19. Levine, S. and Friesen, W. I., "Flocculation of Colloid Particles by Water-Soluble Polymers," in "Flocculation in Biotechnology and Separation Systems-Proceedings of the International Symposium on Flocculation in Biotechnology and Separation Systems, San Francisco, July, 1986," Attia, Y. A. Ed., Elsevier, Amsterdam, 3, 1987.

20. Worrall, W. E., Clays and Ceramic Raw Materials, Elsevier, London, 1986.

21. Chander, S. and Hogg, R., "Sedimentation and Consolidation in Destabilized Suspensions," in "Flocculation in Biotechnology and Separation Systems- Proceedings of the International Symposium on Flocculation in Biotechnology and Separation Systems, San Francisco, July, 1986," Attia, Y. A., Ed., Elsevier, Amsterdam, 279, 1987.

22. Kessick, M.A., " Clay Slimes from the Extraction of Alberta Oil Sands, Florida Phosphate Matrix and Other Mined Deposits," *CIM Bull.* , 71(790),80, 1978.

23. Mittal, H.K., "Tailings Disposal Concepts in Oil Sands Open Pit Mines," Design and Construction of Tailings Dams, Wilson, D., Ed., Colorado School of Mines Press, 206, 1981.

24. Erskine, H.L., "Separation of Clay and Mineral from Heavy Oil Production," in "The Future of Heavy Crude and Tar Sands," Meyer, R.F., Wynn, J.C. and Olson, J.C., Ed., 519,1982.

25. Kasperski, K.L., "Studies of the Physical Chemistry of Clays," Ph. D. Thesis, The Department of Chemistry, University of Alberta, 1988.

26. Hepler, L.G., Dobrogowska, C. and Kasperski, K., "Water Soluble Substances from Heavy Oils and Bitumen," in " Oil in Fresh Water: Chemistry, Biology, Countermeasure Technology," Vandermeulen, J.H., and Hrudey, S.E., Ed., Pergamon Press, 3, 1987.

27. Burchfield, T. E. and Hepler, L.G., "Some Chemical and Physical Properties of Tailings Water from Oil Sands Extraction Plants," *Fuel*, 58, 745, 1979.

28. May, A., " Electrophoretic Mobilities and Cation Exchange Capacities of Florida Phosphate Slimes," US Bureau of Mines, RI 8046, 1975.

29. Environmental Science & Technology, Feature article " Those Nasty Phosphatic Clay Ponds," 8, 312, 1974.

30. Hoppe, R. W., "Phosphates Are Vital to Agriculture - and Florida Mine for One-Third the World," *E/MJ*, 177, 79, May, 1976.

31. O'Gorman, J.V. and Kitchener, J.A., "The Flocculation and De-watering of Kimberlite Clay Slimes," *Int. J. Miner. Process.*, 1, 33, 1974

32. Hood, G. D. and Wilemon, G. M., "Dewatering of Red Mud," in "Flocculation in Biotechnology and Separation Systems-Proceedings of the International Symposium on Flocculation in Biotechnology and Separation Systems, San Francisco, July, 1986," Attia, Y. A. Ed., Elsevier, Amsterdam, 773, 1987.

33. Vogt, M. F. and Stein, D. L., "Dewatering Large Volume Aqueous Slurries - Sand Bed Filtration of Bauxite Residue," in " Light Met., Proc. of Sess., AIME Annual Meeting," 105th, New York, V.2, 117, 1976.

34. Sparrow, G.J.and Ihle, S.,"Dewatering Clay Slimes - an Approach to the Problem," Minerals Research Laboratory, Melbourne Australia, CSIRO Investigation Report 126, 1978.

35. Crickmore, P. J., Schutte, R. and Causgrove, J., " Fractal Geometry and the Settling of Oil Sands Tailings Sludge," in "Proceedings of 4th Unitar Conference on Heavy Crude and Tar Sands, Edmonton, August, 1988," V.1, 217, 1988.

36. Mikula, R. J., Payette, C. and Lam, W. W., "Microscopic Conservation of Structure in Oil Sands Sludge," in "Preprint of the Petroleum Society of CIM and AOSTR A. 1991 Technical Meeting, Banff, April, 1991," V.3, Paper No.120, 1991.

37. Baillie, R. A. and Malmberg, "Removal of Clay from the Water Streams of the Hot Water Process by Flocculation," United States Patent 3,487,003, 1969.

38. Lang, W. J. and Hentz, D. A., "Process for Flocculanting Oil and Clay-Containing Slimes," United States Patent 3,723,310, 1973.

39. Camp, F.W., "Removing Suspended Solids from a Liquid," United States Patent 3,526,585, 1970.

40. Schutte, R., "Clarification of Tar Sands Middlings Water," United States Patent 3,816,305, 1974.

41. Hepp, P. S. and Camp, F. W., "Treating Hot Water Process Discharge Water by Flocculation and Vacuum Precoat Filtration," United States Patent 3,502,575, 1970 and Canadian Patent 892,548, 1972.

42. Pittman, W. E. Jr., McLendon, J. T. and Sweeney, J. W., " A Review of Phosphatic Clay Dewatering Research," US Bureau of Mines Information Circular 8980, 1984.

43. Schulz, K. F. and Morrison, D. N., " Great Canadian Oil Sands Tailings Disposal Problem," Alberta Research Council Open File Report 1973-38.

44. Hocking, M. B. and Lee, G.W., "Effect of Chemical Agents on Settling Rates of Sludges from Effluent of Hot Water Extraction of Athabasca Oil Sands," *Fuel*, 56, 325, 1977

45. Hall, E. S and Tollefson, E. L., "Stabilization and Destabilization of Mineral Fines-Bitumen-Water Dispersions in Tailings from Oil Sands Extraction Plants That Use the Hot Water Process," in "Proceedings of the 2nd World Congress of Chemical Engineering, Montreal, 1981," V.2, 457, 1981.

46. Stastny, G. J., "Some Methods for Treating Tar Sands Tailings," Report to Alberta Environment, Part I & II, 1973 and 1974.

47. Kingery, W.D., Bowen, H.R. and Uhlmann, D.R., Introduction to Ceramics, John Wiley & Sons, New York, 1976.

48. Beutelspacher, H. and van der Marcel, H. W., Ed., Atlas of Electron Microscopy of Clay Minerals and Their Admixtures, Elsevier, Amsterdam, 1968.

49. van Olphen, H., An Introduction to Clay Colloid Chemistry, Interscience, New York, 1963.

50. Swartzen-Allen, S. L. and Matijevic, E., "Surface and Colloid Chemistry of Clays," *Chemical Reviews*, 74, 35,1974.

51. Hunter, R. J. and Nicol, S. K., " The Dependence of Plastic Flow Behavior of Clay Suspensions on Surface Properties," *J.Colloid Interface Sci.*, **28**, 250. 1968.

52. Rowell, D. L., "Influence of Positive Charge on the Inter- and Intra-Crystalline Swelling of Oriented Aggregates of Na-montmorillonite in NaCl Solution," *Soil Sci.*, **100**, 340, 1965.

53. Flegmann, A.W., Goodwin, J. W. and Ottewill, R. H., "Rheological Studies on Kaolinite Suspensions,' *Proc. Br. Ceram. Soc.*, 31, June, 1969.

54. Mitra, R. P. and Kapoor, B. S., "Acid Character of Montmorillonite - Titration Curve in Water and Some Non-aqueous Solvents," *Soil Sci.*, **108**, 11, 1969.

55. Schofield, R. K., "Effect of pH on Electric Charge Carried by Clay Particles," *J. Soil Sci.*, **1**, 1, 1949.

56. O'Brien, N. R., "Fabric of Kaolinite and Illite Floccules," *Clays & Clay Minerals*, **19**, 353, 1971.

57. Babchin, A., Reitman, V. and Rispler, K., "Settling of Synthetic Sludges and Kaolinites," in "Preprint of the Petroleum Society of CIM and AOSTRA, 1991 Technical Meeting, Banff, April, 1991," V.3, Paper No.127, 1991.

58. Schutte, R., Czarnecki, J. A. and Liu, J. K., "Structure of Sludge," in "Preprint of the Petroleum Society of CIM and AOSTRA, 1991 Technical Meeting, Banff, April, 1991," V.3, Paper No.119, 1991.

59. Arora, H. S. and Coleman, N. T., "The Influence of Electrolytes Concentration on Flocculation of Clay Suspensions," *Soil Sci.*, **127**, 134, 1979.

60. Greene, R. S. B., Posner, A. M. and Quirk, J. P., "A Studies of the Coagulation of Montmorillonite and Illite Suspensions by $CaCl_2$ Using the Electron Microscope," in " Modification of Soil Structure," Emerson, W. W., Bond, R. D. and Dexter, A. R., Ed., John Wiley & Sons, New York, 1978.

61. Swartzen-Allen, S. L. and Matijevic, E., "Colloid and Surface Properties of Clay Suspensions, III. Stability of Montmorillonite and Kaolinite," *J. Colloid Interface Sci.*, **56**, 159,1976.

62. Swartzen-Allen, S. L. and Matijevic, E., "Colloid and Surface Properties of Clay Suspensions, II. Electrophoresis and Cation Adsorption of Montmorillonite", *J. Colloid Interface Sci.*, **50**, 143, 1975.

63. Goldberg, S. and Glaubig, R. A., "Effect of Saturating Cation, pH, and Aluminum and Iron Oxide on the Flocculation of Kaolinite and Montmorillonite," *Clays & Clay Minerals*, **35**, 220, 1987.

64. Gregory, J., "Flocculation by Inorganic Salts," in "The Scientific Basis of Flocculation-Proceedings of the NATO Advanced Study Institute on the Scientific Basis of Flocculation, Cambridge, July, 1977," Ives, K.J., Ed., Sijthoff & Noordhoff, Alphen aan den Rijn, 89, 1978.

65. Blackmore, A. V., "Aggregation of Clay by the Products of Iron (III) Hydrolysis," *Aust. J. Soil Res.*, **11**, 75, 1973.

66. Lutz, J.F., "The Relation of Free Iron in the Soil to Aggregation", *Proc. Soil Sci. Soc. Am.*, **1**, 43, 1936.

67. El Rayah, H. M. E. and Rowell, D.L., "The Influence of Iron and Aluminium Hydroxides on the Swelling of Na-Montmorillonite and the Permeability of a Na-Soil," *J. Soil Sci.*, **24**, 137, 1973.

68. Fitch, B., "Sedimentation Process Fundamentals," *AIME Trans.*, **223**, 129, 1962.

69. Hogg, R., Klimpel, R. C. and Ray, D. T., "Agglomerate Structure in Flocculated Suspensions and its Effect on Sedimentation and Dewatering," *Minerals & Metallurgical Processing*, **4**, 108, 1987.

70. Smellie, R. H. Jr. and La Mer, V. K., "Flocculation, Subsidence, and Filtration of Phosphate Slimes, III. Subsidence Behavior," *J. Colloid Sci.*, **11**, 720, 1956.

71. Michaels, A. and Bolger, J. C., "Settling Rates and Sediment Volumes of Flocculated Kaolin Suspensions," *I & EC Fundam.*, **10**, 24, 1962.

72. Norrish, K., "The Swelling of Montmorillonite," *Disc. Faraday Soc.*, **18**, 120, 1954.

73. Khandal, R. K. and Tadros, Th. F., "Application of Viscoelastic Measurements to the Investigation of the Swelling of Sodium Montmorillonite Suspensions," *J. Colloid Interface Sci.*, **125**, 122, 1988.

74. Emerson, W. W., "The Swelling of Na-Montmorillonite due to Water Adsorption," *Aust. J. Soil Res.*, **1**, 129, 1963.

75. Newman, A. C. D., "The Interaction of Water with Clay Mineral Surfaces," Chemistry of Clays and Clay Minerals, Newman, A. C. D., Ed., Longman Scientific & Technical, Essex, 1987.

76. Helmy, A. K. and Natale, I. M., "Effect of the Dielectric Constant on the Double Layer on Clays," *Clays & Clay Minerals*, **33**, 329, 1985.

77. Moore, F., "The Mechanism of Moisture Movement in Clays with Particular Reference to Drying: A Concise Review," *Trans. Br. Ceram. Soc.*, **60**, 517, 1961.

78. Kingery, W. D. and Francl, J., "Fundamental Study of Clay: XIII, Drying Behavior and Plastic Properties," *J. Am. Ceram. Soc.*, **37**, 596, 1954.

79. Livage, J., Henry, M. and Sanchez, C., "Sol-Gel Chemistry of Transition Metal Oxides," *Prog. Solid State Chem.*, **18**, 259, 1989.

80. Jorgensen, C. K., Inorganic Complexes, Acadamic Press, London, 1963.

81. Matijevic, E., "The Role of Chemical Complexing in the Formation and Stability of Colloidal Suspensions," *J. Colloid Interface Sci.*, **58**, 374, 1977.

82. Brindley, G. W. and Brown. G., Crystal Structures of Clay Minerals and Their X-Ray Identification, Mineralogical Society, London, 1980.

83. Kodama, H., Kotlyar, L. S. and Ripmeester, J. A., "Quantification of Crystalline and Noncrystalline Material in Ground Kaolinite by X-ray Powder Diffraction, Infrared, Solid-State Nuclear Magnetic Resonance, and Chemical-Dissolution Analysis," *Clays & Clay Minerals*, **37**, 364, 1989.

84. van Olphen, H. and Fripiat, J. J., Data Handbook for Clay Materials and Other Non-Metallic Minerals, Pergamon, Oxford, 1979.

85. Bohor, B. F. and Hughes, R. E., "Scanning Electron Microscopy of Clays and Clay Minerals," *Clays & Clay Minerals*, **19**, 49, 1971.

86. Witten, T. A. Jr. and Meakin, P., "Diffusion-Limited Aggregation at Multiple Growth Sites," *Phys. Rev. B*, **28**, 5632, 1983.

87. Fricke, J., " Aerogel - Highly Tenuous Solids with Fascinating Properties," *J. Non-Cryst. Solids*, **100**, 169, 1988.

88. Deshpande, T. L., Greenland, D. J., and Quirk, J. P., "Changes in Soil Properties Associated with the Removal of Iron and Aluminium Oxides," *J. Soil Sci.*, **19**, 108, 1968.

89. Macey, H. H., *Trans. Brit. Cera. Soc.*, **37**, 131, 1938.

90. Westman, A. E. R., "Capillary Suction of Some Ceramic Materials," *J. Amer. Ceram. Soc.*, **15**, 552, 1932.

91. Hasted, J. B., Aqueous Dielectrics, Chapman and Hall, London, 1973.

92. Meites, L., Handbook of Analytical Chemistry, McGraw-Hill, New York, 1963.

93. Dean, J. A., Lange's Handbook of Chemistry, McGraw-Hill, New York, 1985.

94. Kramers, J.K. and Brown, R. A. S., " Survey of Heavy Minerals in Surface-Minerable Area of the Athabasca Oil Sand Deposit," *CIM Bull.*, **69**, 92, 1976.

95. Majid, A., Ripmeester, J. A. and Davidson, D.W., "Organic Matter Adsorbed to Heavy Metal Minerals in Oil Sands," National Research Council of Canada Report, Report No. C1095-82S, 1982.

96. Aksay, I. A. and Schilling, C. H., "Colloidal Filtration Route to Uniform Mictrostructure," in "Ultrastructure Processing of Ceramics, Glasses, and Composites," Hench, L. L. and Ulrich, D. R., Ed., John Wiley & Sons, New York, 439, 1984.